INFORMATION TO USERS

This manuscript has been reproduced from the microfilm master. UMI films the text directly from the original or copy submitted. Thus, some thesis and dissertation copies are in typewriter face, while others may be from any type of computer printer.

The quality of this reproduction is dependent upon the quality of the copy submitted. Broken or indistinct print, colored or poor quality illustrations and photographs, print bleedthrough, substandard margins, and improper alignment can adversely affect reproduction.

In the unlikely event that the author did not send UMI a complete manuscript and there are missing pages, these will be noted. Also, if unauthorized copyright material had to be removed, a note will indicate the deletion.

Oversize materials (e.g., maps, drawings, charts) are reproduced by sectioning the original, beginning at the upper left-hand corner and continuing from left to right in equal sections with small overlaps. Each original is also photographed in one exposure and is included in reduced form at the back of the book.

Photographs included in the original manuscript have been reproduced xerographically in this copy. Higher quality 6" x 9" black and white photographic prints are available for any photographs or illustrations appearing in this copy for an additional charge. Contact UMI directly to order.

UMI

A Bell & Howell Information Company
300 North Zeeb Road, Ann Arbor MI 48106-1346 USA
313/761-4700 800/521-0600

NON-LINEAR FREE VIBRATION OF A SPINNING TETHER

by

BYUNG NO MIN

Department of Mechanical Engineering
McGill University, Montreal
August 1996

A thesis submitted to the Faculty of Graduate Studies and Research
in partial fulfillment of the requirement of the degree of
Master of Engineering

Abstract

Non-linear vibration of a spinning tether is studied in this thesis. The tether is thought to be a part of a spinning tethered satellite system in the station-keeping phase so that the tether has a constant nominal length and is forced to spin at a constant rate about its nominal axis. Using the extended Hamilton's principle the governing equations of motion are derived retaining non-linear terms up to the third order that originate from geometric non-linearity. They are discretized by the assumed-modes method, truncated to one-mode equations, and transformed to the phase-space form. Then the method of averaging is applied.

When the tether has high nominal tension, averaging with two variables results in a closed form solution, which shows dependence of the frequency contents on the initial amplitude parameters of the system. In the case of very low nominal tension, averaging with a single variable is useful to obtain the steady state and the limit steady state solutions, both of which result in a circular whirling motion like a skip-rope. Without damping, a general transverse mode appears to be quasi-periodic but it can be periodic under certain initial conditions. Numerical investigations reveal that the material damping through the longitudinal mode derives the steady state to the limit steady state. Also, several interesting shapes are observed in phase plots.

Résumé

Cette thèse étudie les vibrations non linéaires d'un fil en rotation. On considère le fil faisant partie d'un système satellisé en rotation dans la phase de maintien en position. Ceci nous permet de présumer que le fil a une longueur nominale fixe et qu'il est contraint à tourner autour de son axe principal avec une vitesse constante. Les équations du mouvement sont formulées à partir du principe d'Hamilton en gardant les termes non linéaires jusqu'au troisième ordre. Ces derniers apparaissent en raison de la géométrie non linéaire du système. Les équations du mouvement sont discrétisées en utilisant la méthode des modes imposés, où seul le premier mode est considéré. Ensuite, ces équations sont transformées dans l'espace des phases avant d'y appliquer la méthode de la moyenne.

Lorsque le fil a une tension nominale élevée, en appliquant la méthode de la moyenne avec deux variables on obtient une solution analytique. Ceci démontre que les fréquences et les amplitudes initiales du système sont interdépendentes. Dans le cas où la tension nominale du fil est faible, en appliquant la méthode de la moyenne avec une seule variable on obtient la solution ainsi que la solution limite à l'état stationnaire. Ces solutions représentent un tournoiement circulaire ressemblant au mouvement d'une corde à sauter. En omettant les effets d'amortissement, on observe qu'un mode transversal se comporte d'une façon quasi-périodique. Cependant, ce dernier peut devenir périodique sous certaines conditions initiales. Plusieures recherches démontrent que la présence d'amortissement dans le matériau, dans le mode longitudinal, peut entraîner un état stationnaire à la limite. De plus, plusieurs formes intéressantes sont observées dans les courbes de phase.

Acknowledgement

I would like to express my sincere gratitude to my supervisor Prof. Arun K. Misra for his kindness, guidance and encouragement throughout the course of this research, and especially for his precise reviews and the details required in the completion of this thesis.

Sincere thanks are due to all my colleagues, with whom I shared an office and computing facilities on 550 Sherbrooke, for their encouragement and friendship. Among them I would like to extend special thanks to Khin Thatt Tsang-Wai-Sang and Tareck Horchani for their help writing the Résumé. Thanks to Lal Alakkattussery for his help regarding the MECHENG network. I especially thank Ms. Barbara Whiston for her administrative expertise and kindness.

I wish to express my deepest gratitude to my mother for her support and concern.

Contents

Nomenclature

Specific Symbols

A	cross-sectional area of the tether
dx	length of nominal tether element
ds	deformed length of tether element
E	Young's modulus
$\{\hat{\mathbf{i}}, \hat{\mathbf{j}}, \hat{\mathbf{k}}\}$	unit vectors of the tether frame
l	nominal length of the tether
L	Lagrangian of the system
n_o	non-dimensionalized nominal tension
N	local tension in the tether
N_o	nominal tension in the tether
N_l	number of modes along the longitudinal direction
N_t	number of modes along the transverse direction
$q_{(\cdot)}$	generalized external force per unit mass
(q_i, p_i)	phase-space variables in rectangular form
$\mathbf{Q}$	generalized force vector
$\mathbf{r}$	position vector of a mass point of the tether
t	time
T	kinetic energy of the system
u	longitudinal component of the tether deformation
U	discretized coordinate for longitudinal displacement
$\mathbf{v}$	velocity vector of a mass point of the tether

v	transverse component of the tether deformation
V	discretized coordinate for transverse displacement; also potential energy of the system in chapter 2
w	transverse component of the tether deformation
W	work done by the external forces; discretized coordinate for transverse displacement
x	nominal tether coordinate;
$\mathbf{x}$	generalized coordinate vector

Greek Symbols

α_i	disturbance variable for a_i
(a_i, β_i)	phase-space variables in polar form
ε	engineering strain
γ	non-dimensionalized spin rate
η	compound phase angle
φ_i	shape function for longitudinal modes
ν	fundamental frequency of the longitudinal mode
ϑ_i	shape function for transverse modes
ρ	linear density of the tether
ω	fundamental frequency of the transverse mode
Ω	spin rate of the system
ξ	disturbance variable for η
ψ_i	shape function for transverse modes
ζ	damping parameter

List of Tables

List of Figures

Chapter 1

INTRODUCTION

1.1 Introductory Remarks

Tethered satellite systems are considered as one of the promising technologies in space development programs. This simple concept, connecting satellites or space structures with long thin tethers, has led to a large number of proposals for practical applications[1, 2]. Bekey[3] has summarized the potential uses of space tethers putting them into five categories. These are:

- Atmospheric uses: Observation of high altitude atmosphere;
  Orbital wind tunnel;
  Aerobraking in planetary missions for orbital capture.
- Electrodynamic uses: Electric power generation;
  Electrodynamic brake for re-entry.
- Artificial gravity uses: Variable micro-gravity laboratory.
- Constellations: To tie and connect several space platforms together.
- Transportation uses: Orbit transfer of payloads;
  Simultaneous shuttle de-orbit and space station re-boost;
  Waste disposal from the space station.

Two types of tethered satellite systems have been studied and flown in space. One is the non-spinning type such as the SEDS(Small Expendable Deployer System; USA) and TSS(Tethered Satellite System; USA-Italy) missions[Fig. 1.1], while the other is the spinning type like in Gemini XI(USA) and OEDIPUS(Observation of Electric field

Distribution in Inospheric Plasma - a Unique Strategy; Canada) missions[Fig. 1.2]. Both types are in comparatively early stage of development and there is a strong need to understand the complex dynamics of the tether in order to manage the missions successfully. In spite of the simple configurations, it requires rigorous and complicated analysis to understand their dynamics.

The operation of tethered satellite systems is normally composed of three phases: deployment, station-keeping, and retrieval. The deployment and retrieval phases involve a variable tether length that makes the governing equations of the system complex. Moreover, the retrieval has been reported to be intrinsically unstable. That is why many earlier research works were focused on the control of the variable length tether. In the station-keeping phase, during which most of the scientific experiments are conducted, tether length is constant, but the tension in the tether can become very small and the dynamics can belong to the non-linear regime. A comprehensive survey of earlier works on the dynamics and control of tethered systems was done by Misra and Modi[4]. Beletsky and Levin[5] revised and generalized many interesting results published on the theory of space tether dynamics.

1.2 Literature Review on Vibrations of Tethered Satellite Systems

In conjunction with the TSS mission of NASA-Italy, a lot of research work has been conducted on the non-spinning configuration. The earlier studies paid less attention to the tether oscillations compared to its librations, and the vibrations of tether were analyzed usually by the linear theory. Von Flotow[6] suggested the appropriate approximations to keep the bare minimum of the physical effects of a tethered system. Because of the large spectral separation between the motions, he decoupled the fast oscillations of the tether deformation and the attitude motions of the end-bodies from the slow librations of the deformed rigid configuration. Pasca et al.[7] derived the linearized

equations of motion with variable coefficients and solved the corresponding eigenvalue problems by means of a perturbation method. They showed that the in-plane transverse and longitudinal vibrations are weakly coupled with gyroscopic terms such that they could be decoupled from each other approximately. Bergamaschi et al.[8] were able to explain well some of the results from the spectral analysis of TSS-1 mission using the linearized equations derived by Bergamaschi and Catinaccio[9] with an averaged longitudinal stress, and they observed several combination tones of the fundamental modes, which were presumed to be due to non-linear coupling. On the other hand, Luongo and Vestroni[10] considered non-linear oscillations; they used two integro-differential equations with weakly quadratic non-linear terms after ignoring the longitudinal inertia and showed that the frequencies and shapes of the vibrations depended upon the amplitudes.

One of the purposes of spinning the tethered system is to generate an artificial gravity for the spacecraft connected to the ends of the tether and to maintain station-keeping with the sufficient tether tension. In that case, the system is forced to spin about an axis normal to the nominal tether line like a cartwheel. Gemini XI and the proposed BICEPS(BIstatic Canadian Experiment on Plasmas in Space) are examples of this[11, 12]. Elastic oscillations of such tethered systems have been carried out by Quadrelli and Lorenzini[13].

In OEDIPUS missions, on the other hand, the tether spins about an axis parallel to the nominal tether line, and the spin of tether is induced by the end-body rotations for spin stabilization of the attitude. In the first OEDIPUS flight, the attitude of the end-bodies showed some deviation from that expected prior to the flight without detailed consideration of the tether effects. Tyc and Han[14] took tether interactions into account in the analysis of the attitude dynamics in two aspects; by considering the tether tension exerted on the end-bodies and by including the additional energy dissipation. The results of their parametric study were in good agreement with those of the real flight. They, however, did not deal with the motion of the tether. Tyc et al.[15] included tether motion

in the dynamic modeling and obtained closed-form conditions for asymptotic stability of the system from the linearized equations. They showed that the spin of the tether had significant effects on the dynamics and stability. In a later related study, Luo et al.[16] focused their attention on the oscillations of a spinning tether and derived the non-linear equations up to the third order. The resonance and stability conditions were deduced.

1.3 Literature Review on Non-Linear Vibrations of an Elastic String

Motion of an elastic string on which a space tether is modeled has been studied for a long time because it is a simple mechanical system which can verify the mathematical formulation and it can provide good physical intuition. The famous wave equation was formulated over a century ago and could be solved under a variety of boundary conditions. It was possible to extract the resonant frequencies and mode shapes of vibration of a stretched string. It, however, was restricted to linear analysis with the assumption of infinitesimal deformation. Several phenomena, such as jump responses, sub/super-harmonic resonances, saturation, and amplitude-modulated motions, which could not be explained by the linear theory were discovered and they were tackled by introducing non-linear terms into the formulations[17, 18].

Lee[19] considered the local variation of tension caused by the strain up to the second order and derived a modified wave equation with a non-linear term. He obtained an approximate amplitude-frequency relation for a planar forced vibration of a string, but the result was compatible with the experiment in a qualitative way only. Oplinger[20] took the global variation of tension into account and formulated an integro-differential equation. In case of a specific boundary condition, he could obtain an exact solution and the results of his formulation were compatible with those of the experiment until the out-of-plane motion occurred. Murthy and Ramakrishna[21] extended the previous theories to include the out-of-plane vibration, which was coupled with the in-plane vibration

nonlinearly. Using the harmonic balance method, they derived the amplitude-frequency relations from the coupled non-linear equations and explained the tubular whirling motion and the jump phenomena as the normal pattern of resonance response of stretched strings. The stability analysis of these phenomena was done by Miles[22]. Anand[23] considered the coupling between the longitudinal and transverse modes of vibration. Because of the large spectral separation between the two modes, the longitudinal inertia term was ignored and the modified equations for the transverse vibrations were obtained. His formulation was used as a standard in many later analyses. Eller[24] conducted the stability analysis based on a modified and extended form of Anand's theory and compared it with the experiment.

Recently, studies on vibrations of an elastic string were focused on more complex behavior, such as bifurcation phenomena and chaos. Using the method of averaging, many researchers transformed the governing equations of motion into a set of phase-space formulation and tried to observe the behavior by manipulating it. Miles[25] revisited the problem of stability of the string vibrations under a simple harmonic planar excitation and classified the bifurcation points in the frequency parameter domain along with the variation of damping parameter. In the same system, Johnson and Bajaj[26, 27] identified limit cycles, period-doublings, and chaotic attractors for small enough damping. O'Reilly and Holmes[28] added the experiment and more rigorous theoretical analysis.

1.4 Scope and Outline of the Thesis

Spinning tethered satellite systems have emerged recently as a practical application in space. As mentioned in the literature review, the earlier works and real flights have shown the crucial effects of the tether on the dynamics of the system and referred to the need of comprehensive study about the dynamics of the spinning tether. Little research

work, however, has focused on it. It is apparent that the study on non-linear behavior of the spinning tether is in an early development stage.

On that account, the present work considers non-linear free vibration of a spinning tether, which can be regarded as a part of a spinning tethered satellite system in the station-keeping phase. The tether is assumed to spin about its nominal axis due to the rotation of the massive end-satellites and to be under very low nominal tension. It is the most typical condition for a spinning tether in space. Using the extended Hamilton's principle, a set of partial differential equations and boundary conditions that constitute the governing equations of motion are derived. Unfortunately, they are coupled by non-linear terms (retained here up to the third order) and are not amenable to exact solution. Since the energy expressions have been set up during the derivation of the equations of motion, the assumed-modes method is adopted to discretize the system. It results in a set of simultaneous ordinary differential equations that are coupled between the longitudinal and transverse modes as well as between the lower and higher frequency modes. Although they can be solved by a numerical technique, they are truncated to a set of one mode equations, which makes it possible to investigate the significant non-linear features of the system in an analytical way. Van der Pol transformation maps the one mode truncated equations into the phase-space form and then the method of averaging is applied to the formulation.

When the nominal tension is high, averaging is carried out with two variables and results in a closed form solution for the response. On the other hand, when the tension is low, only a single variable is used for averaging. The steady state condition and the corresponding response are obtained, and the effect of the damping, which is modeled as a simplified version of the material damping along the longitudinal mode, is considered as well. Several numerical investigations are presented and discussed. Then, the conclusions follow at the end of the thesis.

The thesis is organized as follows:

- Chapter 2 describes the system configuration and presents the basic assumptions on which the thesis is based. The governing equations of motion are derived using the extended Hamilton's principle.
- Chapter 3 discretizes the system using the assumed-modes method. After truncation to the one mode equations, they are mapped into the phase-space form by the Van der Pol transformation.
- Chapter 4 introduces the method of averaging applied to the phase-space form. Two variables are used for the high nominal tension case, while a single variable is used for the low nominal tension case. The steady state condition, its stability, and the closed form response are obtained, and the effect of damping is analyzed.
- Chapter 5 investigates and discusses several cases of numerical simulation.
- Chapter 6 presents some conclusions of the thesis and recommendations for future work.
- The Bibliography contains the references.

Chapter 2

EQUATIONS OF MOTION

2.1 Description of the System and Basic Assumptions

A schematic diagram of a spinning tethered satellite system is shown in Figure 2.1. A long and thin tether connects two satellites which are supposed to spin at a constant angular rate Ω about their own symmetric axes aligned with the tether. The nominal tether axis passes through the two attachment points, **O** and **E**, of the tether with the satellites, and the x-axis of a tether frame is aligned with it. Two transversal axes are set arbitrarily at **O** in the plane normal to the nominal tether axis to complete a right-handed coordinate system. This tether frame rotates about the x-axis at the same angular rate as that of the satellites. The unit vectors along the tether frame are denoted by $\hat{\mathbf{i}}$, $\hat{\mathbf{j}}$, and $\hat{\mathbf{k}}$, respectively.

The basic assumptions used in the derivation of the equations of motion are as follows:

- The tethered system is in the station-keeping phase. So, the nominal length of tether, l, is constant.
- The length of the tether is not very long so that the gravity gradient effect on the tether motion is negligible.
- The mass of the satellites is much larger than that of the tether. Hence, the vibration of the tether does not alter the global motion of the system and the tether attachment point **O** can be regarded to be fixed inertially.

- The nominal tether axis is aligned with the axes of symmetry of the satellites and its direction remains fixed.
- The spin rate of the tether is the same as that of the satellites such that the tether experiences no twist.
- External forces on the system, such as aerodynamic drag and electrodynamic force, are negligible.
- The material properties of the tether are uniform.
- The constitutive relation of the tether material is given by the Hooke's law.
- The deformations of the tether are not infinitesimal but small.
- There is no internal resonance.

2.2 Kimematic Variables

All points on the tether are described in terms of the nominal tether coordinate x. As shown in Figure 2.1, a point **B** at x in nominal configuration deforms to **A** which is a point in the deformed configuration. u, v, and w are the deformations of the tether along the longitudinal and two transverse directions, respectively, in the tether frame and are functions of the axial coordinate x and time t. Since the origin of the tether frame, which is the tether attachment point **O**, is assumed to be fixed inertially, a position vector of the mass point on the tether at x can be expressed as

$$\mathbf{r}(x,t) = [x + u(x,t)]\hat{\mathbf{i}} + v(x,t)\hat{\mathbf{j}} + w(x,t)\hat{\mathbf{k}} \tag{2.1}$$

Differentiation of the position vector (2.1) with respect to time, which is composed of the differentiation in the rotating frame and the effect due to the rotation of the frame, produces velocity

$$\begin{aligned}\mathbf{v} &= \dot{\mathbf{r}} + \Omega\hat{\mathbf{i}} \times \mathbf{r} \\ &= u_t\hat{\mathbf{i}} + (v_t - \Omega w)\hat{\mathbf{j}} + (w_t + \Omega v)\hat{\mathbf{k}}\end{aligned} \tag{2.2}$$

where the subscript t represents partial differentiation with respect to time t.

Figure 2.2 depicts two infinitesimal elements of the tether in a slightly exaggerated manner. A nominal element **BB′** of length dx deforms to a stretched element **AA′**. The length ds of the deformed element can be calculated by the Pythagorean rule from the geometry:

$$ds = dx\left[(1+u_x)^2 + v_x^{\,2} + w_x^{\,2}\right]^{\frac{1}{2}} \tag{2.3}$$

A local engineering strain is defined as the ratio of the net extension to the nominal length of the element as follows:

$$\begin{aligned}\varepsilon &\equiv \frac{ds}{dx} - 1 \\ &= \left[(1+u_x)^2 + v_x^{\,2} + w_x^{\,2}\right]^{\frac{1}{2}} - 1\end{aligned} \tag{2.4}$$

Using the binomial expansion formula

$$(1+z)^{\frac{1}{2}} = 1 + \frac{1}{2}z - \frac{1\cdot 1}{2\cdot 4}z^2 + \frac{1\cdot 1\cdot 3}{2\cdot 4\cdot 6}z^3 - \frac{1\cdot 1\cdot 3\cdot 5}{2\cdot 4\cdot 6\cdot 8}z^4 + \cdots \tag{2.5}$$

the strain expression of Eq. (2.4) becomes

$$\begin{aligned}\varepsilon = u_x + \tfrac{1}{2}\left(v_x^{\,2} + w_x^{\,2}\right) - \tfrac{1}{2}u_x\left(v_x^{\,2} + w_x^{\,2}\right) \\ - \tfrac{1}{8}\left(v_x^{\,2} + w_x^{\,2}\right)^2 + \tfrac{1}{2}u_x^{\,2}\left(v_x^{\,2} + w_x^{\,2}\right) + \cdots\end{aligned} \tag{2.6}$$

in which the expansion is retained up to the fourth order under the assumption that the deformations, u, v, and w, are not infinitesimal but small.

2.3 Energy Expressions

The system has two kinds of energy, those are kinetic energy and potential energy due to the elasticity of the tether. From the velocity expression (2.2), the kinetic energy of the system is simply

$$\begin{aligned} T &= \tfrac{1}{2}\int_0^l \mathbf{v}\cdot\mathbf{v}\rho dx \\ &= \tfrac{1}{2}\int_0^l \left[\rho u_t^{\,2} + \rho(v_t - \Omega w)^2 + \rho(w_t + \Omega v)^2\right] dx \end{aligned} \tag{2.7}$$

where ρ is the linear density of the tether defined as mass per unit nominal length.

The tether is assumed to be made of an elastic material and its deformation is associated with an elastic potential energy or strain energy. According to Hooke's law the tension in the tether is given by

$$N = N_o + EA\varepsilon \tag{2.8}$$

where E is the Young's modulus and A is the cross-sectional area of the tether. N_o is the nominal tension when the tether is in its nominal configuration and may result, for example, from the gravity gradient effect in an orbit. Since the constitutive relation (2.8) between tension and strain is linear, the potential energy of the system becomes

$$V = \int_0^l \left(N_o\varepsilon + \tfrac{1}{2}EA\varepsilon^2\right) dx \tag{2.9}$$

and substituting the strain expression (2.6) into (2.9) leads to

$$\begin{aligned} V \equiv \int_0^l \Big[& N_o u_x + \tfrac{1}{2}N_o\left(v_x^{\,2} + w_x^{\,2}\right) + \tfrac{1}{2}EAu_x^{\,2} \\ & + \tfrac{1}{2}(EA - N_o)\left\{u_x\left(v_x^{\,2} + w_x^{\,2}\right) + \tfrac{1}{4}\left(v_x^{\,2} + w_x^{\,2}\right)^2 - u_x^{\,2}\left(v_x^{\,2} + w_x^{\,2}\right)\right\}\Big] dx \end{aligned} \tag{2.10}$$

In the above, the deformation variables are kept up to the fourth order to take non-linear effects into account. It is a geometric non-linearity rather than that of the material. In most cases of practical importance, the nominal tension N_o is much smaller than the longitudinal rigidity EA, so the strain energy could be rewritten without losing much accuracy as follows:

$$V \cong \int_0^l \Big[N_o \Big\{ u_x + \tfrac{1}{2}\left(v_x^2 + w_x^2\right) \Big\} + \tfrac{1}{2} EA \Big\{ u_x^2 + u_x\left(v_x^2 + w_x^2\right) + \tfrac{1}{4}\left(v_x^2 + w_x^2\right)^2 - u_x^2\left(v_x^2 + w_x^2\right) \Big\} \Big] dx \tag{2.11}$$

From Eqs. (2.7) and (2.11), the Lagrangian of the system can be obtained as

$$\begin{aligned} L &\equiv T - V \\ &= \tfrac{1}{2} \int_0^l \Big[\rho u_t^2 + \rho\left(v_t - \Omega w\right)^2 + \rho\left(w_t + \Omega v\right)^2 \\ &\qquad - 2N_o \Big\{ u_x + \tfrac{1}{2}\left(v_x^2 + w_x^2\right) \Big\} \\ &\qquad - EA \Big\{ u_x^2 + u_x\left(v_x^2 + w_x^2\right) + \tfrac{1}{4}\left(v_x^2 + w_x^2\right)^2 - u_x^2\left(v_x^2 + w_x^2\right) \Big\} \Big] dx \end{aligned} \tag{2.12}$$

2.4 Governing Equations

According to the extended Hamilton's principle,

$$\int_{t_1}^{t_2} (\delta L + \delta W) dt = 0 \tag{2.13}$$

for any arbitrary time interval (t_1, t_2) where δL is the variation of the Lagrangian L, while δW is the virtual work done by the applied forces. The stationary condition of Eq. (2.13) results in a set of partial differential equations and the corresponding boundary conditions, which constitute the governing equations of motion. The detailed derivation can be found

in Appendix A at the end of the thesis. Under the condition of uniform material property of the tether, the governing equations are:

P.D.E.

$$u_{tt} - \frac{EA}{\rho}\left\{\left(1 - v_x^2 - w_x^2\right)u_{xx} + \left(1 - 2u_x\right)\left(v_x v_{xx} + w_x w_{xx}\right)\right\} = q_u \tag{2.14. a}$$

$$\begin{aligned} & v_{tt} - 2\Omega w_t - \Omega^2 v - \frac{N_o}{\rho} v_{xx} \\ & - \frac{EA}{\rho}\left\{\left(u_x - u_x^2 + \tfrac{3}{2}v_x^2 + \tfrac{1}{2}w_x^2\right)v_{xx} + \left(u_{xx} - 2u_x u_{xx} + w_x w_{xx}\right)v_x\right\} = q_v \end{aligned} \tag{2.14. b}$$

$$\begin{aligned} & w_{tt} + 2\Omega v_t - \Omega^2 w - \frac{N_o}{\rho} w_{xx} \\ & - \frac{EA}{\rho}\left\{\left(u_x - u_x^2 + \tfrac{1}{2}v_x^2 + \tfrac{3}{2}w_x^2\right)w_{xx} + \left(u_{xx} - 2u_x u_{xx} + v_x v_{xx}\right)w_x\right\} = q_w \end{aligned} \tag{2.14. c}$$

B.C.

$$u = v = w = 0 \qquad \text{at} \qquad x = 0 \quad \text{and} \quad x = l \tag{2.15}$$

In Eqs. (2.14), q_u, q_v, and q_w are generalized forces per unit mass along the longitudinal and the two transverse directions, respectively. These are calculated from the external loading applied to the system and the dissipative force due to damping. The partial differential equations (2.14) and boundary conditions (2.15) constitute the mathematical formulation for the continuous system of the spinning tether. The formulation can be comparable to that of Anand's[23] that has been used as a standard in many works on the string vibrations. The formulation (2.14) of the present work contains all the terms of Anand's; in addition, it has the gyroscopic coupling terms and a few more non-linear terms. The gyroscopic terms arise from the spin of the tether about its nominal axis, while

the supplementary non-linear terms are caused by the expansion of the strain expression up to the fourth order rather than the second in Anand's.

The two transverse equations (2.14. b, c) are coupled gyroscopically and all the three equations of motion are coupled to each other by highly non-linear terms as well. It is impossible to obtain the exact closed form solution, and hence there is no choice but to resort to an approximate method.

Chapter 3

DISCRETIZATION

3.1 Assumed-Modes Method

For non-linear continuous systems, it is usually not possible to obtain the exact closed form solution of the governing equations. This is due to the difficulties in solving non-linear partial differential equations. Nonetheless, these equations can be transformed to a set of ordinary differential equations by eliminating the spatial dependence from the problems through discretization, and these can then be solved by analytical or numerical methods. This process, however, implies a certain degree of approximation, although the accuracy of the solution can be achieved up to the level desired.

There is a variety of discretization procedures. They can be categorized into two classes. One is that of analytical procedures, such as the assumed-modes and Galerkin methods, based on the expansion of the solutions in a finite series of known functions. The other is the physical discretization procedure, such as the lumped parameter method or the finite element method. Each procedure has its own features, advantages and disadvantages, which have been discussed by Meirovitch[31].

Since the kinetic and potential energy expressions as well as the Lagrangian of the system have been derived in the previous chapter, the assumed-modes method is preferred here since it is a variational method based on the energy of the system. According to this method, the following forms of the solution are assumed.

$$u(x,t) = \sum_{i=1}^{N_t} \varphi_i(x) U_i(t) = \varphi_i U_i \qquad (3.1.\text{a})$$

$$v(x,t) = \sum_{i=1}^{N_l} \vartheta_i(x) V_i(t) = \vartheta_i V_i \tag{3.1. b}$$

$$w(x,t) = \sum_{i=1}^{N_t} \psi_i(x) W_i(t) = \psi_i W_i \tag{3.1. c}$$

where U_i, V_i, and W_i are the generalized coordinates of the discretized system, while φ_i, ϑ_i, and ψ_i are the assumed shape functions that satisfy the boundary conditions $\varphi_i = \vartheta_i = \psi_i = 0$ at both $x = 0$ and $x = l$. As mentioned earlier, the assumed-modes method is a variational method based on the energy of system, and hence the shape functions need to be only admissible functions, i.e. they need satisfy only the geometric boundary conditions but not necessarily the natural boundary conditions. The specific forms of the shape functions are specified later. N_l and N_t are the numbers of the shape functions utilized for the longitudinal and the transverse displacements, respectively. Note that the tensor summation convention has been used in Eqs. (3.1) for brevity.

Substituting the approximate solution forms (3.1) into the system Lagrangian (2.11) produces the Lagrangian in terms of the discretized coordinates:

$$\begin{aligned}
L = {} & \tfrac{1}{2}\langle \rho\varphi_i\varphi_j \rangle \dot{U}_i\dot{U}_j + \tfrac{1}{2}\langle \rho\vartheta_i\vartheta_j \rangle \dot{V}_i\dot{V}_j + \tfrac{1}{2}\langle \rho\psi_i\psi_j \rangle \dot{W}_i\dot{W}_j \\
& - \Omega\langle \rho\vartheta_i\psi_j \rangle \dot{V}_i W_j + \Omega\langle \rho\psi_i\vartheta_j \rangle \dot{W}_i V_j \\
& - \tfrac{1}{2}\langle EA\varphi_i'\varphi_j' \rangle U_i U_j - \langle N_o\varphi_i' \rangle U_i \\
& + \tfrac{1}{2}\left\{ \Omega^2\langle \rho\vartheta_i\vartheta_j \rangle - \langle N_o\vartheta_i'\vartheta_j' \rangle \right\} V_i V_j \\
& + \tfrac{1}{2}\left\{ \Omega^2\langle \rho\psi_i\psi_j \rangle - \langle N_o\psi_i'\psi_j' \rangle \right\} W_i W_j \\
& - \tfrac{1}{2}\langle EA\varphi_i'\vartheta_j'\vartheta_k' \rangle U_i V_j V_k - \tfrac{1}{2}\langle EA\varphi_i'\psi_j'\psi_k' \rangle U_i W_j W_k \\
& + \tfrac{1}{2}\langle EA\varphi_i'\varphi_j'\vartheta_k'\vartheta_l' \rangle U_i U_j V_k V_l + \tfrac{1}{2}\langle EA\varphi_i'\varphi_j'\psi_k'\psi_l' \rangle U_i U_j W_k W_l \\
& - \tfrac{1}{8}\langle EA\vartheta_i'\vartheta_j'\vartheta_k'\vartheta_l' \rangle V_i V_j V_k V_l - \tfrac{1}{4}\langle EA\vartheta_i'\vartheta_j'\psi_k'\psi_l' \rangle V_i V_j W_k W_l \\
& - \tfrac{1}{8}\langle EA\psi_i'\psi_j'\psi_k'\psi_l' \rangle W_i W_j W_k W_l
\end{aligned} \tag{3.2}$$

where the angle bracket $\langle\cdot\rangle$ means the integral from 0 to l in the nominal coordinate x, i.e., $\langle\cdot\rangle = \int_0^l \cdot dx$.

The general Euler-Lagrange's equations of motion for a discrete system have the form

$$\frac{d}{dt}\left(\frac{\partial L}{\partial \dot{\mathbf{x}}}\right) - \frac{\partial L}{\partial \mathbf{x}} = \mathbf{Q} \tag{3.3}$$

in which $\mathbf{x}$ and $\mathbf{Q}$ are the generalized coordinate and force vectors, respectively. By introducing the Lagrangian (3.2) into Eq. (3.3), the discretized equations of motion are obtained as follows:

$$\begin{aligned}\langle \rho\varphi_i\varphi_j\rangle\ddot{U}_j + \langle EA\varphi_i'\varphi_j'\rangle U_j + \tfrac{1}{2}\langle EA\varphi_i'\vartheta_j'\vartheta_k'\rangle V_jV_k + \tfrac{1}{2}\langle EA\varphi_i'\psi_j'\psi_k'\rangle W_jW_k \\ - \langle EA\varphi_i'\varphi_j'\vartheta_k'\vartheta_l'\rangle U_jV_kV_l - \langle EA\varphi_i'\varphi_j'\psi_k'\psi_l'\rangle U_jW_kW_l + \langle N_o\varphi_i'\rangle = Q_{U_i}\end{aligned} \tag{3.4. a}$$

$$\begin{aligned}\langle \rho\vartheta_i\vartheta_j\rangle\ddot{V}_j - 2\Omega\langle \rho\vartheta_i\psi_j\rangle\dot{W}_j + \left\{\langle N_o\vartheta_i'\vartheta_j'\rangle - \Omega^2\langle \rho\vartheta_i\vartheta_j\rangle\right\}V_j \\ + \langle EA\vartheta_i'\vartheta_j'\varphi_k'\rangle V_jU_k - \langle EA\vartheta_i'\vartheta_j'\varphi_k'\varphi_l'\rangle V_jU_kU_l \\ + \tfrac{1}{2}\langle EA\vartheta_i'\vartheta_j'\vartheta_k'\vartheta_l'\rangle V_jV_kV_l + \tfrac{1}{2}\langle EA\vartheta_i'\vartheta_j'\psi_k'\psi_l'\rangle V_jW_kW_l = Q_{V_i}\end{aligned} \tag{3.4. b}$$

$$\begin{aligned}\langle \rho\psi_i\psi_j\rangle\ddot{W}_j + 2\Omega\langle \rho\psi_i\vartheta_j\rangle\dot{V}_j + \left\{\langle N_o\psi_i'\psi_j'\rangle - \Omega^2\langle \rho\psi_i\psi_j\rangle\right\}W_j \\ + \langle EA\psi_i'\psi_j'\varphi_k'\rangle W_jU_k - \langle EA\psi_i'\psi_j'\varphi_k'\varphi_l'\rangle W_jU_kU_l \\ + \tfrac{1}{2}\langle EA\psi_i'\psi_j'\vartheta_k'\vartheta_l'\rangle W_jV_kV_l + \tfrac{1}{2}\langle EA\psi_i'\psi_j'\psi_k'\psi_l'\rangle W_jW_kW_l = Q_{W_i}\end{aligned} \tag{3.4. c}$$

The above is a set of simultaneous second order ordinary differential equations and the number of degrees of freedom is $N_l + 2N_t$. All the equations are coupled to each other non-linearly. It is still not feasible to obtain the closed form solution for Eqs. (3.4) and further simplification is required.

3.2 Non-Dimensionalization and Truncation

Many practical considerations require the tether to have uniform material properties such as uniform mass distribution, uniform geometry, and constant longitudinal stiffness. In that case, introducing the following dimensionless variables makes the analysis convenient.

$$\left\{x/l,\ \ U/l,\ \ V/l,\ \ W/l,\ \ t\left(EA/\rho l^2\right)^{\frac{1}{2}}\right\} \ \rightarrow\ \{x,\ \ U,\ \ V,\ \ W,\ \ t\} \qquad (3.5)$$

From now on all variables are dimensionless, and the discretized equations (3.4) become

$$\begin{aligned}\left\langle \varphi_i\varphi_j\right\rangle \ddot{U}_j &+\left\langle \varphi_i'\varphi_j'\right\rangle U_j+\tfrac{1}{2}\left\langle \varphi_i'\vartheta_j'\vartheta_k'\right\rangle V_jV_k+\tfrac{1}{2}\left\langle \varphi_i'\psi_j'\psi_k'\right\rangle W_jW_k\\ &-\left\langle \varphi_i'\varphi_j'\vartheta_k'\vartheta_l'\right\rangle U_jV_kV_l-\left\langle \varphi_i'\varphi_j'\psi_k'\psi_l'\right\rangle U_jW_kW_l+{n_o}^2\left\langle \varphi_i'\right\rangle = q_{U_i}\end{aligned} \qquad (3.6.\text{ a})$$

$$\begin{aligned}\left\langle \vartheta_i\vartheta_j\right\rangle \ddot{V}_j &-2\gamma\left\langle \vartheta_i\psi_j\right\rangle \dot{W}_j+\left\{{n_o}^2\left\langle \vartheta_i'\vartheta_j'\right\rangle-\gamma^2\left\langle \vartheta_i\vartheta_j\right\rangle\right\}V_j\\ &+\left\langle \vartheta_i'\vartheta_j'\varphi_k'\right\rangle V_jU_k-\left\langle \vartheta_i'\vartheta_j'\varphi_k'\varphi_l'\right\rangle V_jU_kU_l\\ &+\tfrac{1}{2}\left\langle \vartheta_i'\vartheta_j'\vartheta_k'\vartheta_l'\right\rangle V_jV_kV_l+\tfrac{1}{2}\left\langle \vartheta_i'\vartheta_j'\psi_k'\psi_l'\right\rangle V_jW_kW_l=q_{V_i}\end{aligned} \qquad (3.6.\text{ b})$$

$$\begin{aligned}\left\langle \psi_i\psi_j\right\rangle \ddot{W}_j &+2\gamma\left\langle \psi_i\vartheta_j\right\rangle \dot{V}_j+\left\{{n_o}^2\left\langle \psi_i'\psi_j'\right\rangle-\gamma^2\left\langle \rho\psi_i\psi_j\right\rangle\right\}W_j\\ &+\left\langle \psi_i'\psi_j'\varphi_k'\right\rangle W_jU_k-\left\langle \psi_i'\psi_j'\varphi_k'\varphi_l'\right\rangle W_jU_kU_l\\ &+\tfrac{1}{2}\left\langle \psi_i'\psi_j'\vartheta_k'\vartheta_l'\right\rangle W_jV_kV_l+\tfrac{1}{2}\left\langle \psi_i'\psi_j'\psi_k'\psi_l'\right\rangle W_jW_kW_l=q_{W_i}\end{aligned} \qquad (3.6.\text{ c})$$

where

$$\begin{cases} q_{(\cdot)}=Q_{(\cdot)}/EA\\ \gamma=\Omega\left(EA/\rho l^2\right)^{-\frac{1}{2}}\\ n_o=\left(N_o/EA\right)^{\frac{1}{2}}\end{cases} \qquad (3.7)$$

Because of the symmetry of the tether about the nominal axis, the two transverse modes can be expanded by the same set of shape functions. Besides, it is expected from many earlier studies that the response in the higher modes would be smaller than that of the fundamental mode. Contribution to the motion from the higher modes could be negligible unless internal resonance occurs and the response described by the fundamental mode could show most of the salient characteristics of the system. With that in mind, to obtain approximate solutions, the following is assumed:

$$\begin{cases} U_1 = U, \quad V_1 = V, \quad W_1 = W \\ U_i = V_i = W_i = 0, \quad i = 2,3,4,\cdots \\ \Psi_1 = \vartheta_1 = \vartheta \end{cases} \tag{3.8}$$

Applying Eqs. (3.8) to Eqs. (3.6) and simplifying lead to the one-mode truncated equations of motion:

$$\ddot{U} + \nu^2 U = f_U + \left(-h_1 + k_1 U\right)\left(V^2 + W^2\right) \tag{3.9. a}$$

$$\ddot{V} - 2\gamma\dot{W} + \left(\omega^2 - \gamma^2\right)V = f_V + \left\{-h_2 U + k_2 U^2 - k_3\left(V^2 + W^2\right)\right\}V \tag{3.9. b}$$

$$\ddot{W} + 2\gamma\dot{V} + \left(\omega^2 - \gamma^2\right)W = f_W + \left\{-h_2 U + k_2 U^2 - k_3\left(V^2 + W^2\right)\right\}W \tag{3.9. c}$$

where the dimensionless forces and the coefficients are given by

$$f_U = Q_U / \langle \varphi^2 \rangle, \qquad f_V = Q_V / \langle \vartheta^2 \rangle, \qquad f_W = Q_W / \langle \vartheta^2 \rangle \tag{3.10}$$

$$\begin{cases} \nu = \left\{ \langle \varphi'^2 \rangle / \langle \varphi^2 \rangle \right\}^{\frac{1}{2}}, \quad \omega = n_o \left\{ \langle \vartheta'^2 \rangle / \langle \vartheta^2 \rangle \right\}^{\frac{1}{2}} \\ h_1 = \langle \varphi' \vartheta'^2 \rangle / \langle 2\varphi^2 \rangle, \quad h_2 = \langle \vartheta'^2 \varphi' \rangle / \langle \vartheta^2 \rangle \\ k_1 = \langle \varphi'^2 \vartheta'^2 \rangle / \langle \varphi^2 \rangle, \quad k_2 = \langle \vartheta'^2 \varphi'^2 \rangle / \langle 2\vartheta^2 \rangle, \quad k_3 = \langle \vartheta'^4 \rangle / \langle 2\vartheta^2 \rangle \end{cases} \tag{3.11}$$

3.3 Phase-Space Formulation

The left-hand sides of the truncated set of equations (3.9) are linear and the general solutions with the right-hand sides put equal to zero can be found without much difficulty. From those, the following form of solution for Eqs. (3.9) is suggested:

$$U(t) = a_1(t)\cos[\nu t + \beta_1(t)] \qquad (3.12.\text{ a})$$

$$V(t) = a_2(t)\cos[(\omega-\gamma)t + \beta_2(t)] + a_3(t)\cos[(\omega+\gamma)t + \beta_3(t)] \qquad (3.12.\text{ b})$$

$$W(t) = a_2(t)\sin[(\omega-\gamma)t + \beta_2(t)] - a_3(t)\sin[(\omega+\gamma)t + \beta_3(t)] \qquad (3.12.\text{ c})$$

The above reduces to the linear solution when both a_i's and β_i's become constants. A set of equations (3.12) is a sort of transformation from the configuration-space (U, V, W) to the phase-space (a_1, a_2, a_3, β_1, β_2, β_3). Sometimes it is called the Van der Pol transformation. It is obvious that the phase-space variables, a_i's and β_i's, in the transformation (3.12) cannot be determined completely, because the dimension of the phase-space is six as opposed to that of the configuration-space which is three. Hence, three more restrictions are needed. Thus, one can impose three conditions that the time derivatives of the discretized coordinates have the same form as they do when the phase variables are constants, i.e.,

$$\dot{U}(t) = -a_1(t)\nu\sin[\nu t + \beta_1(t)] \qquad (3.13.\text{ a})$$

$$\dot{V}(t) = -a_2(t)(\omega-\gamma)\sin[(\omega-\gamma)t + \beta_2(t)] - a_3(t)(\omega+\gamma)\sin[(\omega+\gamma)t + \beta_3(t)]$$
..... (3.13. b)

$$\dot{W}(t) = a_2(t)(\omega-\gamma)\cos[(\omega-\gamma)t + \beta_2(t)] - a_3(t)(\omega+\gamma)\cos[(\omega+\gamma)t + \beta_3(t)]$$
..... (3.13. c)

Substituting the transformation (3.12) into both the restriction (3.13) and the set of equations of motion (3.9) and then rewriting them in matrix form yield

$$\begin{bmatrix} \cos[\nu t+\beta_1] & -\sin[\nu t+\beta_1] \\ \sin[\nu t+\beta_1] & \cos[\nu t+\beta_1] \end{bmatrix} \begin{bmatrix} \dot{a}_1 \\ a_1\dot{\beta}_1 \end{bmatrix} = \begin{bmatrix} 0 \\ -\frac{1}{\nu} f_U - \frac{1}{\nu}\left\{-h_1 + k_1 a_1 \cos[\nu t+\beta_1]\right\}\left\{a_2^{\,2} + a_3^{\,2} + 2a_2 a_3 \cos[2\omega t+\beta_2+\beta_3]\right\} \end{bmatrix} \qquad (3.14.\text{ a})$$

$$\begin{bmatrix} \cos[(\omega-\gamma)t+\beta_2] & -\sin[(\omega-\gamma)t+\beta_2] & \cos[(\omega+\gamma)t+\beta_3] & -\sin[(\omega+\gamma)t+\beta_3] \\ \sin[(\omega-\gamma)t+\beta_2] & \cos[(\omega-\gamma)t+\beta_2] & -\sin[(\omega+\gamma)t+\beta_3] & -\cos[(\omega+\gamma)t+\beta_3] \\ -(\omega-\gamma)\sin[(\omega-\gamma)t+\beta_2] & -(\omega-\gamma)\cos[(\omega-\gamma)t+\beta_2] & -(\omega+\gamma)\sin[(\omega+\gamma)t+\beta_3] & -(\omega+\gamma)\cos[(\omega+\gamma)t+\beta_3] \\ (\omega-\gamma)\cos[(\omega-\gamma)t+\beta_2] & -(\omega-\gamma)\sin[(\omega-\gamma)t+\beta_2] & -(\omega+\gamma)\cos[(\omega+\gamma)t+\beta_3] & (\omega+\gamma)\sin[(\omega+\gamma)t+\beta_3] \end{bmatrix} \begin{bmatrix} \dot{a}_2 \\ a_2\dot{\beta}_2 \\ \dot{a}_3 \\ a_3\dot{\beta}_3 \end{bmatrix}$$

$$= \begin{bmatrix} 0 \\ 0 \\ f_V + \left\{-h_2 a_1 \cos[\nu t+\beta_1] + k_2 a_1^{\,2}\cos^2[\nu t+\beta_1] - k_1\left(a_2^{\,2}+a_3^{\,2}+2a_2a_3\cos[2\omega t+\beta_2+\beta_3]\right)\right\} \\ \quad \times\left\{a_2\cos[(\omega-\gamma)t+\beta_2] + a_3\cos[(\omega+\gamma)t+\beta_3]\right\} \\ f_W + \left\{-h_2 a_1 \cos[\nu t+\beta_1] + k_2 a_1^{\,2}\cos^2[\nu t+\beta_1] - k_1\left(a_2^{\,2}+a_3^{\,2}+2a_2a_3\cos[2\omega t+\beta_2+\beta_3]\right)\right\} \\ \quad \times\left\{a_2\sin[(\omega-\gamma)t+\beta_2] - a_3\sin[(\omega+\gamma)t+\beta_3]\right\} \end{bmatrix}$$

..... (3.14. b)

In the case of free oscillations with light material damping, which is a practical situation for tethers in space, dissipative forces act on the tether although no external force is applied to the system. The dissipative force due to material damping corresponds to the rate of deformation of the material, and it can be approximated to be along the longitudinal direction if the configuration of the system is linear such as a string or tether. Then, the generalized forcing terms in Eqs. (3.14) could be expressed as

$$\begin{cases} f_U = -2\zeta\dot{U} = 2\zeta a_1 \nu \sin[\nu t + \beta_1] \\ f_V = 0 \\ f_W = 0 \end{cases} \tag{3.15}$$

where ζ is a damping parameter.

The coefficient matrices of Eqs. (3.14. a, b) are invertible. Pre-multiplication of Eqs. (3.14. a, b) by their inverses and use of Eqs. (3.15) result in a set of first order simultaneous ordinary differential equations in phase-space as follows:

$$\begin{bmatrix} \dot{a}_1 \\ a_1\dot{\beta}_1 \\ \dot{a}_2 \\ a_2\dot{\beta}_2 \\ \dot{a}_3 \\ a_3\dot{\beta}_3 \end{bmatrix} = \begin{bmatrix} -2\zeta a_1 \sin^2[\nu t + \beta_1] + \frac{1}{\nu}\{h_1 \sin[\nu t + \beta_1] - k_1 a_1 \cos[\nu t + \beta_1]\sin[\nu t + \beta_1]\} \\ \quad \times \{a_2^2 + a_3^2 + 2a_2 a_3 \cos[2\omega t + \beta_2 + \beta_3]\} \\ -2\zeta a_1 \cos[\nu t + \beta_1]\sin[\nu t + \beta_1] + \frac{1}{\nu}\{h_1 \cos[\nu t + \beta_1] - k_1 a_1 \cos^2[\nu t + \beta_1]\} \\ \quad \times \{a_2^2 + a_3^2 + 2a_2 a_3 \cos[2\omega t + \beta_2 + \beta_3]\} \\ \frac{1}{2\omega}\{-h_2 a_1 \cos[\nu t + \beta_1] + k_2 a_1^2 \cos^2[\nu t + \beta_1] - k_3(a_2^2 + a_3^2 + 2a_2 a_3 \cos[2\omega t + \beta_2 + \beta_3])\} \\ \quad \times \{-a_3 \sin[2\omega t + \beta_2 + \beta_3]\} \\ \frac{1}{2\omega}\{-h_2 a_1 \cos[\nu t + \beta_1] + k_2 a_1^2 \cos^2[\nu t + \beta_1] - k_3(a_2^2 + a_3^2 + 2a_2 a_3 \cos[2\omega t + \beta_2 + \beta_3])\} \\ \quad \times \{-a_2 - a_3 \sin[2\omega t + \beta_2 + \beta_3]\} \\ \frac{1}{2\omega}\{-h_2 a_1 \cos[\nu t + \beta_1] + k_2 a_1^2 \cos^2[\nu t + \beta_1] - k_3(a_2^2 + a_3^2 + 2a_2 a_3 \cos[2\omega t + \beta_2 + \beta_3])\} \\ \quad \times \{-a_2 \sin[2\omega t + \beta_2 + \beta_3]\} \\ \frac{1}{2\omega}\{-h_2 a_1 \cos[\nu t + \beta_1] + k_2 a_1^2 \cos^2[\nu t + \beta_1] - k_3(a_2^2 + a_3^2 + 2a_2 a_3 \cos[2\omega t + \beta_2 + \beta_3])\} \\ \quad \times \{-a_2 \cos[2\omega t + \beta_2 + \beta_3] - a_3\} \end{bmatrix} \tag{3.16}$$

Chapter 4

ANALYSIS USING THE METHOD OF AVERAGING

4.1 Averaging with Two Variables

Under the assumption of small deformation the response of the system, Eq. (3.12), has a small magnitude, i.e. the coefficients a_i's are small. When the nominal tension is high, the transverse frequency parameter ω is large and its reciprocal becomes sufficiently small. Besides, the longitudinal frequency parameter v is always high and its reciprocal is small. Then the right hand side of the phase-space equation (3.16) can be regarded to have small elements and so do the derivatives of the phase-space variables. It can be interpreted that the phase-space variables, a_i's and β_i's, are slowly varying functions of time and the variations in these variables are negligible compared to the main response of the system. According to the method of averaging, the effect of the minute variations in slowly varying functions can be accounted for by taking an average with respect to the rapidly varying variables.

It can easily be noticed that the right-hand side of the phase-space equation (3.16) is composed of the terms which are either constant or periodic with a period of 2π with respect to the variables vt and $2\omega t$. Since the longitudinal frequency v is usually high and so is ω as mentioned in the previous paragraph, both vt and $2\omega t$ are rapidly varying variables and can be used as averaging variables in order to discard the minute variations

caused by the rapidly varying variables in the phase-space equation (3.16). Averaging the phase-space equation over a period with respect to the variables νt and $2\omega t$, one obtains

$$\begin{bmatrix} \dot{a}_1 \\ a_1\dot{\beta}_1 \\ \dot{a}_2 \\ a_2\dot{\beta}_2 \\ \dot{a}_3 \\ a_3\dot{\beta}_3 \end{bmatrix} = \frac{1}{4\pi^2}\int_0^{2\pi}\int_0^{2\pi}\begin{bmatrix} \text{R.H.S.} \\ \text{of} \\ \text{Eq. (3.16)} \end{bmatrix} d(\nu t)d(2\omega t) \tag{4.1}$$

which results in the following approximate equation:

$$\begin{bmatrix} \dot{a}_1 \\ a_1\dot{\beta}_1 \\ \dot{a}_2 \\ a_2\dot{\beta}_2 \\ \dot{a}_3 \\ a_3\dot{\beta}_3 \end{bmatrix} = \begin{bmatrix} -\zeta a_1 \\ -\frac{k_1}{2\nu}a_1\left(a_2^{\,2}+a_3^{\,2}\right) \\ 0 \\ \frac{1}{4\omega}a_2\left\{-k_2a_1^{\,2}+2k_3\left(a_2^{\,2}+2a_3^{\,2}\right)\right\} \\ 0 \\ \frac{1}{4\omega}a_3\left\{-k_2a_1^{\,2}+2k_3\left(2a_2^{\,2}+a_3^{\,2}\right)\right\} \end{bmatrix} \tag{4.2}$$

The above equation is easy to solve. First, the solution for the amplitude variables is

$$\begin{cases} a_1 = a_{1o}e^{-\zeta\nu} \\ a_2 = a_{2o} \\ a_3 = a_{3o} \end{cases} \tag{4.3}$$

where a_{io}'s are constants of integration dependent on the initial conditions. Inserting them into the equations governing the phase angle variables, the β_i's in Eq. (4.2), and integrating, one obtains

$$\begin{cases} \beta_1 = -\frac{k_1}{2\nu}\left(a_{2o}^{\ 2} + a_{3o}^{\ 2}\right)t + \beta_{1o} \\ \beta_2 = \frac{1}{4\omega}\left\{-\frac{k_2}{2\zeta}a_{1o}^{\ 2}\left(1-e^{-2\zeta t}\right) + 2k_3\left(a_{2o}^{\ 2} + 2a_{3o}^{\ 2}\right)t\right\} + \beta_{2o} \\ \beta_3 = \frac{1}{4\omega}\left\{-\frac{k_2}{2\zeta}a_{1o}^{\ 2}\left(1-e^{-2\zeta t}\right) + 2k_3\left(2a_{2o}^{\ 2} + a_{3o}^{\ 2}\right)t\right\} + \beta_{3o} \end{cases} \tag{4.4}$$

where β_{io}'s are constants of integration.

Substituting Eqs. (4.3) and (4.4) into Eq. (3.12), the first order approximations for the response in discretized coordinates are obtained in closed forms as follows:

$$U(t) = a_{1o}e^{-\zeta t}\cos\left[\left\{\nu - \frac{k_1}{2\nu}\left(a_{2o}^{\ 2} + a_{3o}^{\ 2}\right)\right\}t + \beta_{1o}\right] \tag{4.5. a}$$

$$\begin{aligned} V(t) = {} & a_{2o}\cos\left[(\omega-\gamma)t + \frac{1}{4\omega}\left\{-\frac{k_2}{2\zeta}a_{1o}^{\ 2}\left(1-e^{-2\zeta t}\right) + 2k_3\left(a_{2o}^{\ 2} + 2a_{3o}^{\ 2}\right)t\right\} + \beta_{2o}\right] \\ & + a_{3o}\cos\left[(\omega+\gamma)t + \frac{1}{4\omega}\left\{-\frac{k_2}{2\zeta}a_{1o}^{\ 2}\left(1-e^{-2\zeta t}\right) + 2k_3\left(2a_{2o}^{\ 2} + a_{3o}^{\ 2}\right)t\right\} + \beta_{3o}\right] \end{aligned}$$

..... (4.5. b)

$$\begin{aligned} W(t) = {} & a_{2o}\sin\left[(\omega-\gamma)t + \frac{1}{4\omega}\left\{-\frac{k_2}{2\zeta}a_{1o}^{\ 2}\left(1-e^{-2\zeta t}\right) + 2k_3\left(a_{2o}^{\ 2} + 2a_{3o}^{\ 2}\right)t\right\} + \beta_{2o}\right] \\ & - a_{3o}\sin\left[(\omega+\gamma)t + \frac{1}{4\omega}\left\{-\frac{k_2}{2\zeta}a_{1o}^{\ 2}\left(1-e^{-2\zeta t}\right) + 2k_3\left(2a_{2o}^{\ 2} + a_{3o}^{\ 2}\right)t\right\} + \beta_{3o}\right] \end{aligned}$$

..... (4.5. c)

The response (4.5) shows some interesting characteristics. The amplitude of the longitudinal vibration decays exponentially due to the damping but those of the transverse vibrations are not affected. On the other hand, the frequency content shows the reverse behavior. By differentiating the arguments of the sinusoidal functions in Eqs. (4.5), the longitudinal and transverse frequency contents are respectively given by

$$\nu_1 = \nu - \frac{k_1}{2\nu}\left(a_{2o}^{\ 2} + a_{3o}^{\ 2}\right) \tag{4.6}$$

$$\begin{cases} \omega_1 = \omega - \gamma + \frac{1}{4\omega}\left\{-k_2 a_{1o}{}^2 e^{-2\zeta t} + 2k_3\left(a_{2o}{}^2 + 2a_{3o}{}^2\right)\right\} \\ \omega_2 = \omega + \gamma + \frac{1}{4\omega}\left\{-k_2 a_{1o}{}^2 e^{-2\zeta t} + 2k_3\left(2a_{2o}{}^2 + a_{3o}{}^2\right)\right\} \end{cases} \tag{4.7}$$

The frequency content of the transverse motion is affected by the structural damping while that for the longitudinal motion is not, at least up to the first order. Both of them, however, depend on the initial amplitude parameters a_{io}'s, which is one of the typical features in non-linear oscillations.

After a transient period, the response (4.5) approaches a limit state, which can be easily deduced by replacing the exponential terms with zero.

When the damping is absent, the limit process

$$\lim_{\zeta \to 0} \frac{1 - e^{-2\zeta t}}{2\zeta} = t \tag{4.8}$$

can be used, which changes Eqs. (4.5) to yield free *undamped* vibration response given by

$$U(t) = a_{1o} \cos\left[\left\{\nu - \frac{k_1}{2\nu}\left(a_{2o}{}^2 + a_{3o}{}^2\right)\right\}t + \beta_{1o}\right] \tag{4.9. a}$$

$$\begin{aligned} V(t) = {} & a_{2o} \cos\left[\left\{(\omega - \gamma) + \frac{1}{4\omega}\left(-k_2 a_{1o}{}^2 + 2k_3\left\{a_{2o}{}^2 + 2a_{3o}{}^2\right\}\right)\right\}t + \beta_{2o}\right] \\ & + a_{3o} \cos\left[\left\{(\omega + \gamma) + \frac{1}{4\omega}\left(-k_2 a_{1o}{}^2 + 2k_3\left\{2a_{2o}{}^2 + a_{3o}{}^2\right\}\right)\right\}t + \beta_{3o}\right] \end{aligned} \tag{4.9. b}$$

$$\begin{aligned} W(t) = {} & a_{2o} \sin\left[\left\{(\omega - \gamma) + \frac{1}{4\omega}\left(-k_2 a_{1o}{}^2 + 2k_3\left\{a_{2o}{}^2 + 2a_{3o}{}^2\right\}\right)\right\}t + \beta_{2o}\right] \\ & - a_{3o} \sin\left[\left\{(\omega + \gamma) + \frac{1}{4\omega}\left(-k_2 a_{1o}{}^2 + 2k_3\left\{2a_{2o}{}^2 + a_{3o}{}^2\right\}\right)\right\}t + \beta_{3o}\right] \end{aligned} \tag{4.9. c}$$

It may be noted that the longitudinal vibration (4.9. a) is purely harmonic with the frequency of

$$\nu_1 = \nu - \frac{k_1}{2\nu}\left(a_{2o}{}^2 + a_{3o}{}^2\right) \tag{4.10}$$

while the two transverse vibrations are quasi-periodic with the frequencies of

$$\begin{cases} \omega_1 = \omega - \gamma + \frac{1}{4\omega}\left\{-k_2 a_{1o}{}^2 + 2k_3\left(a_{2o}{}^2 + 2a_{3o}{}^2\right)\right\} \\ \omega_2 = \omega + \gamma + \frac{1}{4\omega}\left\{-k_2 a_{1o}{}^2 + 2k_3\left(2a_{2o}{}^2 + a_{3o}{}^2\right)\right\} \end{cases} \tag{4.11}$$

4.2 Averaging with a Single Variable

In the case of small nominal tension, which is usual condition for short tethered satellite systems in the station-keeping phase, the transverse frequency parameter ω is small so that the corresponding time variable $2\omega t$ is no longer fast-varying. Hence, it cannot play a role as an averaging variable in the method of averaging.

The longitudinal frequency parameter ν, however, is still high and νt is acceptable as an averaging variable. Taking an average on the phase space equation (3.16) over a period 2π with the fast varying time νt only, one has

$$\begin{bmatrix} \dot{a}_1 \\ a_1\dot{\beta}_1 \\ \dot{a}_2 \\ a_2\dot{\beta}_2 \\ \dot{a}_3 \\ a_3\dot{\beta}_3 \end{bmatrix} = \frac{1}{2\pi}\int_0^{2\pi} \begin{bmatrix} \text{R.H.S} \\ \text{of} \\ \text{Eq. (3.16)} \end{bmatrix} d(\nu t) \tag{4.12}$$

which results in the following approximate phase-space form:

$$\begin{bmatrix} \dot{a}_1 \\ a_1\dot{\beta}_1 \\ \dot{a}_2 \\ a_2\dot{\beta}_2 \\ \dot{a}_3 \\ a_3\dot{\beta}_3 \end{bmatrix} = \begin{bmatrix} -\zeta a_1 \\ -\frac{k_1}{2v} a_1 \left\{a_2^{\,2} + a_3^{\,2} + 2a_2a_3\cos[2\omega t + \beta_2 + \beta_3]\right\} \\ \frac{1}{2\omega}\left\{-\frac{1}{2}k_2a_1^{\,2} + k_3\left(a_2^{\,2} + a_3^{\,2} + 2a_2a_3\cos[2\omega t + \beta_2 + \beta_3]\right)\right\} \\ \quad \times \left\{a_3 \sin[2\omega t + \beta_2 + \beta_3]\right\} \\ \frac{1}{2\omega}\left\{-\frac{1}{2}k_2a_1^{\,2} + k_3\left(a_2^{\,2} + a_3^{\,2} + 2a_2a_3\cos[2\omega t + \beta_2 + \beta_3]\right)\right\} \\ \quad \times \left\{a_2 + a_3\cos[2\omega t + \beta_2 + \beta_3]\right\} \\ \frac{1}{2\omega}\left\{-\frac{1}{2}k_2a_1^{\,2} + k_3\left(a_2^{\,2} + a_3^{\,2} + 2a_2a_3\cos[2\omega t + \beta_2 + \beta_3]\right)\right\} \\ \quad \times \left\{a_2 \sin[2\omega t + \beta_2 + \beta_3]\right\} \\ \frac{1}{2\omega}\left\{-\frac{1}{2}k_2a_1^{\,2} + k_3\left(a_2^{\,2} + a_3^{\,2} + 2a_2a_3\cos[2\omega t + \beta_2 + \beta_3]\right)\right\} \\ \quad \times \left\{a_2\cos[2\omega t + \beta_2 + \beta_3] + a_3\right\} \end{bmatrix} \tag{4.13}$$

Eq. (4.13) is a set of coupled ordinary differential equations with six dependent variables. By introducing a new variable of compound phase, $\eta = 2\omega t + \beta_2 + \beta_3$, it is possible to divide Eq. (4.13) into a set of core ordinary differential equations involving three dependent variables a_2, a_3, and η

$$\dot{a}_2 = \frac{1}{2\omega}\left\{-\frac{1}{2}k_2a_1^{\,2} + k_3\left(a_2^{\,2} + a_3^{\,2} + 2a_2a_3\cos\eta\right)\right\}\cdot a_3 \sin\eta \tag{4.14. a}$$

$$\dot{a}_3 = \frac{1}{2\omega}\left\{-\frac{1}{2}k_2a_1^{\,2} + k_3\left(a_2^{\,2} + a_3^{\,2} + 2a_2a_3\cos\eta\right)\right\}\cdot a_2 \sin\eta \tag{4.14. b}$$

$$a_2a_3\dot{\eta} = 2\omega a_2a_3 + \frac{1}{2\omega}\left\{-\frac{1}{2}k_2a_1^{\,2} + k_3\left(a_2^{\,2} + a_3^{\,2} + 2a_2a_3\cos\eta\right)\right\} \times \left\{2a_2a_3 + \left(a_2^{\,2} + a_3^{\,2}\right)\cos\eta\right\} \tag{4.14. c}$$

and the following supplementary equations.

$$a_1 = a_{1o}e^{-\zeta t} \tag{4.15. a}$$

$$\begin{cases} \beta_1 = -\frac{k_1}{2v}\int_0^t (a_2^2 + a_3^2 + 2a_2 a_3 \cos\eta)dt + \beta_{1o} \\ \beta_2 = \frac{1}{2\omega}\int_0^t \left[\left\{-\frac{1}{2}k_2 a_1^2 + k_3(a_2^2 + a_3^2 + 2a_2 a_3 \cos\eta)\right\}\cdot\left\{1 + \frac{a_3}{a_2}\cos\eta\right\}\right]dt + \beta_{2o} \\ \beta_3 = \frac{1}{2\omega}\int_0^t \left[\left\{-\frac{1}{2}k_2 a_1^2 + k_3(a_2^2 + a_3^2 + 2a_2 a_3 \cos\eta)\right\}\cdot\left\{\frac{a_2}{a_3}\cos\eta + 1\right\}\right]dt + \beta_{3o} \end{cases}$$

..... (4.15. b)

where β_{io}'s are constants of integration.

Eq. (4.15. a) gives the longitudinal amplitude as an exponential function of time and completes Eqs. (4.14) as a set of simultaneous ordinary differential equations that govern the phase-space response. In general, since a_1 is a function of time, Eqs. (4.14) are non-autonomous so that their general solution requires the use of numerical means. In some restricted cases, however, it can be solved analytically to yield the steady state response. After solving Eqs. (4.14) the phase angle variables β_i's can be determined by integrating Eq. (4.15. b).

4.3 Steady State Solution

The steady state of a dynamical system can be characterized as a state in which the system repeats a certain kind of regular motion. In the phase-space, the steady state is identified as a stationary point. Hence, the steady state solution can be obtained by solving the equations governing the phase-space for their stationary solution.

When damping is absent, the longitudinal amplitude a_1 becomes a constant a_{1o} determined from the initial conditions and plays a role as a constant parameter in Eqs. (4.14), which become an autonomous set of ordinary differential equations of the form

$$\dot{a}_2 = \frac{1}{2\omega}\left\{-\tfrac{1}{2}k_2 a_{1o}{}^2 + k_3\left(a_2{}^2 + a_3{}^2 + 2a_2 a_3 \cos\eta\right)\right\}\cdot a_3 \sin\eta \equiv f_1(a_2, a_3, \eta) \tag{4.16. a}$$

$$\dot{a}_3 = \frac{1}{2\omega}\left\{-\tfrac{1}{2}k_2 a_{1o}{}^2 + k_3\left(a_2{}^2 + a_3{}^2 + 2a_2 a_3 \cos\eta\right)\right\}\cdot a_2 \sin\eta \equiv f_2(a_2, a_3, \eta) \tag{4.16. b}$$

$$a_2 a_3 \dot{\eta} = 2\omega a_2 a_3 + \frac{1}{2\omega}\left\{-\tfrac{1}{2}k_2 a_1{}^2 + k_3\left(a_2{}^2 + a_3{}^2 + 2a_2 a_3 \cos\eta\right)\right\} \times \left\{2a_2 a_3 + \left(a_2{}^2 + a_3{}^2\right)\cos\eta\right\} \equiv f_3(a_2, a_3, \eta) \tag{4.16. c}$$

The above set of equations governs the phase-space of the undamped system. It can be expected that the set of Eqs. (4.16) contains some stationary solutions that determine the steady state solutions of the system.

In steady state, the principal variables of Eqs. (4.16), a_2, a_3, and η, have no variation with time and respectively become constants, a_{2s}, a_{3s}, and η_s, such that they satisfy the following algebraic equations:

$$0 = \frac{1}{2\omega}\left\{-\tfrac{1}{2}k_2 a_{1o}{}^2 + k_3\left(a_{2s}{}^2 + a_{3s}{}^2 + 2a_{2s}a_{3s}\cos\eta_s\right)\right\}\cdot a_{3s}\sin\eta_s \tag{4.17. a}$$

$$0 = \frac{1}{2\omega}\left\{-\tfrac{1}{2}k_2 a_{1o}{}^2 + k_3\left(a_{2s}{}^2 + a_{3s}{}^2 + 2a_{2s}a_{3s}\cos\eta_s\right)\right\}\cdot a_{2s}\sin\eta_s \tag{4.17. b}$$

$$0 = 2\omega a_{2s}a_{3s} + \frac{1}{2\omega}\left\{-\tfrac{1}{2}k_2 a_{1o}{}^2 + k_3\left(a_{2s}{}^2 + a_{3s}{}^2 + 2a_{2s}a_{3s}\cos\eta_s\right)\right\} \times \left\{2a_{2s}a_{3s} + \left(a_{2s}{}^2 + a_{3s}{}^2\right)\cos\eta_s\right\} \tag{4.17. c}$$

Since the degenerate case in which both a_{2s} and a_{3s} are zero should be avoided, Eqs. (4.17. a, b) suggest

$$\sin\eta_s = 0 \quad \rightarrow \quad \eta_s = \begin{cases} 0 \\ \pi \end{cases} \tag{4.18}$$

Substituting the above values into Eq. (4.17. c) and solving for a_{1o}^2, one obtains the steady state condition in the phase-space:

$$a_{1o}^2 = \frac{2}{k_2}\left\{k_3(a_{2s} \pm a_{3s})^2 \pm \frac{4\omega^2 a_{2s}a_{3s}}{(a_{2s} \pm a_{3s})^2}\right\} \tag{4.19}$$

where the positive and negative signs correspond to $\eta_s = 0$ and π, respectively. Of course, one can choose the bracketed term in Eqs. (4.17. a, b) to be zero as another possibility. Eq. (4.17. c) then forces either a_{2s} or a_{3s} to be zero, and the corresponding solution is also included in the steady state condition of Eq. (4.19).

Using the condition (4.19), the phase angle variables can be obtained from Eq. (4.15. b) to be as follows:

$$\begin{cases} \beta_1 = -\frac{k_1}{2\nu}(a_{2s} \pm a_{3s})^2 t + \beta_{1o} \\ \beta_2 = -\frac{2\omega(\pm a_{3s})}{a_{2s} \pm a_{3s}} t + \beta_{2o} \\ \beta_3 = -\frac{2\omega a_{2s}}{a_{2s} \pm a_{3s}} t + \beta_{3o} \end{cases} \tag{4.20}$$

where β_{io}'s are constants of integration such that $\beta_{2o} + \beta_{3o} = \eta_s = \begin{cases} 0 \\ \pi \end{cases}$.

By inserting both the phase angle variables β_i's of Eq. (4.20) and the steady amplitude variables into Eq. (3.12) and then replacing β_{3o} with $\eta_s - \beta_{2o}$, the response of the steady state in the discretized coordinates becomes

$$U_s(t) = a_{1o}\cos\left[\left\{\nu - \frac{k_1}{2\nu}(a_{2s} \pm a_{3s})^2\right\}t + \beta_{1o}\right] \tag{4.21. a}$$

$$V_s(t) = (a_{2s} \pm a_{3s}) cos\left[\left\{\frac{a_{2s} \mp a_{3s}}{a_{2s} \pm a_{3s}}\omega - \gamma\right\}t + \beta_{2o}\right] \tag{4.21. b}$$

$$W_s(t) = (a_{2s} \pm a_{3s}) sin\left[\left\{\frac{a_{2s} \mp a_{3s}}{a_{2s} \pm a_{3s}}\omega - \gamma\right\}t + \beta_{2o}\right] \tag{4.21. c}$$

The expressions of Eqs. (4.21. b, c) for the transverse motion can be interpreted as a circular whirling motion of the tether about its longitudinal axis(skip-rope mode) though the longitudinal oscillation also exists. It is interesting to note that the steady transverse vibrations have a characteristic of monofrequency, which could not be expected in linear theory.

In order to verify the stability of the steady states, let us introduce the disturbance variables, α_2, α_3, and ξ, such that

$$\begin{cases} a_2 = a_{2s} + \alpha_2 \\ a_3 = a_{3s} + \alpha_3 \\ \eta = \eta_s + \xi \end{cases} \tag{4.22}$$

By applying Eq. (4.22) to the autonomous set of Eqs. (4.16) and taking series expansions up to the first order about the steady state, the following disturbance equation is obtained in matrix form:

$$\begin{bmatrix} \dot{\alpha}_2 \\ \dot{\alpha}_3 \\ \dot{\xi} \end{bmatrix} = \left[\frac{\partial(f_1 \quad f_2 \quad f_3)}{\partial(a_2 \quad a_3 \quad \eta)}\bigg|_s\right] \begin{bmatrix} \alpha_2 \\ \alpha_3 \\ \xi \end{bmatrix} \tag{4.23}$$

where the specific expression for the coefficient matrix is

$$\left[\frac{\partial(f_1 \quad f_2 \quad f_3)}{\partial(a_2 \quad a_3 \quad \eta)}\bigg|_s\right]=\begin{bmatrix} 0 & 0 & -\frac{2\omega a_{2s}a_{3s}^2}{(a_{2s}\pm a_{3s})^2} \\ 0 & 0 & -\frac{2\omega a_{2s}^2 a_{3s}}{(a_{2s}\pm a_{3s})^2} \\ \frac{k_3}{\omega}(\pm a_{2s}+a_{3s})^3+2\omega a_{3s}\frac{-a_{2s}\pm a_{3s}}{a_{2s}\pm a_{3s}} & \frac{k_3}{\omega}(a_{2s}\pm a_{3s})^3+2\omega a_{2s}\frac{\pm a_{2s}-a_{3s}}{\pm a_{2s}+a_{3s}} & 0 \end{bmatrix}$$

..... (4.24)

The characteristic of solutions of the disturbance equation (4.23) governs stability of the steady state. It mainly depends on the eigenvalues of the coefficient matrix (4.24). If one of the real parts of the eigenvalues has a positive value, the solution of Eq. (4.23) would diverge, and the steady state would be unstable. If all of the real parts are negative, then the solution of Eq. (4.23) would go to zero and the steady state would be stable. If all the real parts are zero, then the steady state would belong to neutral stability.

The three eigenvalues of the coefficient matrix (4.24) are calculated to be

$$\begin{Bmatrix} 0 \\ i\left\{2k_3(a_{2s}\pm a_{3s})^2+\left(2\omega\cdot\frac{a_{2s}\mp a_{3s}}{a_{2s}\pm a_{3s}}\right)^2\right\}^{\frac{1}{2}} \\ -i\left\{2k_3(a_{2s}\pm a_{3s})^2+\left(2\omega\cdot\frac{a_{2s}\mp a_{3s}}{a_{2s}\pm a_{3s}}\right)^2\right\}^{\frac{1}{2}} \end{Bmatrix} \qquad (4.25)$$

The real parts of all the eigenvalues are zero. It means that the circular whirling steady state response has neutral stability under the condition of no damping.

4.4 Limit Steady State Solution

The limit steady state is a steady state after a long time when the transient response decays out. If there exists a limit steady state in the system, then it should satisfy certain conditions.

According to Eq. (4.15. a), the longitudinal amplitude variable a_1 would decay to zero. If the system approaches the steady state such that the phase-space variables, a_2, a_3, and η, approach steady values, $a_{2\infty}$, $a_{3\infty}$, and η_∞, respectively, their first derivatives with respect to time would vanish. Then, the equation set (4.14) produces algebraic equations for the limit steady state as follows:

$$0 = \frac{k_3}{2\omega}\left\{a_{2\infty}^{\,2} + a_{3\infty}^{\,2} + 2a_{2\infty}a_{3\infty}\cos\eta_\infty\right\}\cdot a_{3\infty}\sin\eta_\infty \qquad (4.26.\text{ a})$$

$$0 = \frac{k_3}{2\omega}\left\{a_{2\infty}^{\,2} + a_{3\infty}^{\,2} + 2a_{2\infty}a_{3\infty}\cos\eta_\infty\right\}\cdot a_{2\infty}\sin\eta_\infty \qquad (4.26.\text{ b})$$

$$0 = 2\omega a_{2\infty}a_{3\infty} + \frac{k_3}{2\omega}\left\{a_{2\infty}^{\,2} + a_{3\infty}^{\,2} + 2a_{2\infty}a_{3\infty}\cos\eta_\infty\right\}\cdot\left\{2a_{2\infty}a_{3\infty} + \left(a_{2\infty}^{\,2} + a_{3\infty}^{\,2}\right)\cos\eta_\infty\right\}$$

..... (4.26. c)

It can be seen at a glance that Eqs. (4.26) are identical to the set of algebraic equations (4.17) for the steady state when the a_{1o} terms are dropped off and the subscript s is substituted by ∞. Hence, the limit values of the amplitude parameters must satisfy Eq. (4.19) with $a_{1o} = 0$, i.e.,

$$0 = k_3\left(a_{2\infty} \pm a_{3\infty}\right)^2 \pm \frac{4\omega^2 a_{2\infty}a_{3\infty}}{\left(a_{2\infty} \pm a_{3\infty}\right)^2} \qquad (4.27)$$

Since the amplitude variables are non-negative, it is apparent that the case corresponding to the positive (+) signs in Eq. (4.27) is not valid, i.e. only the case corresponding to the negative (−) signs must be chosen, which, from Eq. (4.18), means that η_∞ goes to π only. Therefore, the first condition for the limit steady state becomes

$$\begin{cases} \eta_{\infty} = \pi \\ \dfrac{(a_{2\infty} - a_{3\infty})^4}{a_{2\infty} a_{3\infty}} = \dfrac{4\omega^2}{k_3} \end{cases} \tag{4.28}$$

Multiplying Eq. (4.14. a) and Eq. (4.14. b) by a_3 and a_2, respectively, and then subtracting, one obtains

$$a_2 \dot{a}_2 - a_3 \dot{a}_3 = 0 \tag{4.29}$$

which is valid at all times. The left-hand side of the above equation is an exact differential form, so the integration of Eq. (4.29) yields the second condition for the limit steady state:

$$a_{2\infty}{}^2 - a_{3\infty}{}^2 = a_{2o}{}^2 - a_{3o}{}^2 \tag{4.30}$$

where a_{2o} and a_{3o} are constants determined from the initial conditions.

Eqs. (4.28) and (4.30) constitute the two algebraic equations to determine the two limit values $a_{2\infty}$ and $a_{3\infty}$. It should be noted that the compound phase, η, has only a single value π for the limit steady state instead of 0 and π for the steady state.

Under these conditions, Eq. (4.15. b) leads to the asymptotic form of the phase angle variables

$$\begin{cases} \beta_2 \rightarrow 2\omega \dfrac{a_{2\infty}}{a_{2\infty} - a_{3\infty}} t + \beta_{\infty} \\ \beta_3 \rightarrow -2\omega \dfrac{a_{2\infty}}{a_{2\infty} - a_{3\infty}} t - \beta_{\infty} + \pi \end{cases} \qquad \text{as} \quad t \rightarrow \infty \tag{4.31}$$

in which β_{∞} is a constant of integration but it is not determined directly from the initial conditions because Eq. (4.31) is an asymptotic expression. Substituting the above phase angles and the amplitudes determined by Eqs. (4.28) and (4.30) into Eqs. (3.12) results in the response of the limit steady state as follows:

$$U_{-}(t) = 0 \tag{4.32. a}$$

$$V_{-}(t) = (a_{2-} - a_{3-})\cos\left[\left\{\frac{a_{2-} + a_{3-}}{a_{2-} - a_{3-}}\omega - \gamma\right\}t + \beta_{-}\right] \tag{4.32. b}$$

$$W_{-}(t) = (a_{2-} - a_{3-})\sin\left[\left\{\frac{a_{2-} + a_{3-}}{a_{2-} - a_{3-}}\omega - \gamma\right\}t + \beta_{-}\right] \tag{4.32. c}$$

The above response of the limit steady state is similar to that of the steady state of Eqs. (4.21). The two transverse components produce a perfectly circular motion in a plane. Since the longitudinal motion decays out to zero, the entire tether motion in the limit steady state can be interpreted as circular whirling.

Verification of stability for the limit steady state solution follows a similar procedure as that for the steady state solution in the previous section. Unlike the case of no damping when Eq. (4.14) is autonomous, it is non-autonomous in the present case. To get an autonomous set of equations, let us modify Eq. (4.15. a) to a differential form. Then, Eqs. (4.15. a) and (4.14) constitute an autonomous set of

$$\begin{cases} \dot{a}_1 = -\zeta a_1 \equiv g_1(a_1, a_2, a_3, \eta) \\ \dot{a}_2 = g_2(a_1, a_2, a_3, \eta) \\ \dot{a}_3 = g_3(a_1, a_2, a_3, \eta) \\ a_2 a_3 \dot{\eta} = g_4(a_1, a_2, a_3, \eta) \end{cases} \tag{4.33}$$

where g_2, g_3, and g_4 represent the expressions in the right hand sides of Eqs. (4.14), respectively. The stationary values of Eq. (4.33) are the limit steady state values $(0, a_{2-}, a_{3-}, \pi)$.

The disturbance variables, α_1, α_2, α_3, and ξ, are defined as

$$\begin{cases} a_1 = 0 + \alpha_1 = \alpha_1 \\ a_2 = a_{2_\infty} + \alpha_2 \\ a_3 = a_{3_\infty} + \alpha_3 \\ \eta = \pi + \xi \end{cases} \tag{4.34}$$

Substituting Eq. (4.34) into the autonomous set of Eq. (4.33) and taking a series expansion up to the first order about the limit steady state values, one obtains the perturbation equations in the matrix form:

$$\begin{bmatrix} \dot{\alpha}_1 \\ \dot{\alpha}_2 \\ \dot{\alpha}_3 \\ \dot{\xi} \end{bmatrix} = \left[\frac{\partial(g_1 \quad g_2 \quad g_3 \quad g_4)}{\partial(a_1 \quad a_2 \quad a_3 \quad \eta)}\bigg|_\infty \right] \begin{bmatrix} \alpha_1 \\ \alpha_2 \\ \alpha_3 \\ \xi \end{bmatrix} \tag{4.35}$$

where the coefficient matrix is

$$\left[\frac{\partial(g_1 \quad g_2 \quad g_3 \quad g_4)}{\partial(a_1 \quad a_2 \quad a_3 \quad \eta)}\bigg|_\infty \right] = \begin{bmatrix} -\zeta & 0 & 0 & 0 \\ 0 & 0 & 0 & -\frac{k_3}{2\omega} a_{3_\infty} (a_{2_\infty} - a_{3_\infty})^2 \\ 0 & 0 & 0 & -\frac{k_3}{2\omega} a_{2_\infty} (a_{2_\infty} - a_{3_\infty})^2 \\ 0 & -\frac{2k_3}{\omega} \frac{(a_{2_\infty} - a_{3_\infty})^3}{a_{2_\infty} a_{3_\infty}} + \frac{2\omega}{a_{2_\infty}} & \frac{2k_3}{\omega} \frac{(a_{2_\infty} - a_{3_\infty})^3}{a_{2_\infty} a_{3_\infty}} + \frac{2\omega}{a_{3_\infty}} & 0 \end{bmatrix}$$

..... (4.36)

Examining matrix (4.36), it can easily be seen that the perturbation equation (4.35) can be decoupled such that

$$\dot{\alpha}_1 = -\zeta \alpha_1 \tag{4.37. a}$$

$$\begin{bmatrix} \dot{\alpha}_2 \\ \dot{\alpha}_3 \\ \dot{\xi} \end{bmatrix} = \begin{bmatrix} 0 & 0 & -\frac{k_3}{2\omega} a_{3_\infty} (a_{2_\infty} - a_{3_\infty})^2 \\ 0 & 0 & -\frac{k_3}{2\omega} a_{2_\infty} (a_{2_\infty} - a_{3_\infty})^2 \\ -\frac{2k_3}{\omega} \frac{(a_{2_\infty} - a_{3_\infty})^3}{a_{2_\infty} a_{3_\infty}} + \frac{2\omega}{a_{2_\infty}} & \frac{2k_3}{\omega} \frac{(a_{2_\infty} - a_{3_\infty})^3}{a_{2_\infty} a_{3_\infty}} + \frac{2\omega}{a_{3_\infty}} & 0 \end{bmatrix} \begin{bmatrix} \alpha_2 \\ \alpha_3 \\ \xi \end{bmatrix}$$

..... (4.37. b)

Eq. (4.37. a) tells us that the disturbance variable α_1 decays out and therefore the longitudinal limit steady state value 0 is stable. The stability for the other variables is determined by the eigenvalues of the coefficient matrix in Eq. (4.37. b). The three eigenvalues are

$$\begin{cases} 0 \\ i\left[k_3\left(a_{2\infty}-a_{3\infty}\right)^2\left\{2+\dfrac{\left(a_{2\infty}+a_{3\infty}\right)^2}{a_{2\infty}a_{3\infty}}\right\}\right]^{\frac{1}{2}} \\ -i\left[k_3\left(a_{2\infty}-a_{3\infty}\right)^2\left\{2+\dfrac{\left(a_{2\infty}+a_{3\infty}\right)^2}{a_{2\infty}a_{3\infty}}\right\}\right]^{\frac{1}{2}} \end{cases} \tag{4.38}$$

in which all the real parts of the eigenvalues are zero. Hence, it can be concluded that the limit steady state values, $a_{2\infty}$, $a_{3\infty}$, and π, of the two transverse amplitude variables and compound phase angle, respectively, have neutral stability.

Chapter 5

NUMERICAL INVESTIGATION

The introduction of the phase-space variables a_i's and β_i's, onto which the discretized coordinates of the system are mapped by the Van der Pol transformation, has led to the phase-space formulation and allowed us to examine the system in an analytical manner. In some cases it is possible to obtain closed form results as was seen in the previous chapter. The analytical results, however, are restricted to a limited number of cases and in general the analysis of the phase-space formulation needs augmentation by a numerical method.

From the closed form results for the system responses such as Eqs. (4.9), (4.21), and (4.32), it can easily be observed that the phase angle variables β_i's increase to large values with time t. It is not easy in that case to grasp the characteristics of the system response obtained from numerical analysis. For better understanding, the following variables are introduced:

$$\begin{cases} q_i = a_i \cos\beta_i \\ p_i = a_i \sin\beta_i \end{cases} \qquad i = 1,2,3 \tag{5.1}$$

The above is a sort of transformation from the polar coordinates of the phase-space variables (a_i, β_i) to the rectangular coordinates (q_i, p_i). Using Eqs. (5.1) and (3.12), the response of the tether motion in the configuration-space can be represented as:

$$U(t) = q_1 \cos \nu t - p_1 \sin \nu t \tag{5.2. a}$$

$$V(t) = q_2 \cos(\omega-\gamma)t - p_2 \sin(\omega-\gamma)t + q_3 \cos(\omega+\gamma)t - p_3 \sin(\omega+\gamma)t \quad (5.2.\ b)$$

$$W(t) = p_2 \cos(\omega-\gamma)t + q_2 \sin(\omega-\gamma)t - p_3 \cos(\omega+\gamma)t - q_3 \sin(\omega+\gamma)t \quad (5.2.\ c)$$

In the q_i - p_i plane each method discussed in the previous chapter leads to a distinct feature. When damping is absent, a response of the linear approximation is represented as a point, because both the amplitude and the phase angle variables are constant. The results from the averaging with two variables, on the other hand, appear as a circle whose radius is equal to the constant amplitude as the phase angle variables vary with time. In the case of averaging with a single variable, a variety of shapes show up in q_i - p_i plane and they are dependent upon the system parameters such as the nominal tension, longitudinal stiffness, initial conditions, and so on.

Several cases have been investigated numerically. Since the present work considers the vibration of the fundamental mode of the tether whose ends are fixed, the half sine function has been used for the shape functions, φ and ϑ. It vanishes at both ends so that it satisfies the conditions for the admissible function. Values of the system parameters and the initial conditions for each case are shown in Table 5.1. The results of the linear approximation are calculated from Eqs. (3.12) with constant parameters. The results of the averaging with two variables are obtained from Eqs. (4.5). In the case of averaging with a single variable, calculations are based on a set of first order ordinary differential equations (4.14) and the expression (4.15. a) for the longitudinal amplitude. After solving them, the phase angle variables are integrated by (4.15. b) and the response is obtained. For the numerical solutions, the second order ordinary differential equations (3.9) are integrated directly.

Through the first three cases, results from the four methods — the linear approximation, averaging with two variables, averaging with a single variable, and numerical — are compared with each other. Values of the nominal tension vary from reasonably high to very low. As expected, the longitudinal modes reveal higher frequency

oscillations than the transverse modes and they are not much affected by variations in the nominal tension. As shown in Figs. 5.1 (a) ~ 5.3 (a), all the four methods yield almost the same response for the longitudinal motion such that the four curves in each graph look like one. For this reason, the linear approximation can be regarded to be accurate enough for representing the longitudinal mode.

In transverse modes, however, the response with the linear approximation deviates significantly from those of the other methods even in the high nominal tension of case 1. Responses from both the averaging with a single variable and the direct numerical integration show pretty good agreement with each other such that it is hard to distinguish between them in Figs. 5.1 (b, c) ~ 5.3 (b, c). Since the solutions from the direct numerical integration are thought to be exact, it can be said that averaging with a single variable gives sufficient accuracy to analyze the system behavior properly even in the case of low nominal tension.

Results obtained by averaging over two variables are in good agreement with those of the averaging with a single variable and the numerical method in the case of high tension, but they deviates from the exact as the tension decreases. These tendencies can be observed in Figs. 5.4 ~ 5.6 as well. When the tension is high the phase diagrams in q_i - p_i plane obtained from averaging with a single variable look like circles as shown in Figs. 5.4 (d) and (f). As discussed earlier, these responses can be interpreted as those obtained from averaging with two variables. As the tension goes down to a low value, diagrams in q_i - p_i plane deviate from circles showing a lot of fringes in Figs. 5.5 (d, f) and 5.6 (d, f), so averaging with two variables cannot be thought to be accurate any more. Nevertheless, averaging with two variables can be used to analyze high tension systems quite efficiently because it is possible to derive a closed form solution.

Investigation of the steady state mentioned in section 4.3 has been conducted through cases 4 ~ 10. Values for the initial amplitude parameters a_{io}'s are chosen so as to

satisfy the steady state condition (4.19). It can be observed that only positive (+) sign condition is valid for the steady state condition (4.19) when the steady amplitude parameters a_{2s} and a_{3s} are close to each other. In that case only zero is allowed to be the steady value for the compound phase angle η and the lower and higher frequency components of the transverse mode are in-phase. This is the situation for cases 4 ~ 6, where the sum of β_{2o} and β_{3o} is set to 0 as an initial value of the steady compound phase angle. Without damping the two components of the transverse motion constitute an exact circle as shown in Fig. 5.7 (h), and the response is in perfect agreement with that of the closed form deduced in section 4.3.

When damping is involved, the system shows several interesting features. The damping is modeled as a simplified version of material damping through the longitudinal mode of the motion. So, its primary effect appears in the longitudinal phase-space variables q_1 and p_1, and they decay out such that the curve in q_1 - p_1 plane spirals in toward the origin of the graph as shown in Figs. 5.8 (a) and (b). The damping affects the transverse mode, too, but in a quite different manner. In the beginning the two pairs of the transverse phase-space variables, (q_2, p_2) and (q_3, p_3), decay up to a certain time. The former, starting with a bigger initial amplitude value than the latter, experiences phase change from 0 to π, and after that each element of the (q_2, p_2) pair grows slightly to converge to the limit steady state[Fig. 5.8 (c)]. In q_2 - p_2 phase plane[Fig. 5.8 (d)], the curve spirals in and at a certain instant its direction reverses completely experiencing a phase change. Afterwards, it spirals out to approach a circle whose radius has the value predicted by the limit steady state conditions of Eqs. (4.28) and (4.30) in section 4.4. In contrast, the pair (q_3, p_3) does not experience any phase change but decreases completely to zero magnitude when (q_2, p_2) experiences the phase change. Subsequently it recovers, grows, and converges to the limit steady state[Figs. 5.8 (e, f)]. In configuration-space, the pair of the transverse components (V, W) shows a very similar feature as (q_2, p_2) as presented in Figs. 5.8 (g) and (h). They decay in the beginning, at a certain time the phase

change occurs, and after that the response converges to the limit steady state that is predicted by Eqs. (4.32).

In case 6 the initial values for the transverse mode are reversed with respect to case 5 such that the pair (q_3, p_3) corresponding to the higher frequency content has bigger initial magnitude than (q_2, p_2) corresponding to the lower frequency content. Since the set of differential equations (4.14) in the phase-space formulation by the averaging with a single variable is symmetric between a_2 and a_3, the amplitude variables of the lower and higher frequency contents, respectively, the transverse phase-space results of case 6 must be in reverse order compared to those of case 5. Figure 5.9 shows that the (q_2, p_2) response of case 6 is identical to the (q_3, p_3) response of case 5 and the (q_3, p_3) of case 6 is the same as the (q_2, p_2) of case 5. The response in the configuration-space, however, shows a difference. As opposed to the phase change in case 5, the transverse motion in the configuration-space in case 6 does not experience it, spirals in and approaches the limit steady state without any change of direction. It should be noted that the radius of the circle in Fig. 5.9 (h), to which the trajectory approaches, is identical to that in Fig. 5.8 (h), although the frequencies are different in the two cases. It means that the limit steady state of case 6 is different from that of case 5. It is natural because the initial conditions in the configuration-space are different in the two cases.

When the steady amplitude parameters a_{2s} and a_{3s} are not close to each other, both positive (+) and negative (−) sign conditions are valid in Eq. (4.19). For the positive (+) sign condition the steady value of the compound phase angle should be 0, and hence the two initial phase angle parameters β_{2o} and β_{3o} are chosen such that their sum η_o is 0. This is the case when the lower and the higher frequency components for the transverse mode are in-phase. For the negative (−) sign condition under which the two components of the transverse mode are out-of-phase, the sum should be π. These are examined through cases 7 ~ 10. Without damping, both positive (+) and negative (−) sign conditions lead to circular whirling motions as shown in Figs. 5.10 and 5.12.

In the presence of damping, the system exhibits some interesting features similar to those in cases 5 and 6. Since the damping acts mainly along the longitudinal component of motion, the trajectory in the q_1 - p_1 plane for the longitudinal mode spirals in and decays out in cases of both positive and negative sign conditions[Figs. 5.11 (a, b) and 5.13 (a, b)]. Under the positive sign condition, the component corresponding to the lower frequency of the transverse mode, which starts from a bigger initial magnitude than that of the higher one, decays, experiences phase change, and grows slightly to the limit steady state[Figs. 5.11 (c, d)]. The component corresponding to the higher frequency decays completely to zero without experiencing phase change and recovers to approach the limit steady state[Figs. 5.11 (e, f)]. In the transverse plane of the configuration-space, the motion spirals inward and at a certain point it reverses direction. After that it spirals in continuously to converge to the limit steady state that is predicted by Eqs. (4.32). The response is very similar to that of case 5 which has smaller initial values than the present case[Figs. 5.11 (g, h)].

In contrast, under the negative sign condition when the lower and higher frequency components of the transverse mode are out-of-phase, the response shows some differences compared to the in-phase case. It is examined in case 10. As can be seen in Figs. 5.13 (c) and (e), both components corresponding to the lower and higher frequencies grow to approach the limit steady state values, respectively, without experiencing phase change. It should be noted that this does not imply the energy increment of the transverse mode. It can be seen easily that the higher frequency component (q_3, p_3) increases at a much larger rate than the lower one (q_2, p_2). Since the amplitude of the transverse motion is determined by subtracting the magnitude of higher frequency component from that of lower one while the system approaches the limit steady state of Eqs. (4.32), the amplitude of transverse motion actually decreases, which might be interpreted as the dissipation of energy from the system. In the configuration-space, the transverse motion spirals in monotonically to converge to the limit steady state[Figs. 5.13 (g, h)].

One of the interesting observations is that some initial parameters produce single closed curve in the transverse plane as in Figs. 5.14 (h) and 5.15 (h). A slight disturbance appears, however, around the curve under the very low nominal tension of case 12. The time histories of the responses repeat regularly as seen in Figs. 5.14 (g) and 5.15 (g). This might be interpreted that the transverse modes are periodic. It is certain that they are not results of the steady state from Eqs. (4.16) because the phase-space variables fluctuate[Figs. 5.14 (d, f) ~ 5.15 (d, f)]. Unfortunately, these results could not be predicted in an analytical way.

Several interesting patterns can be observed in the phase-space. These are Figs. 5.16 (d), 5.17 (d), and 5.18 (f). They are all closed curves so that they seem to be periodic, although the transverse modes in the configuration-space show quasi-periodicity. It was observed that they are quite sensitive to the initial conditions. Even a small change in the initial conditions can eliminate these patterns. Further work is needed to analyze them in detail.

Chapter 6

CONCLUSIONS

6.1 Summary of the Findings

This thesis studied non-linear free vibrations of a spinning tether. The tethered system is assumed to be in the station-keeping phase so that the nominal length of the tether remains constant and the tether is forced to spin at a constant rate about its nominal axis. The governing equations of motion were derived using the extended Hamilton's principle, retaining non-linear terms which originate from the geometric non-linearity up to the third order. The equations have been discretized, truncated, and transformed to the phase-space form. The method of averaging made it possible to analyze the phase-space formulation. From the analytical and numerical analyses, the following conclusions can be drawn:

- The linear approximation is adequate to analyze the longitudinal modes but not the transverse modes.
- The method of averaging with two variables is valid when the tethered system has a high nominal tension. This leads to a closed form solution that shows the dependence of the frequency content on the initial amplitude parameters.
- The method of averaging with a single variable is useful for the whole range of nominal tension, especially for very low tension. The corresponding solution predicts the steady state and the limit steady state; in both cases the system shows a circular whirling motion.

- Material damping in the longitudinal mode drives the steady state to the limit steady state.
- General transverse motion is quasi-periodic, but it can be periodic depending on the initial conditions of the system.

6.2 Recommendations for Future Work

There are many possibilities for extension of the present work. Some of them are given below:

- The present work is confined to the case in which both ends of the tether are fixed under the assumption of very large mass of the end-bodies. In general, however, motions of the end-bodies and the tether would affect each other. They should be considered simultaneously.
- The model for material damping in the longitudinal mode is so simple in the present work that some phenomena might be missed. A more rigorous model should be introduced for the damping.
- Interaction between the lower and the higher frequency modes should be considered to include the case of internal resonance.
- The deployment and retrieval phases are part of the mission of a tethered system along with the station-keeping phase. The preset work can be modified for the case of variable nominal length to study the deployment and retrieval phases.

BIBLIOGRAPHY

1. Cron, A. C., *Applications of Tethers in Space*, NASA CP - 2365, June 1983.

2. Penzo, P. A. and Ammann, P. W., *Tethers in Space Handbook*, NASW - 4341, May 1989.

3. Bekey, I., "Tethers Open New Space Options", *Astronautics and Aeronautics*, Vol. 21, No. 4, 1983, pp. 32 - 40.

4. Misra, A. K. and Modi, V. J., "A Survey on the Dynamics and Control of Tethered Satellite Systems", Tethers in Space, *Advances in the Astronautical Sciences*, Vol. 62, 1987, pp. 667 - 720.

5. Beletsky, V. V. and Levin, E. M., "Dynamics of Space Tether Systems", *Advances in the Astronautical Sciences*, Vol. 83, 1993.

6. Von Flotow, A. H., "Some Approximations for the Dynamics of Spacecraft Tethers", *Journal of Guidance, Control, and Dynamics*, Vol. 11, No. 4, July-August 1988, pp. 357 - 364.

7. Pasca, M., Pignataro, M., and Luongo, A., "Three-Dimensional Vibrations of Tethered Satellite Systems", *Journal of Guidance, Control, and Dynamics*, Vol. 14, No. 2, March-April 1991, pp. 312 - 320.

8. Bergamaschi, S., Bonon, F., and Legnami, M., "Spectral Analysis of TSS-1 Vibrations", *Advances in the Astronautical Sciences*, Vol. 85, 1993, pp. 683 - 700.

9. Bergamaschi, S. and Catinaccio, A., "Further Developments in the Harmonic Analysis of TSS-1", *The Journal of the Astronautical Sciences*, Vol. 40, No. 2, April-June 1992, pp. 189 - 201.

10. Luongo, A. and Vestroni, F., "Non-Linear Free Periodic Oscillations of a Tethered Satellite System", *Journal of Sound and Vibration*, Vol. 175, No. 3, 1994, pp. 299 - 315.

11. Lang, D. D., "Operations with Tethered Space Vehicles", Gemini Summary Conference, NASA SP - 138, 1967, pp. 55 - 64.

12. Tyc, G., Vigneron, F. R., and Jablonski, A. M., "Two - Body Space Dynamics Technology Demonstration for the BICEPS Small Satellite Mission", *Canadian Aeronautics and Space Journal*, Vol. 40, No. 1, March 1994, pp. 3 - 9.

13. Quadrelli, B. M. and Lorenzini, E. C., "Dynamics and Stability of a Tethered Centrifuge in Low Earth Orbit", *The Journal of the Astronautical Sciences*, Vol. 40, No. 1, January - March 1992, pp. 3 - 25.

14. Tyc, G. and Han, R. P. S., "Attitude Dynamics Investigation of the OEDIPUS - A Tethered Rocket Payload", *Journal of Spacecraft and Rockets*, Vol. 32, No. 1, January - February 1995, pp. 133 - 141.

15. Tyc, G., Han, R. P. S., Vigneron, F. R., Jablonski, A. M., Modi, V. J., and Misra, A. K., "Dynamics and Stability of a Spinning Tethered Spacecraft with Flexible Appendages", *Advances in the Astronautical Sciences*, Vol. 85, 1993, pp. 877 - 896.

16. Luo, A. C. J., Han, R. P. S., Modi, V. J., Misra, A. K., and Tyc, G., "Stability and Resonant Motion of a Stretched Spinning Tether", *Journal of Guidance, Control and Dynamics*, in press.

17. Nayfeh, A. H. and Mook, D. T., *Nonlinear Oscillations*, John Wiley & Sons, New York, 1979.

18. Nayfeh, A. H., *Introduction to Perturbation Techniques*, John Wiley & Sons, New York, 1981.

19. Lee, E. W., "Non-linear Forced Vibration of a Stretched String", *British Journal of Applied Physics*, Vol. 8, October 1957, pp. 411 - 413.

20. Oplinger, D. W., "Frequency Response of a Nonlinear Stretched String", *The Journal of the Acoustical Society of America*, Vol. 32, No. 12, December 1960, pp. 1529 - 1538.

21. Murthy, G. S. S. and Ramakrishna, B. S., "Nonlinear Character of Resonance in Stretched Strings", *The Journal of the Acoustical Society of America*, Vol. 38, 1965, pp. 461 - 471.

22. Miles, J. W., "Stability of Forced Oscillations of a Vibrating String", *The Journal of the Acoustical Society of America*, Vol. 38, 1965, pp. 855 - 861.

23. Anand, G. V., "Large-Amplitude Damped Free Vibration of a Stretched String", *The Journal of the Acoustical Society of America*, Vol. 45, No. 5, 1969, pp. 1089 - 1096.

24. Eller, A. I., "Driven Nonlinear Oscillations of a String", *The Journal of the Acoustical Society of America*, Vol. 51, No. 3 (Part 2), 1972, pp. 960 - 966.

25. Miles, J., "Resonant, Nonplanar Motion of a Stretched String", *The Journal of the Acoustical Society of America*, Vol. 75, No. 5, May 1984, pp. 1505 - 1510.

26. Johnson, J. M. and Bajaj, A. K., "Amplitude Modulated and Chaotic Dynamics in Resonant Motion of Strings", *Journal of Sound and Vibration*, Vol. 128, No. 1, 1989, pp. 87 - 107.

27. Bajaj, A. K. and Johnson, J. M., "Asymptotic Techniques and Complex Dynamics in Weakly Non-Linear Forced Mechanical Systems", *International Journal of Non-Linear Mechanics*, Vol. 25, No. 2/3, 1990, pp. 211 - 226.

28. O'Reilly, O. and Holmes, P. J., "Non-Linear, Non-Planar and Non-Periodic Vibrations of a String", *Journal of Sound and Vibration*, Vol. 153, No. 3, 1992, pp. 413 - 435.

29. Tyc, G., Whitehead, W. R., Phillips, J. L., Pierson, J. G., Jablonski, A. M., and Vigneron, F. R., "Design, Qualification and Calibration of the Tether Force Sensor (TFS) for the OEDIPUS - C Mission", *Fourth International Conference on Tethers in Space*, Washington D.C., 10 -14 April, 1995.

30. Butenin, N. V., *Elements of the Theory of Nonlinear Oscillations*, Blaisdell, New York, 1965.

31. Meirovitch, L., *Computational Methods in Structural Dynamics*, Sijthoff & Noordhoff, Rockville, 1980.

TABLES

case	figure	EA [N]	N_o [N]	γ	ζ	a_{1o} a_{2o} a_{3o}	β_{1o} β_{2o} β_{3o}	remark
1	5.1 5.4	4000.	100.	0.05	0.	0.010 0.020 0.013	0 0 0	
2	5.2 5.5	4000.	10.	0.05	0.	0.010 0.020 0.013	0 0 0	
3	5.3 5.6	4000.	1.	0.05	0.	0.010 0.020 0.013	0 0 0	
4	5.7	4000.	1.	0.05	0.	0.03396 0.020 0.013	0 0 0	steady IC (+)
5	5.8	4000.	1.	0.05	0.001	0.03396 0.020 0.013	0 0 0	steady IC (+)
6	5.9	4000.	1.	0.05	0.001	0.03396 0.013 0.020	0 0 0	steady IC (+)
7	5.10	4000.	1.	0.05	0.	0.05347 0.040 0.013	0 0 0	steady IC (+)
8	5.11	4000.	1.	0.05	0.001	0.05347 0.040 0.013	0 0 0	steady IC (+)
9	5.12	4000.	1.	0.05	0.	0.02316 0.040 0.013	0 $2\pi/3$ $\pi/3$	steady IC (-)
10	5.13	4000.	1.	0.05	0.001	0.02316 0.040 0.013	0 $2\pi/3$ $\pi/3$	steady IC (-)
11	5.14	4000.	1.	0.05	0.	0.0291 0.020 0.013	0 0 0	
12	5.15	4000.	0.1	0.05	0.	0.02705 0.020 0.013	0 0 0	
13	5.16	4000.	1.	0.05	0.	0.01055 0.020 0.013	0 0 0	
14	5.17	4000.	1.	0.05	0.	0.031 0.020 0.013	0 0 0	
15	5.18	4000.	1.	0.05	0.	0.033 0.020 0.013	0 0 0	

Table 5.1 Physical and initial parameters

FIGURES

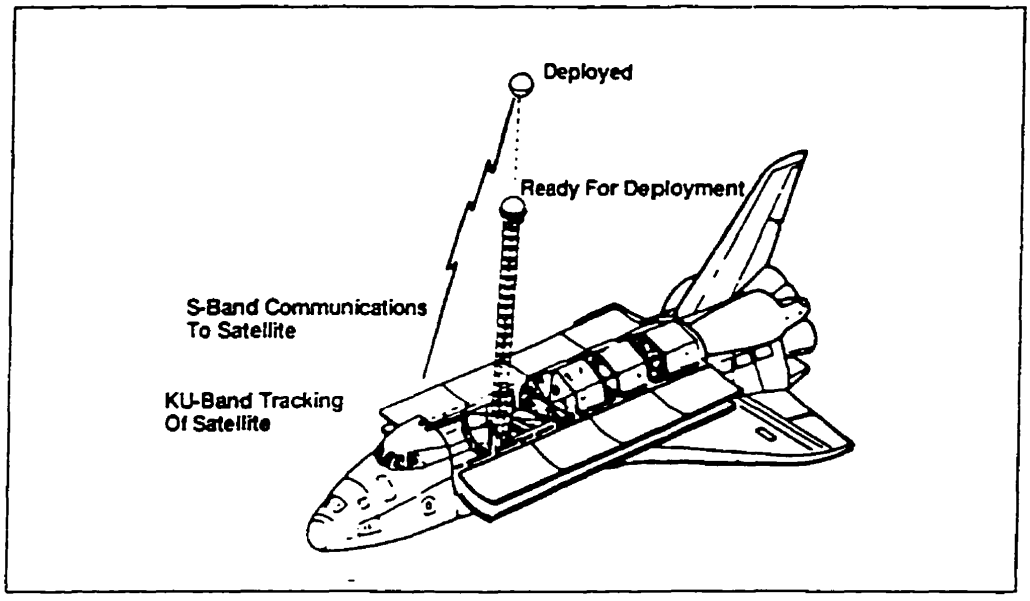

Figure 1.1 TSS-1 Satellite and Tether Attached to 12 meter Extendable Boom(Penzo and Ammann[2])

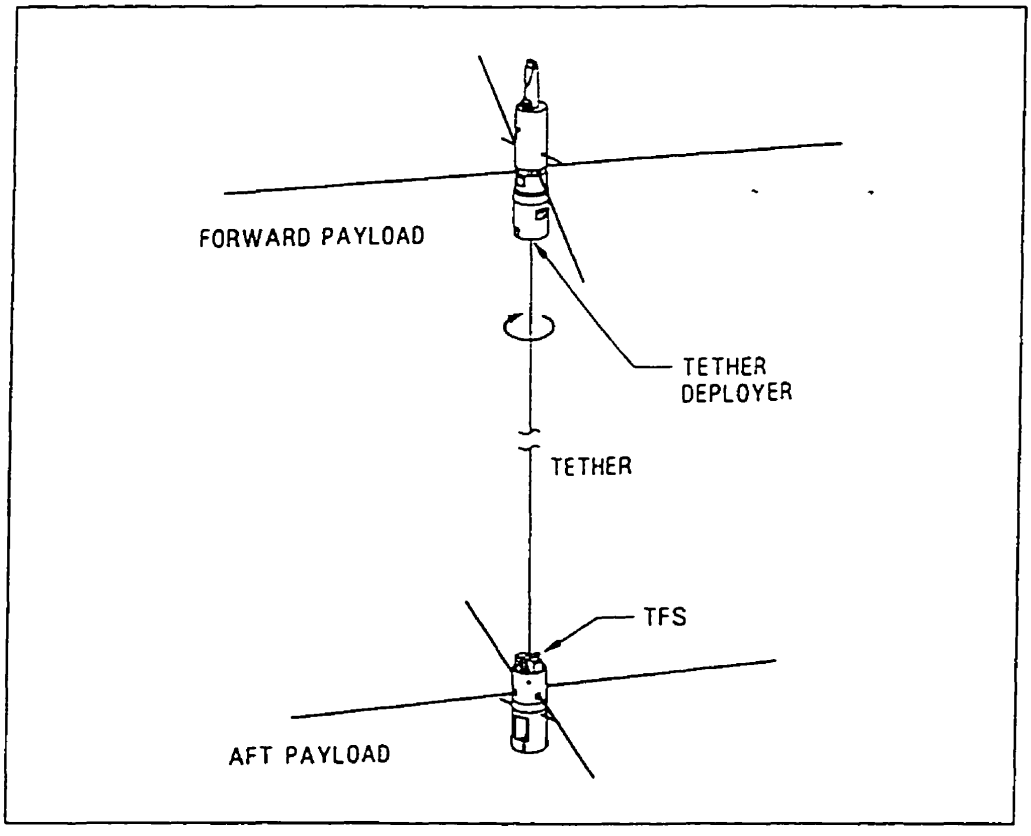

Figure 1.2 OEDIPUS-C Configuration(Tyc et al.[29])

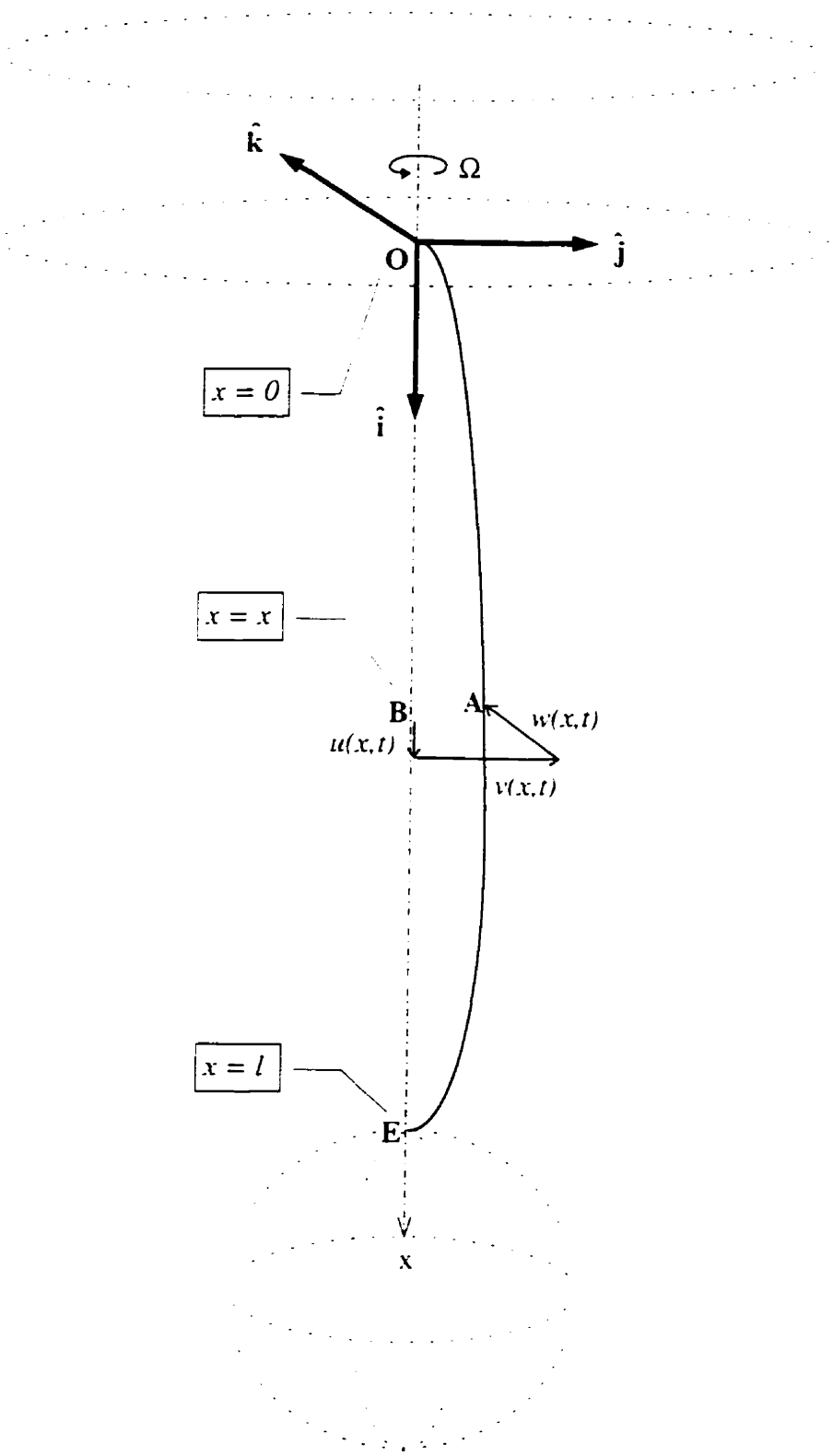

Figure 2.1 A spinning tethered satellite system

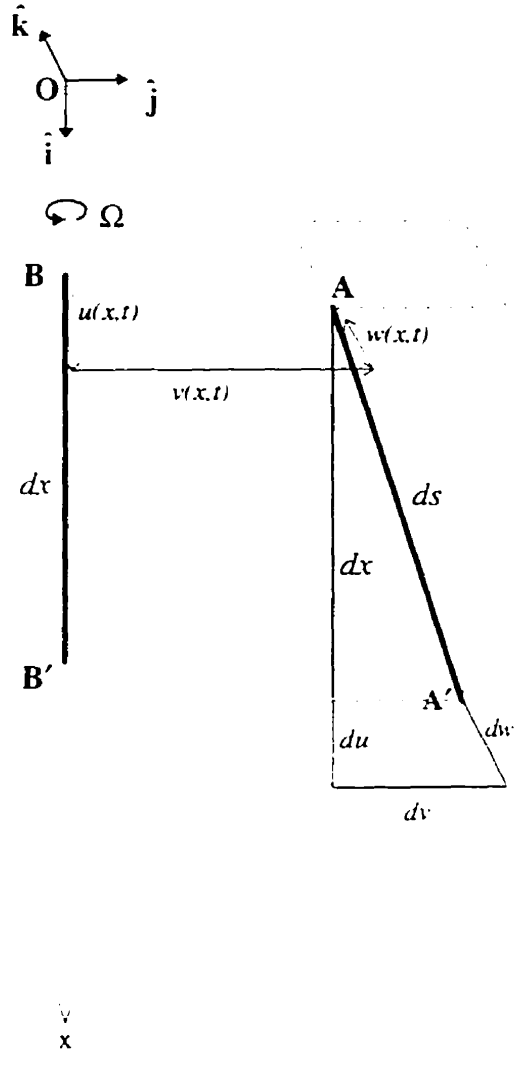

Figure 2.2 Elements of the tether

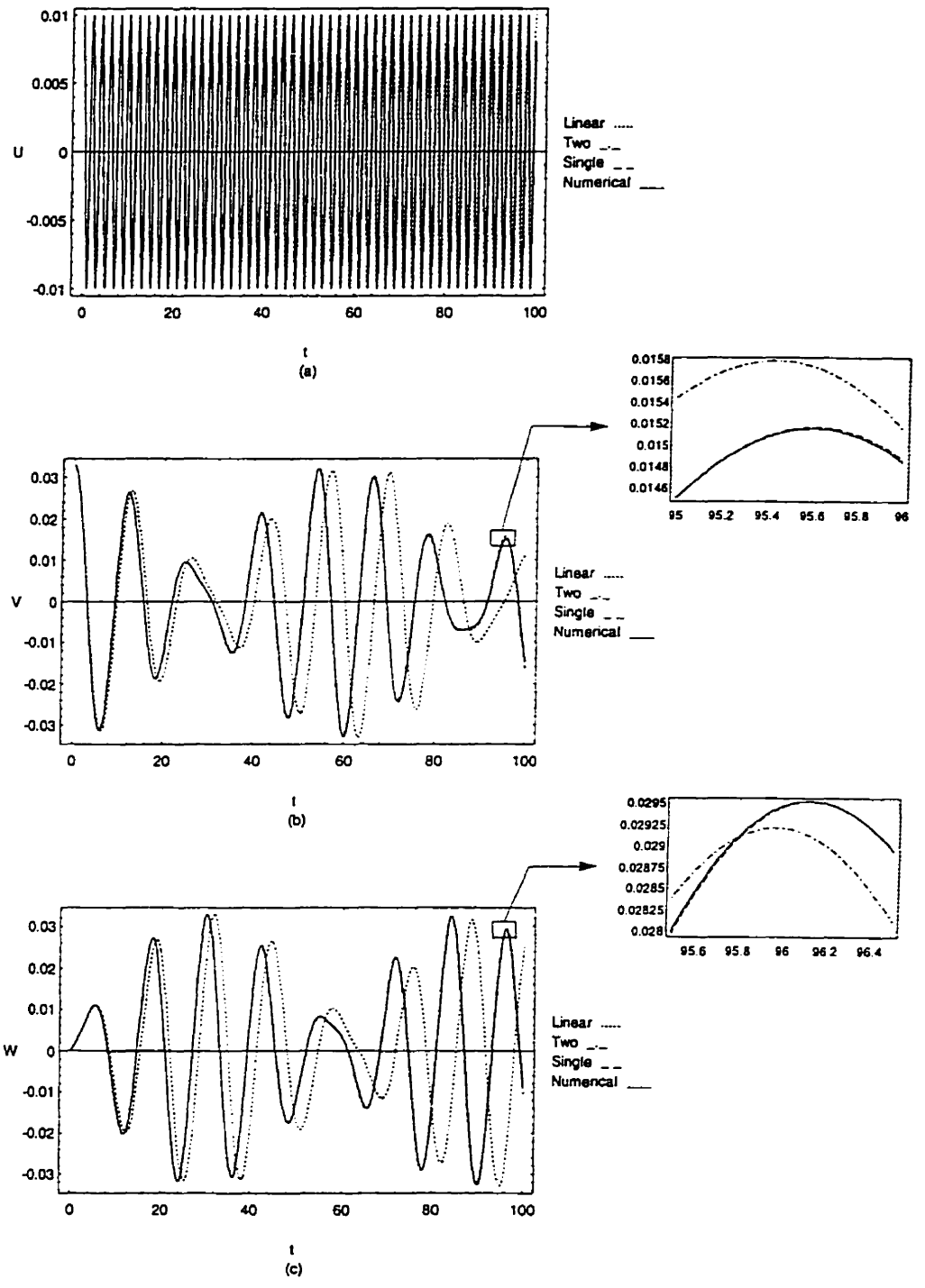

Figure 5.1 Longitudinal and transverse motions in high nominal tension

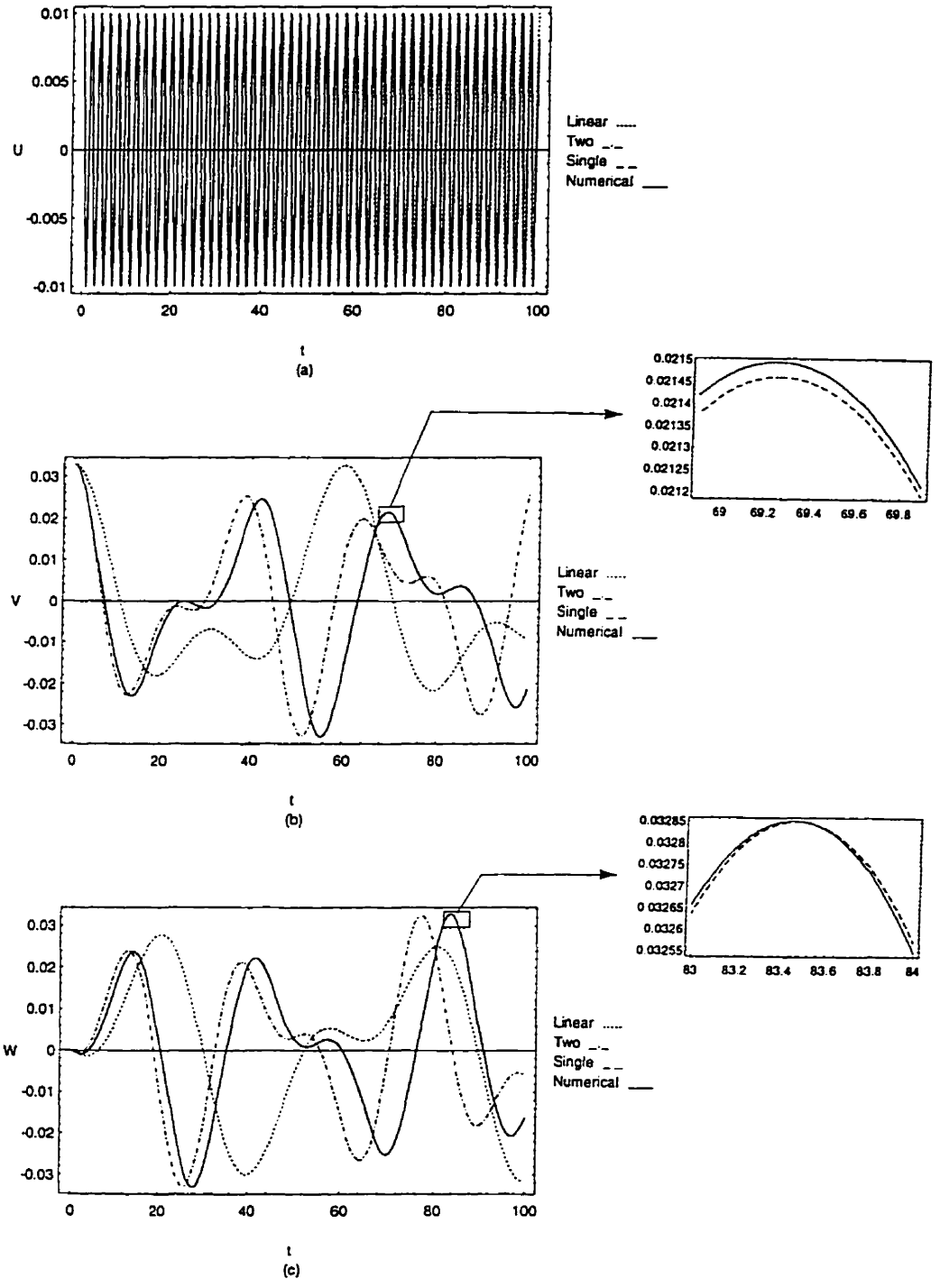

Figure 5.2 Longitudinal and transverse motions in medium nominal tension

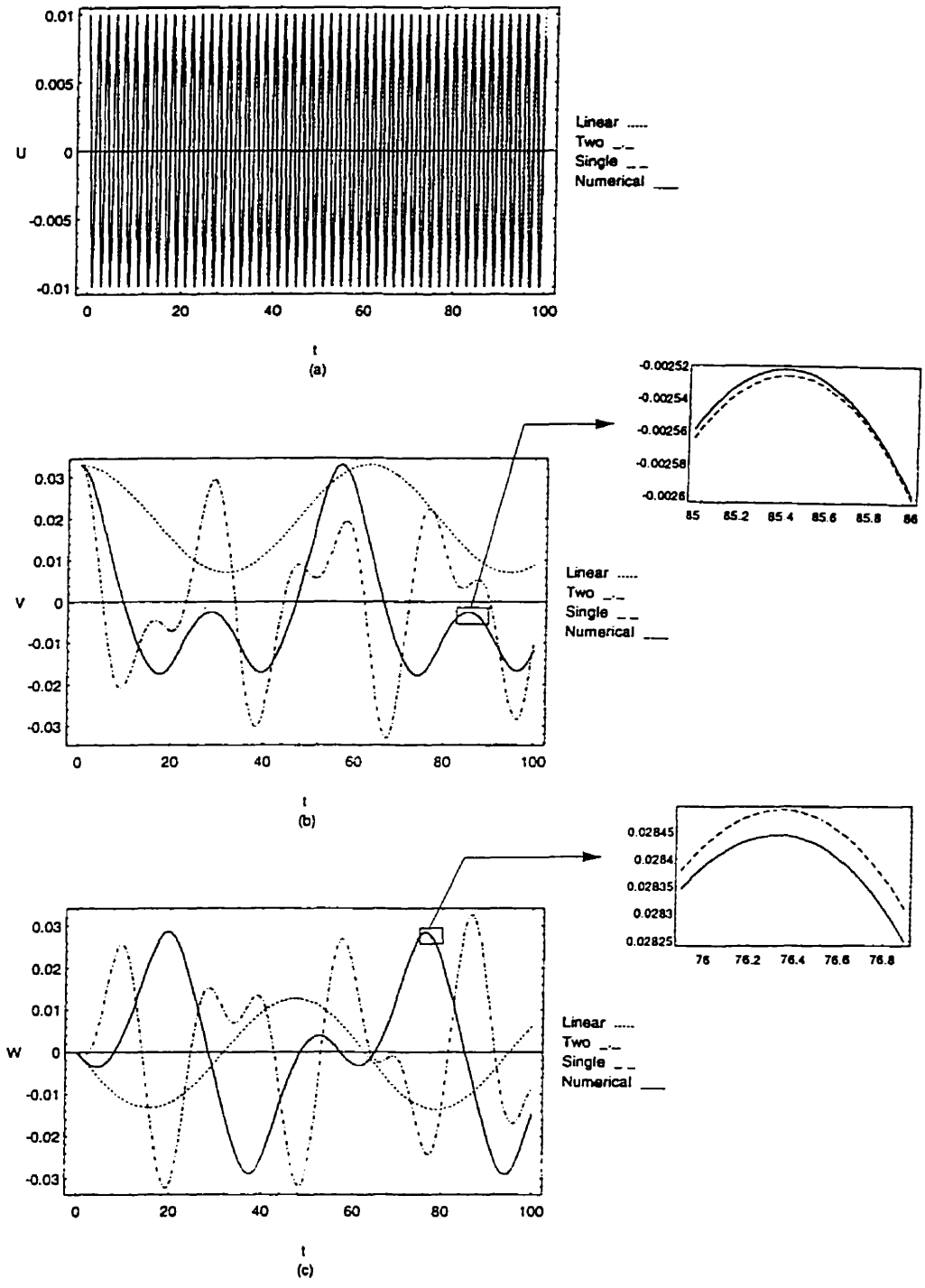

Figure 5.3 Longitudinal and transverse motions in low nominal tension

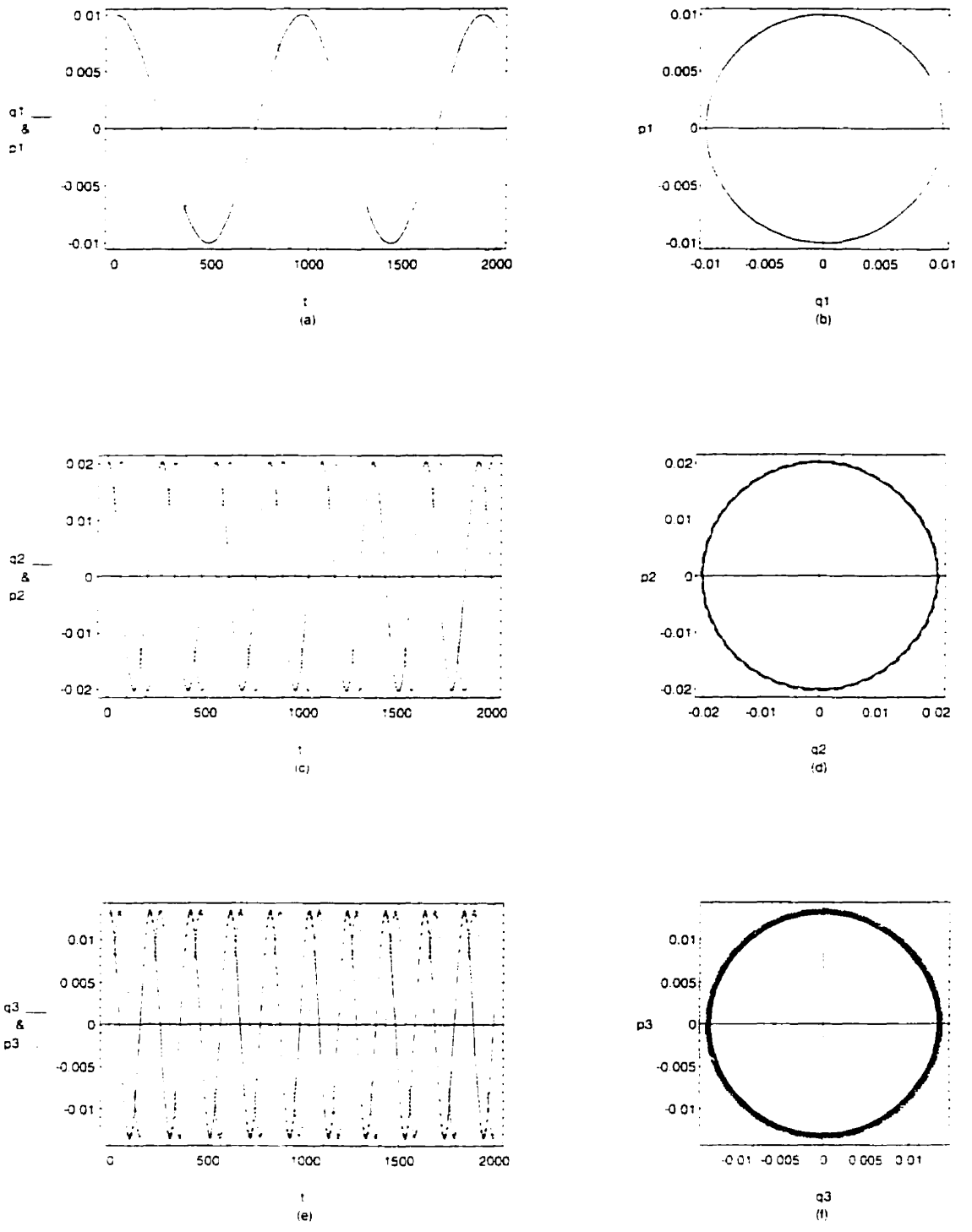

Figure 5.4 Phase-space response and transverse motion in high nominal tension [case 1]

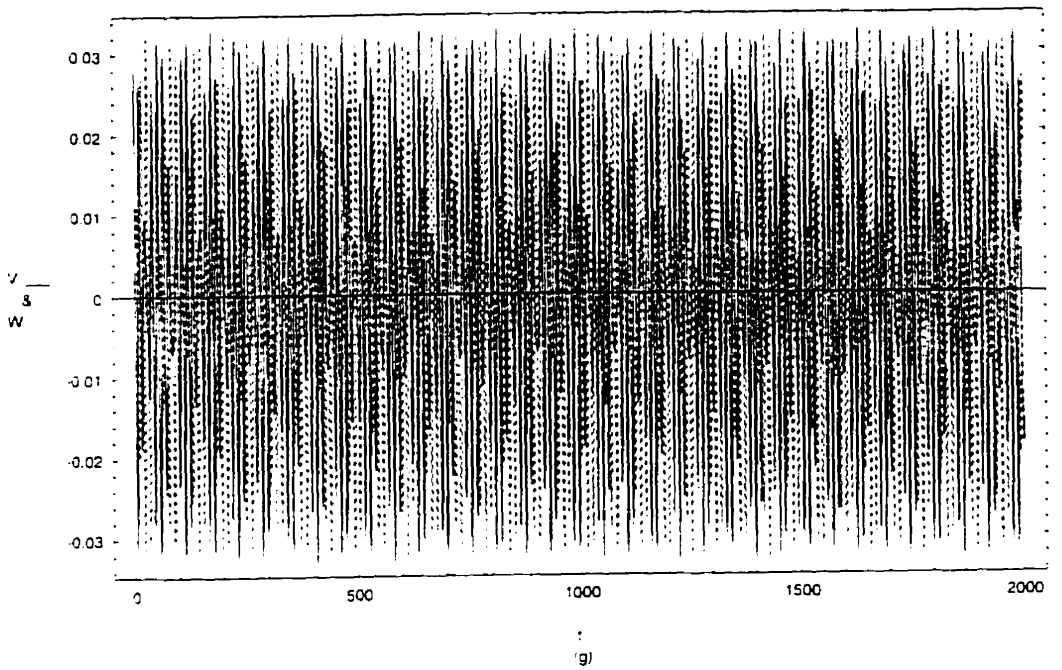

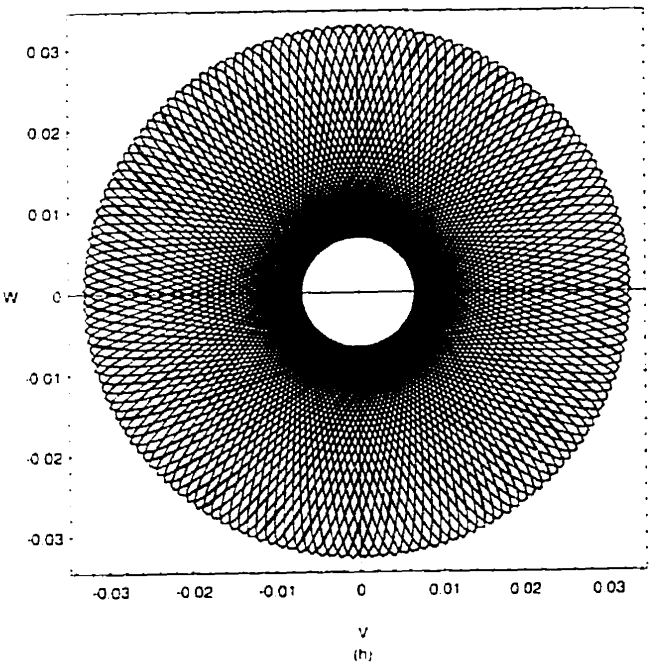

Figure 5.4 (continued)

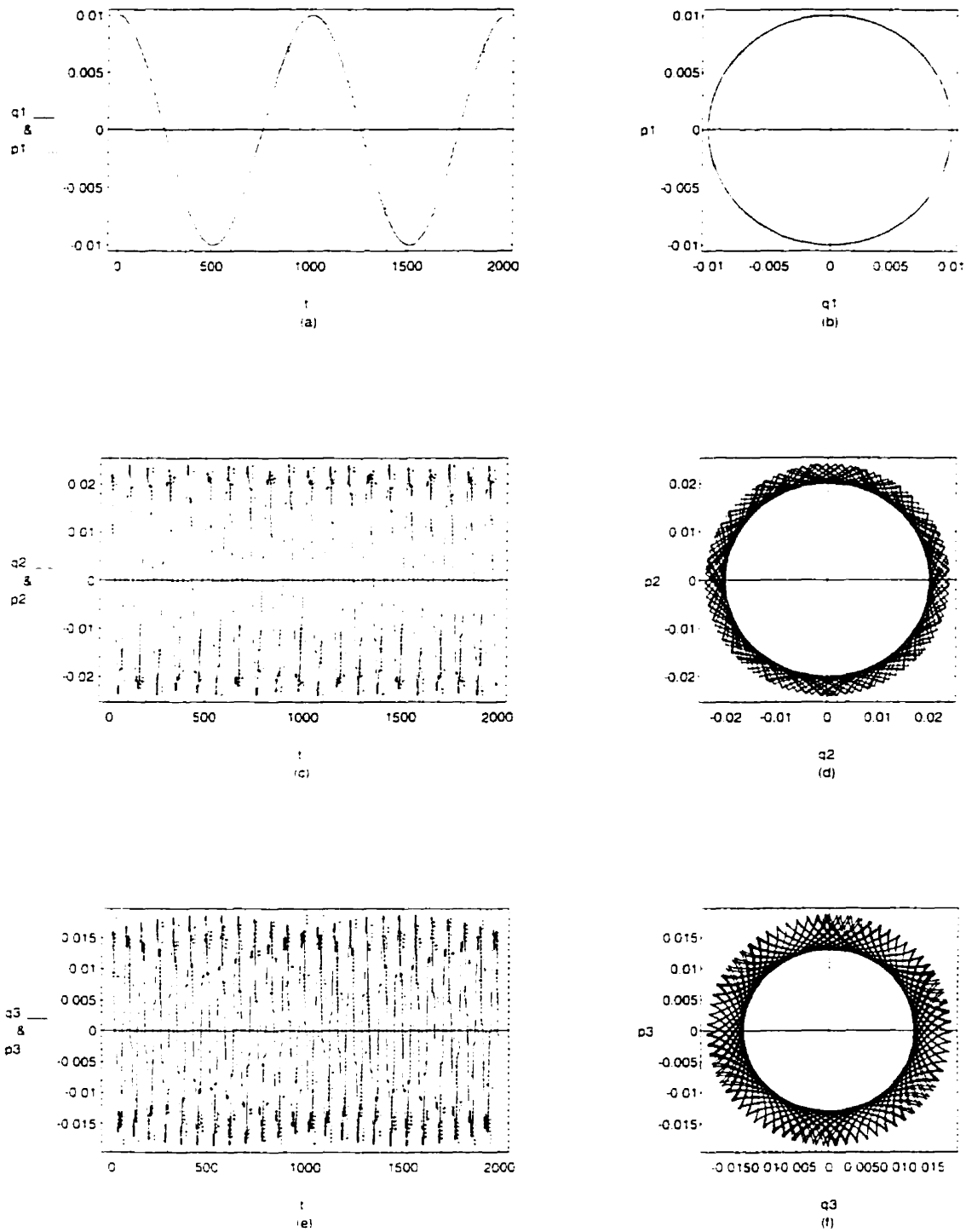

Figure 5.5 Phase-space response and transverse motion in medium nominal tension [case 2]

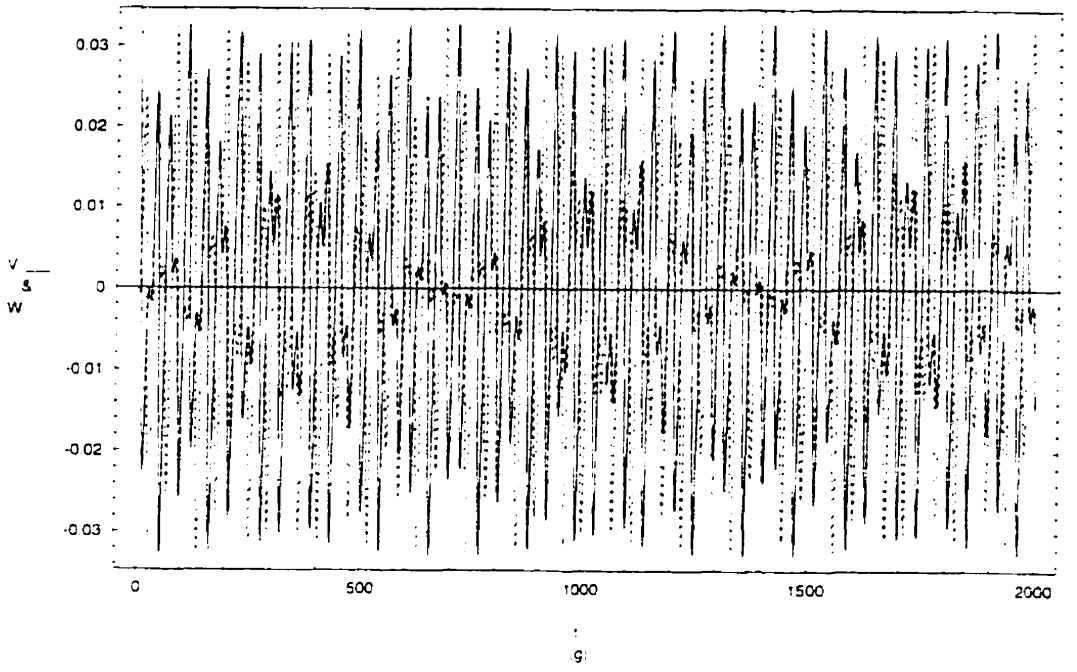

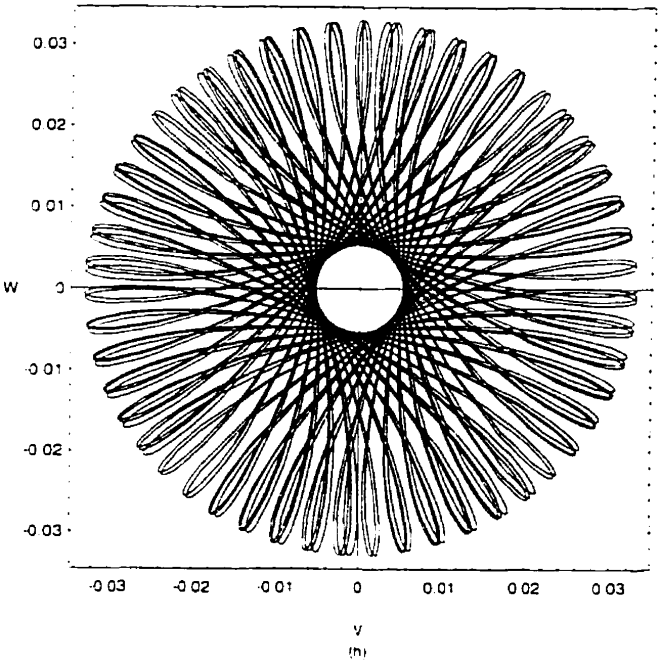

Figure 5.5 (continued)

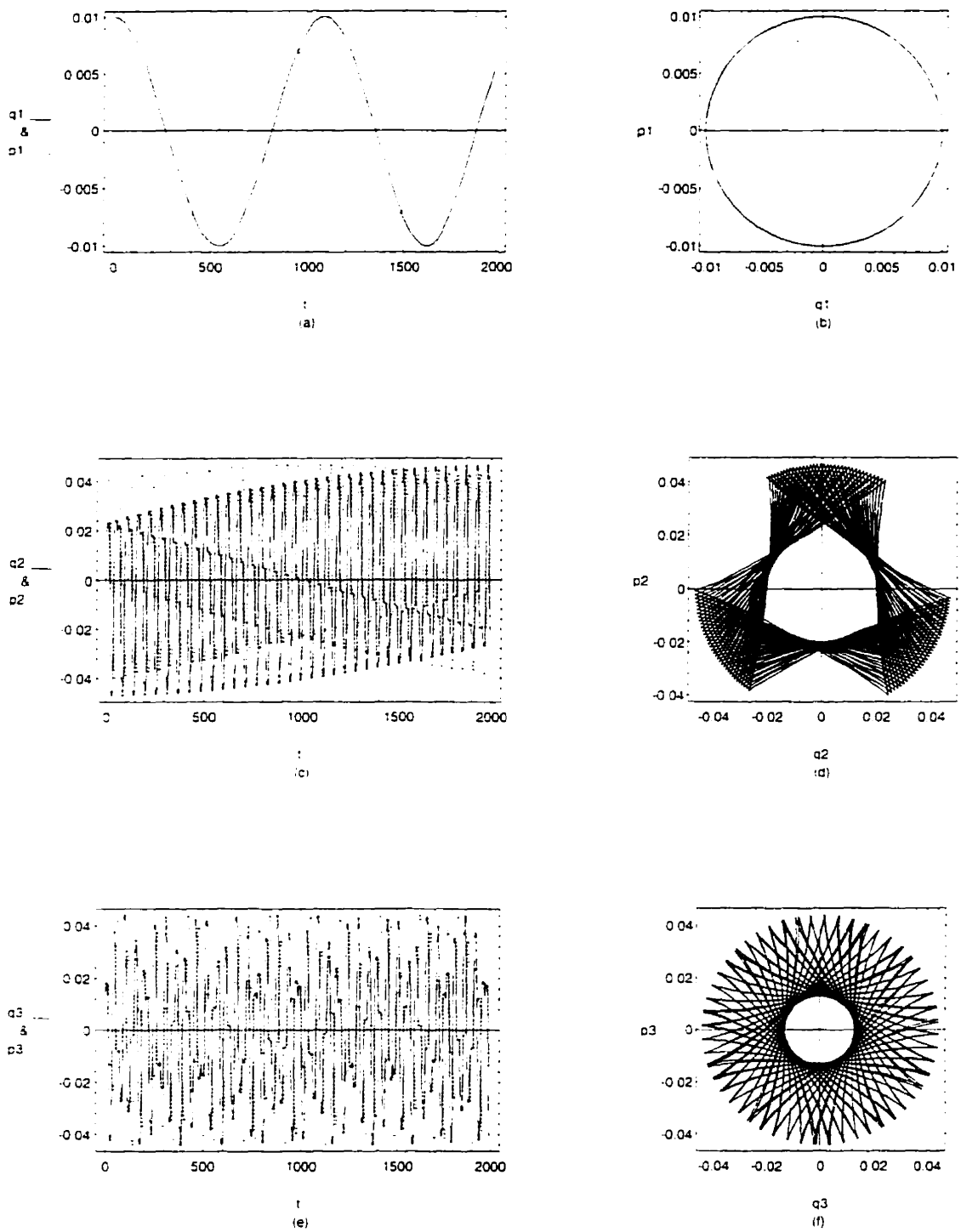

Figure 5.6 Phase-space response and transverse motion in low nominal tension [case 3]

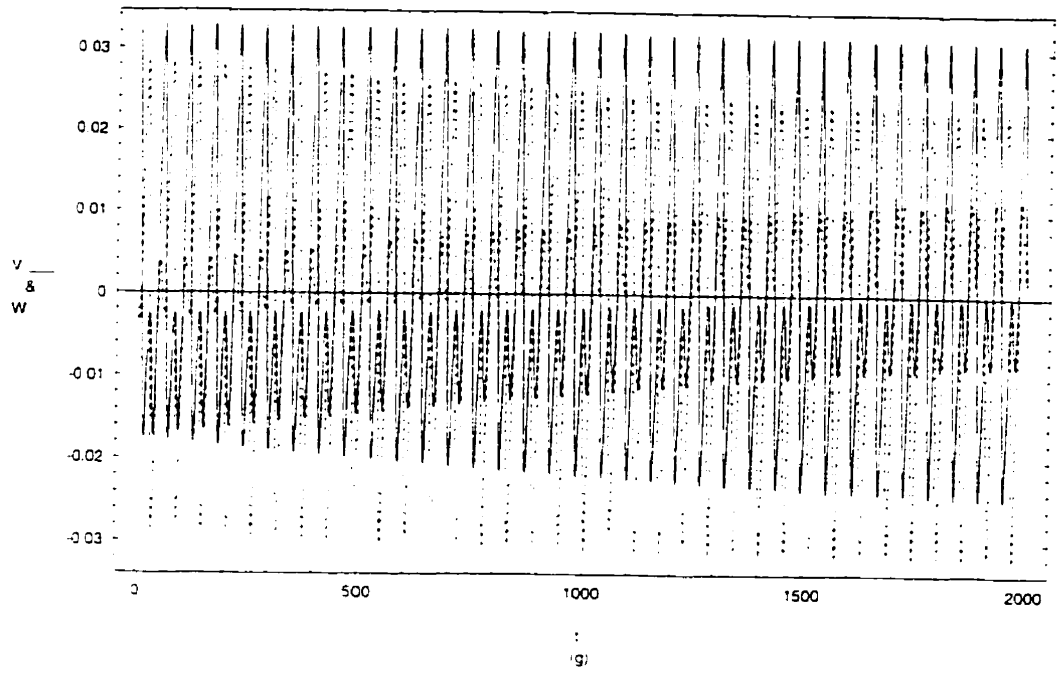

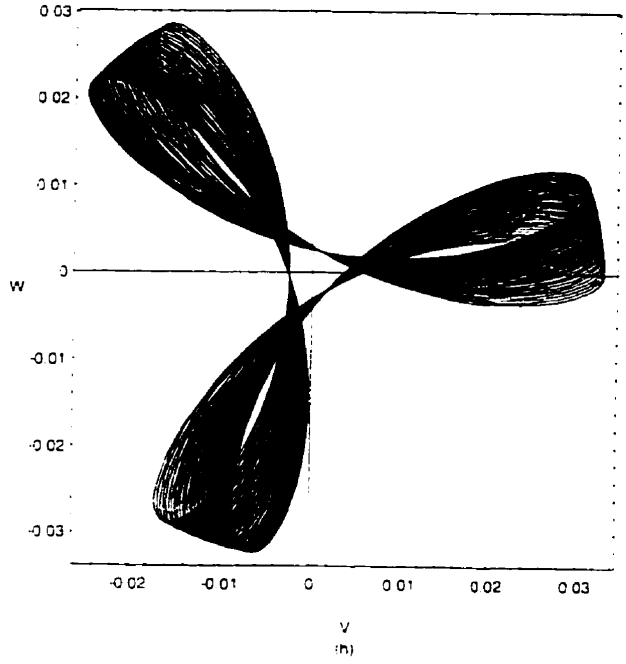

Figure 5.6 (continued)

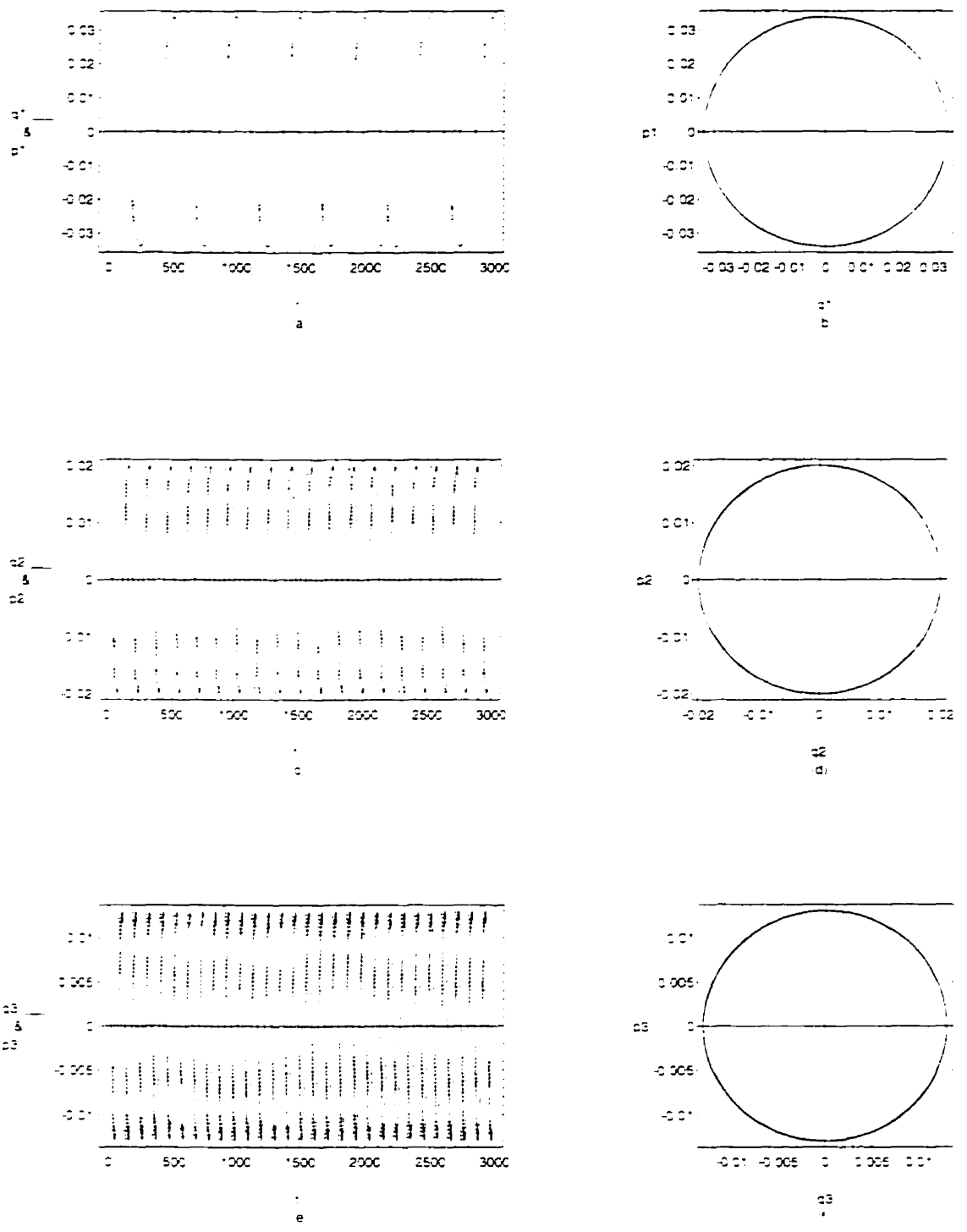

Figure 5.7 Phase-space response and transverse motion in steady state I.C.(+) without damping [case 4]

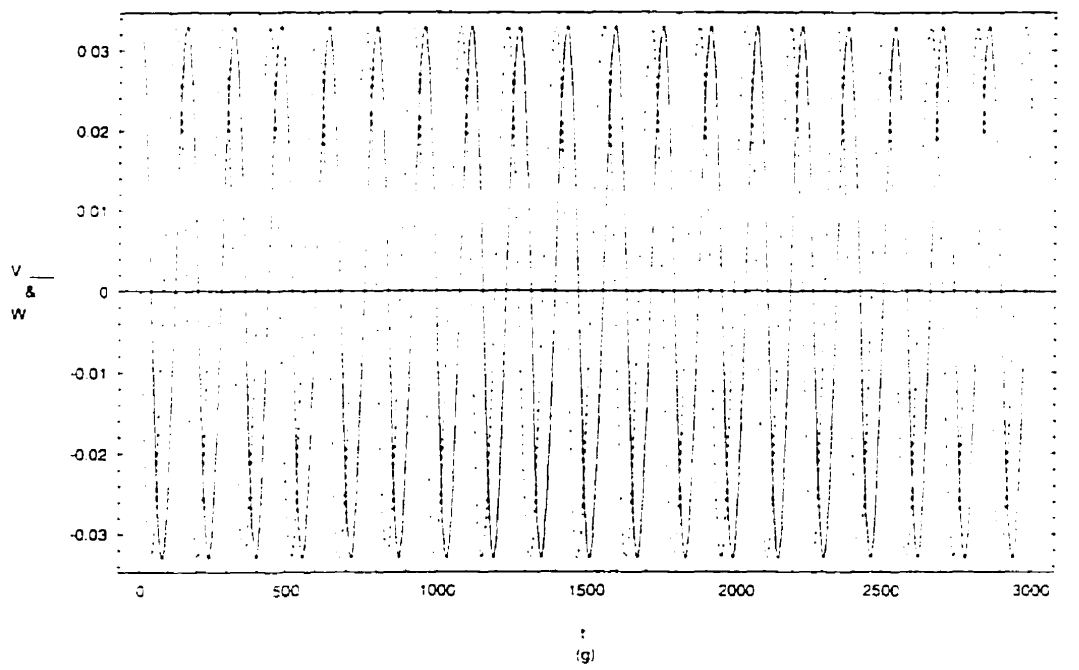

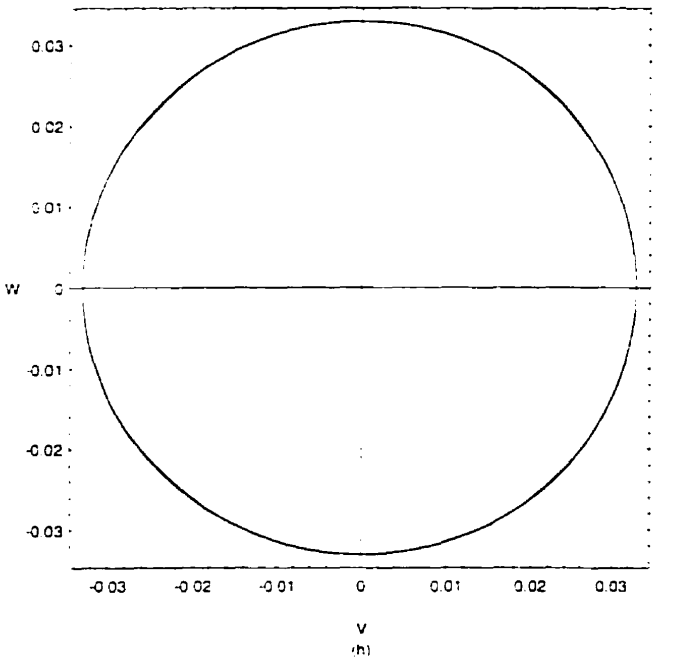

Figure 5.7 (continued)

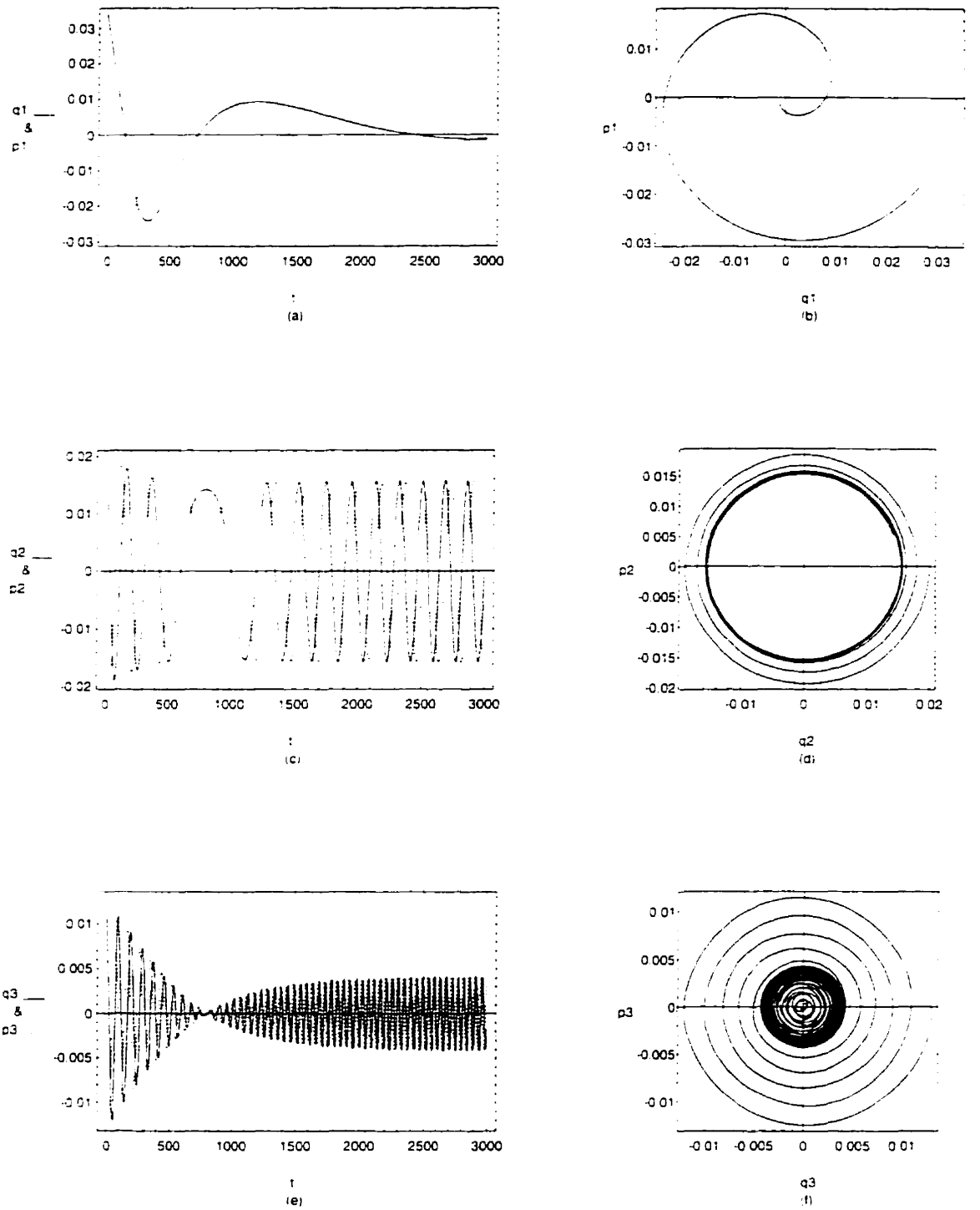

Figure 5.8 Phase-space response and transverse motion in steady state I.C.(+) with damping [case 5]

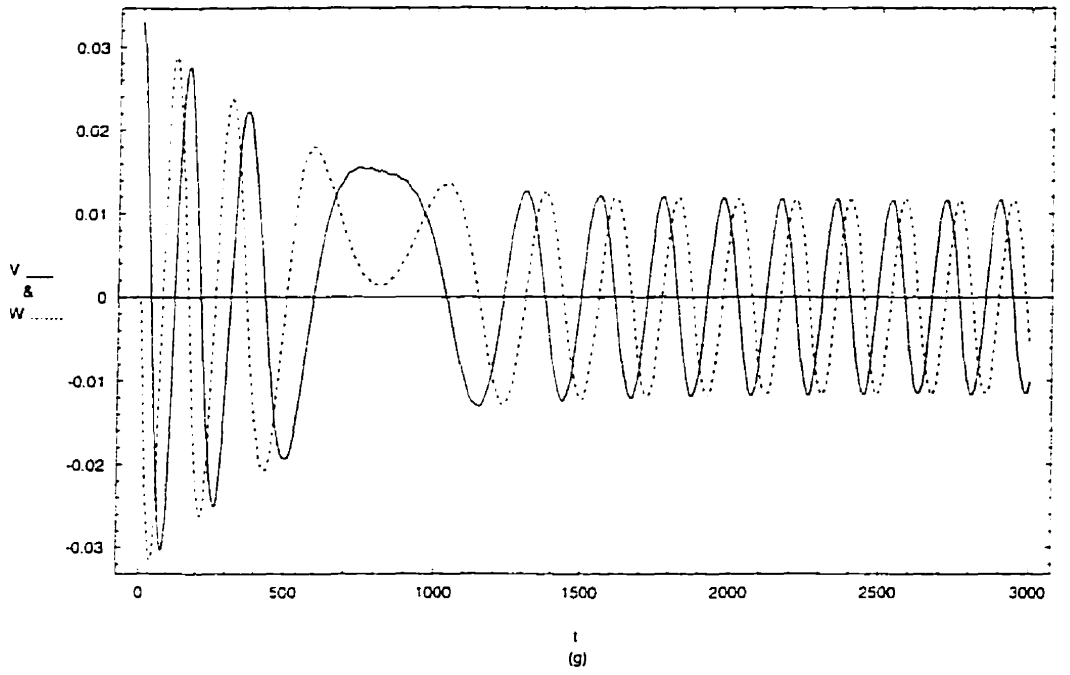

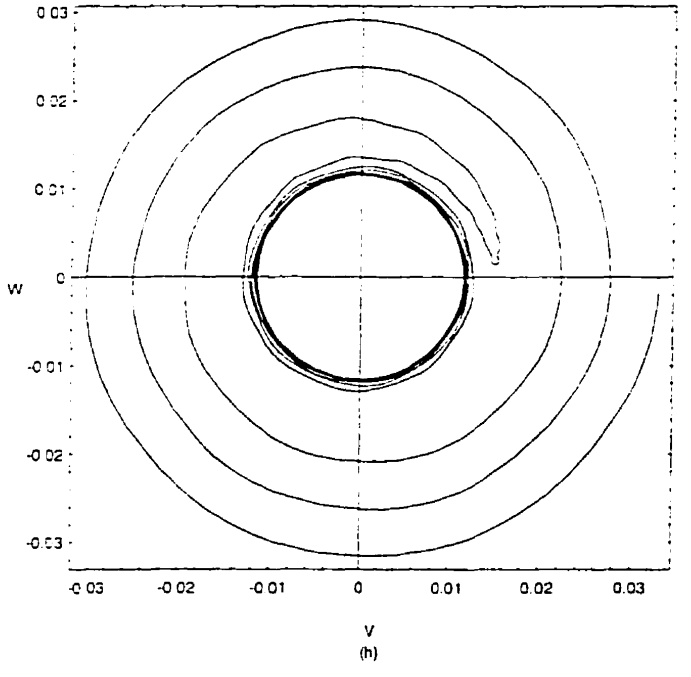

Figure 5.8 (continued)

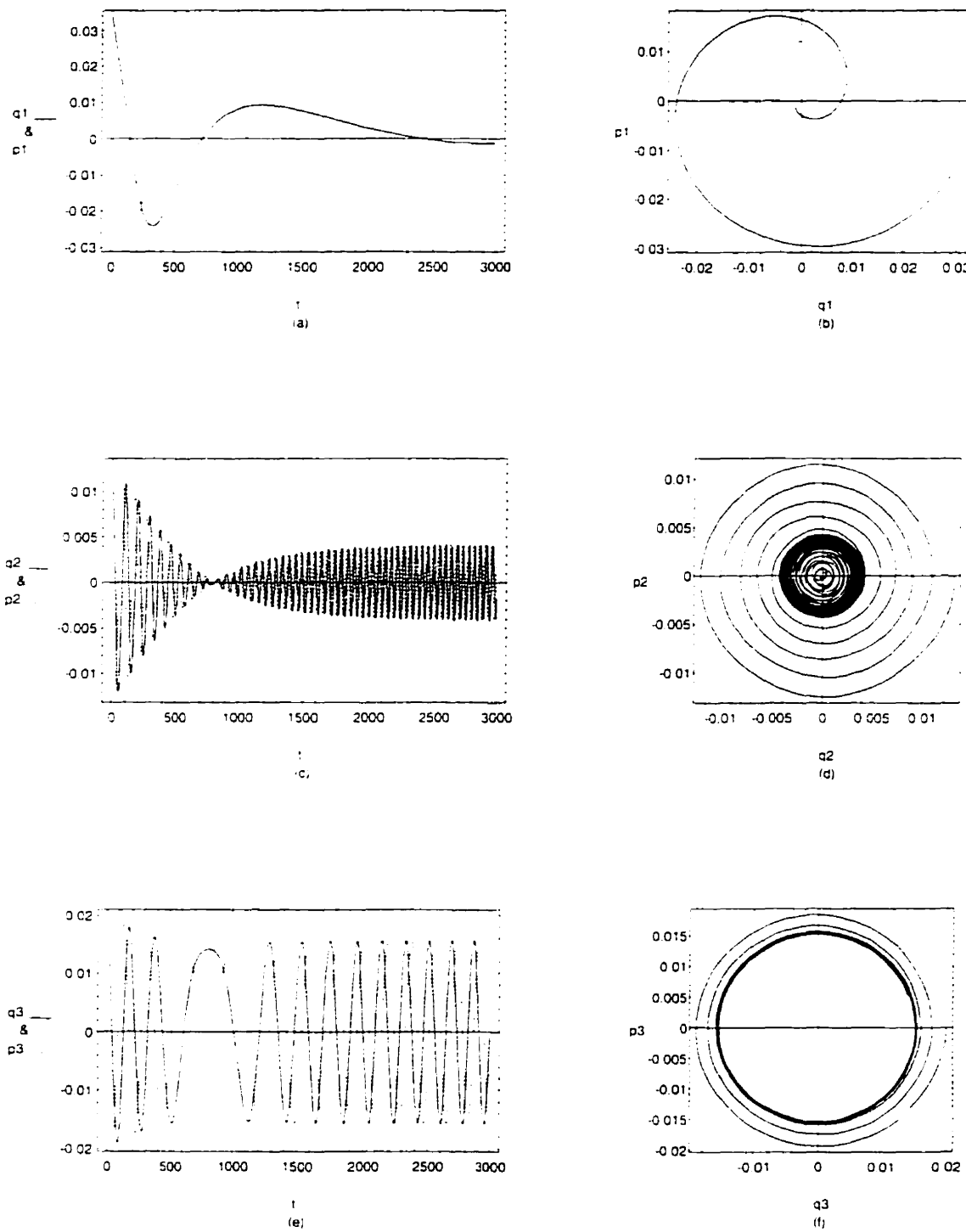

Figure 5.9 Phase-space response and transverse motion in steady state I.C.(+) with damping [case 6]

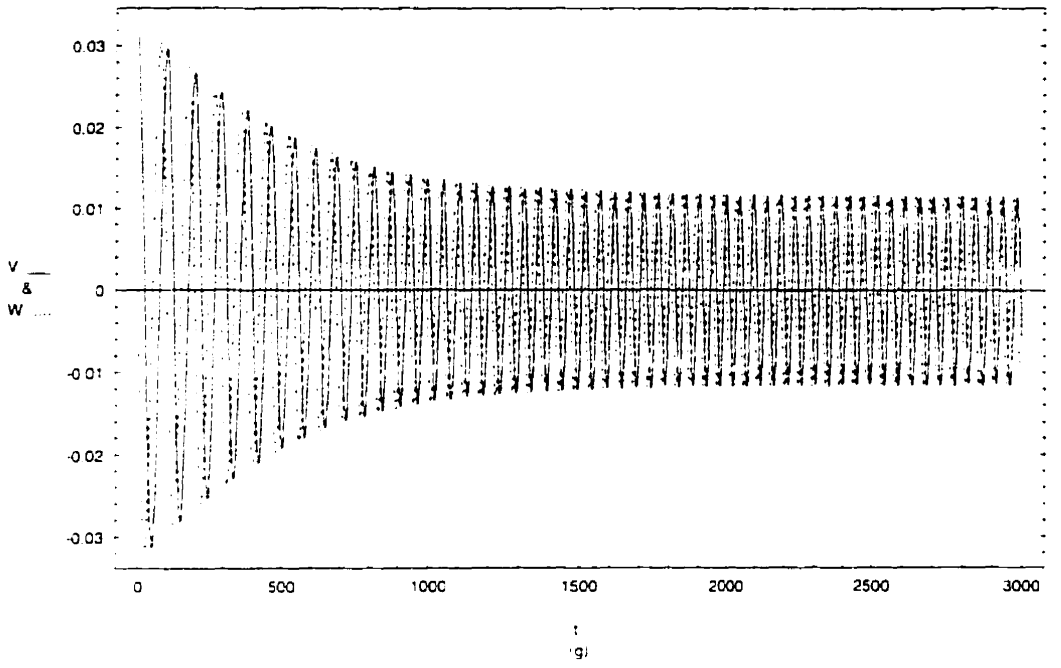

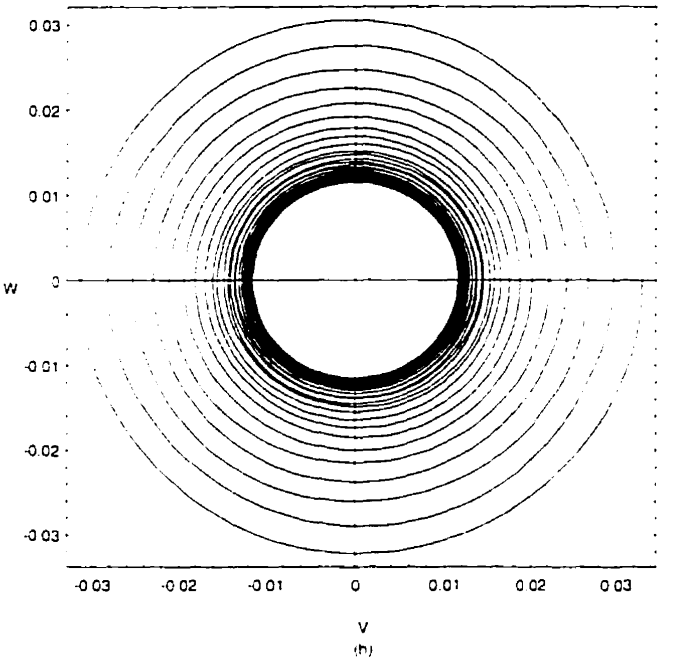

Figure 5.9 (continued)

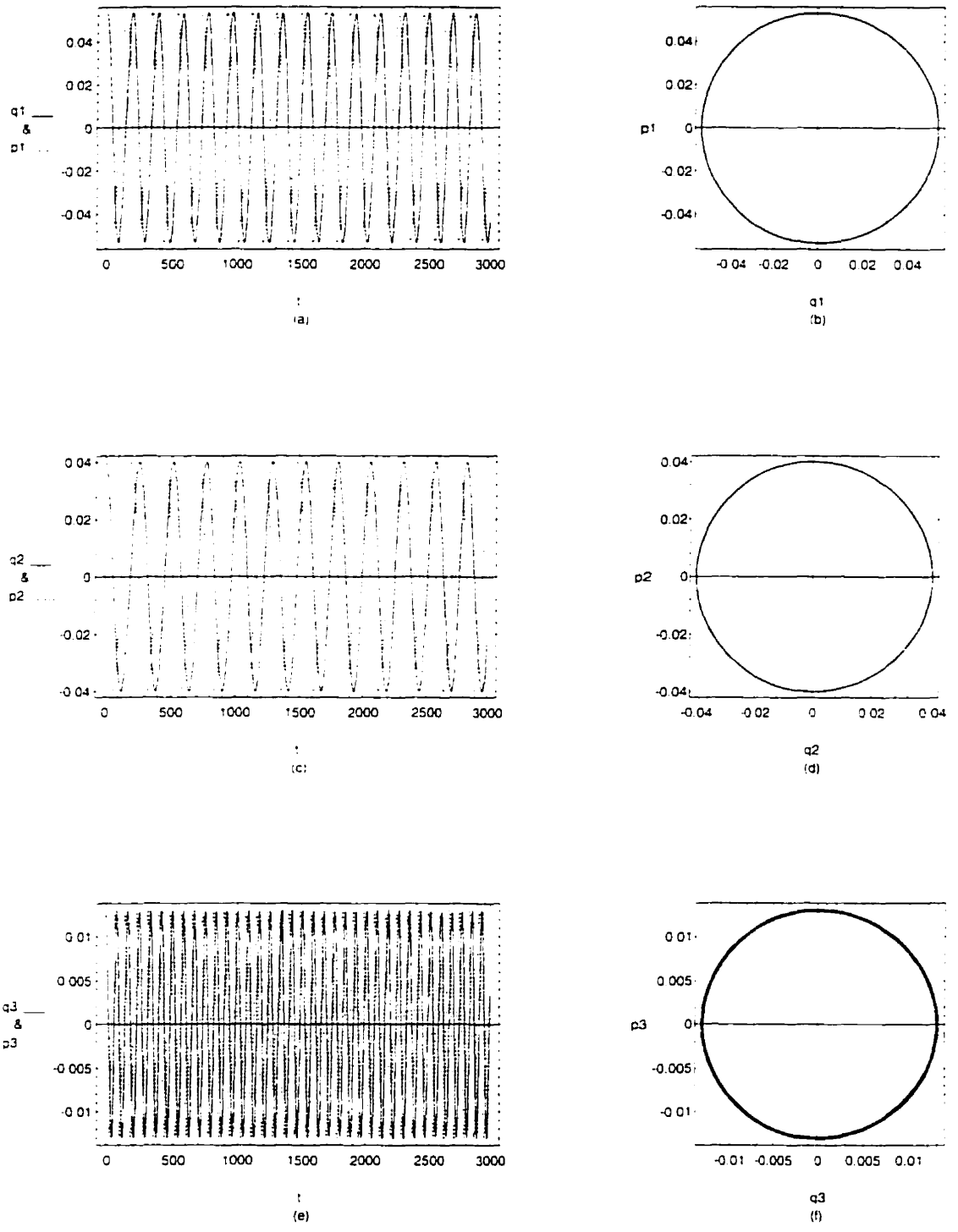

Figure 5.10 Phase-space response and transverse motion in steady state I.C.(+) without damping [case 7]

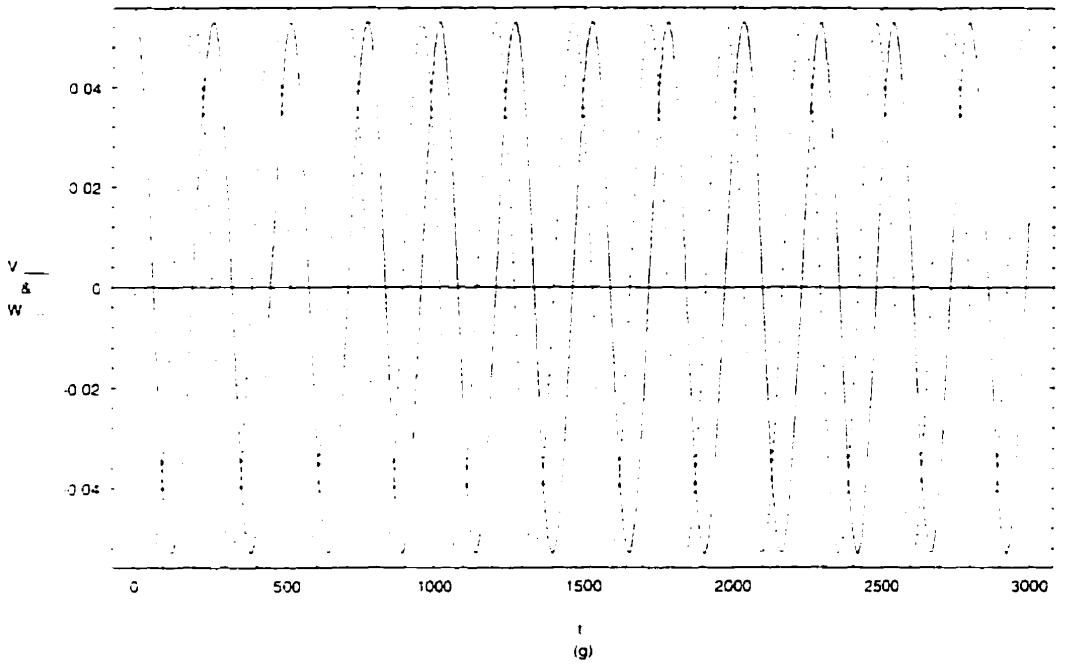

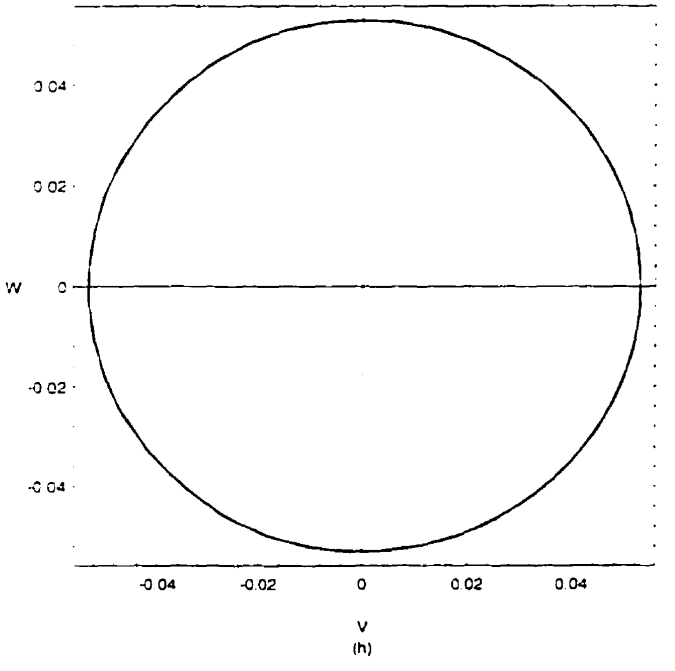

Figure 5.10 (continued)

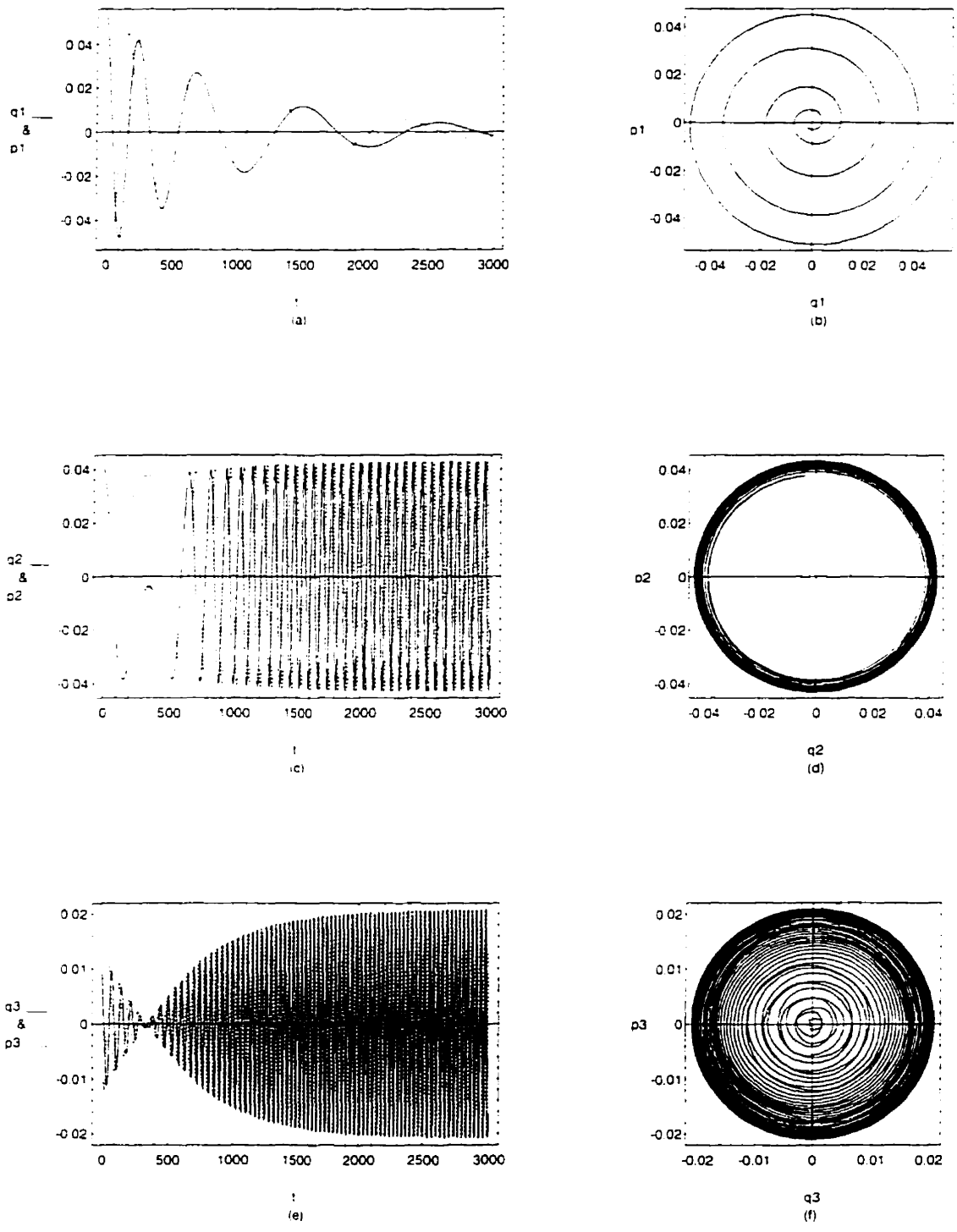

Figure 5.11 Phase-space response and transverse motion in steady state I.C.(+) with damping [case 8]

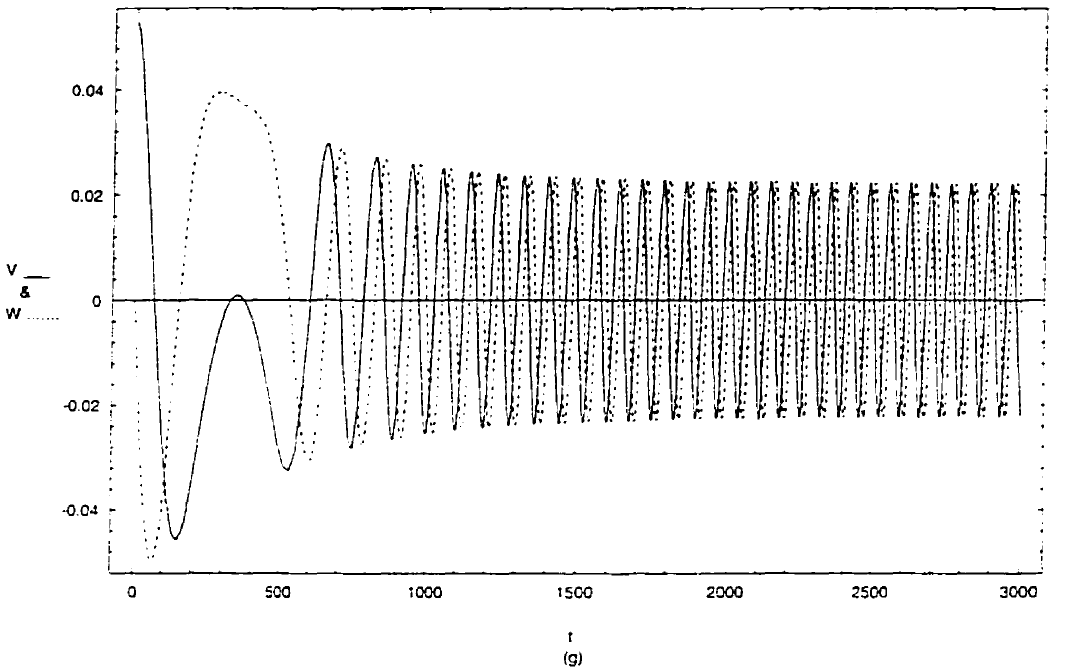

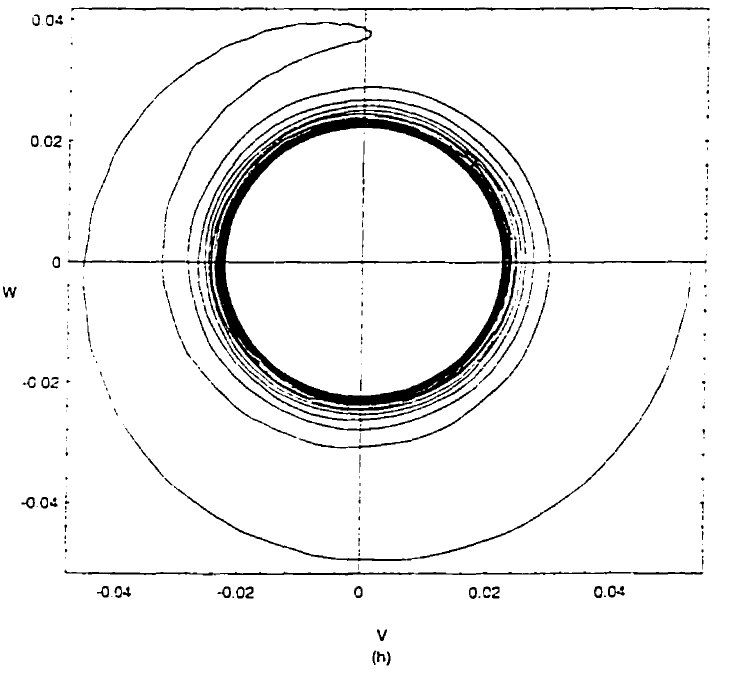

Figure 5.11 (continued)

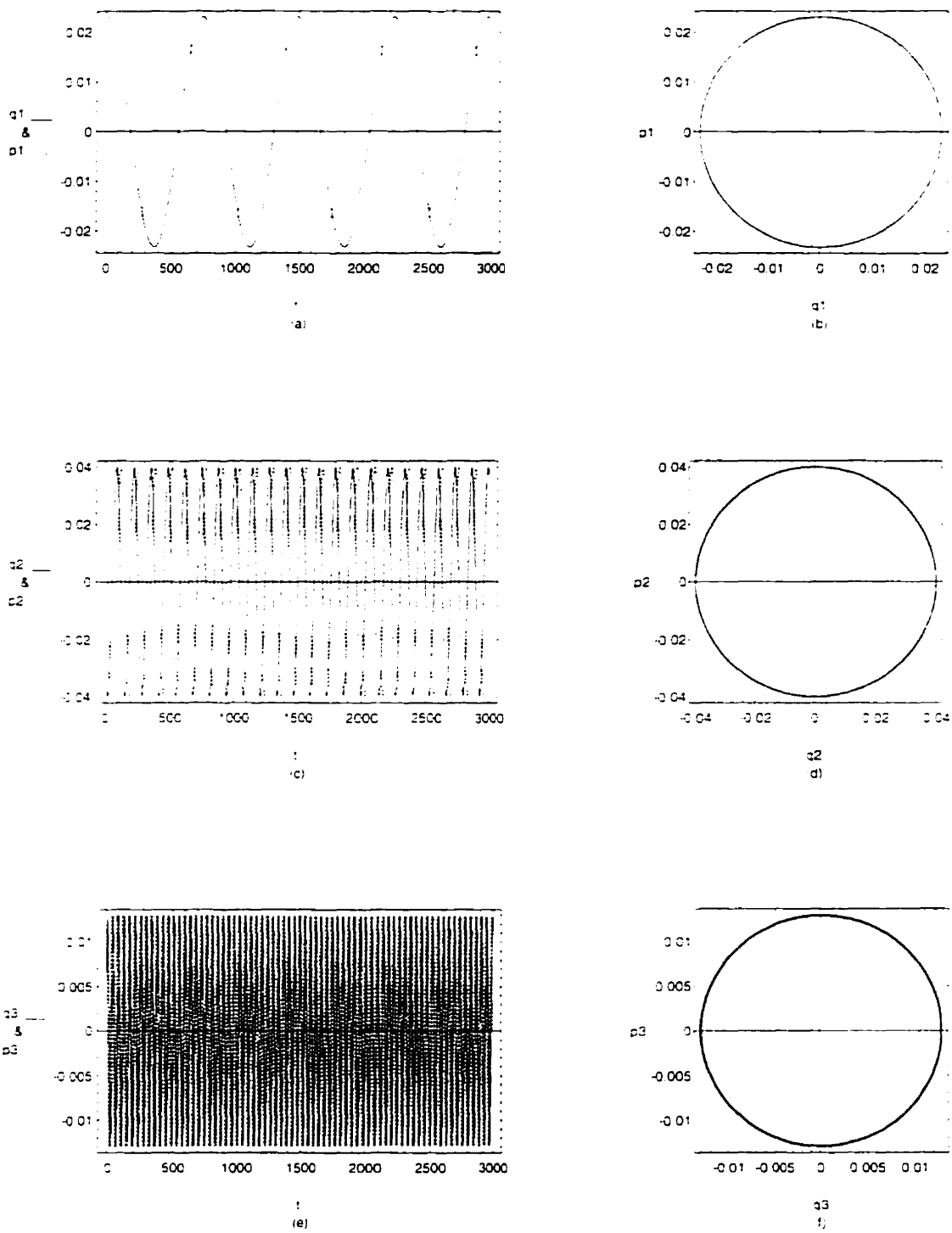

Figure 5.12 Phase-space response and transverse motion in steady state I.C.(-) without damping [case 9]

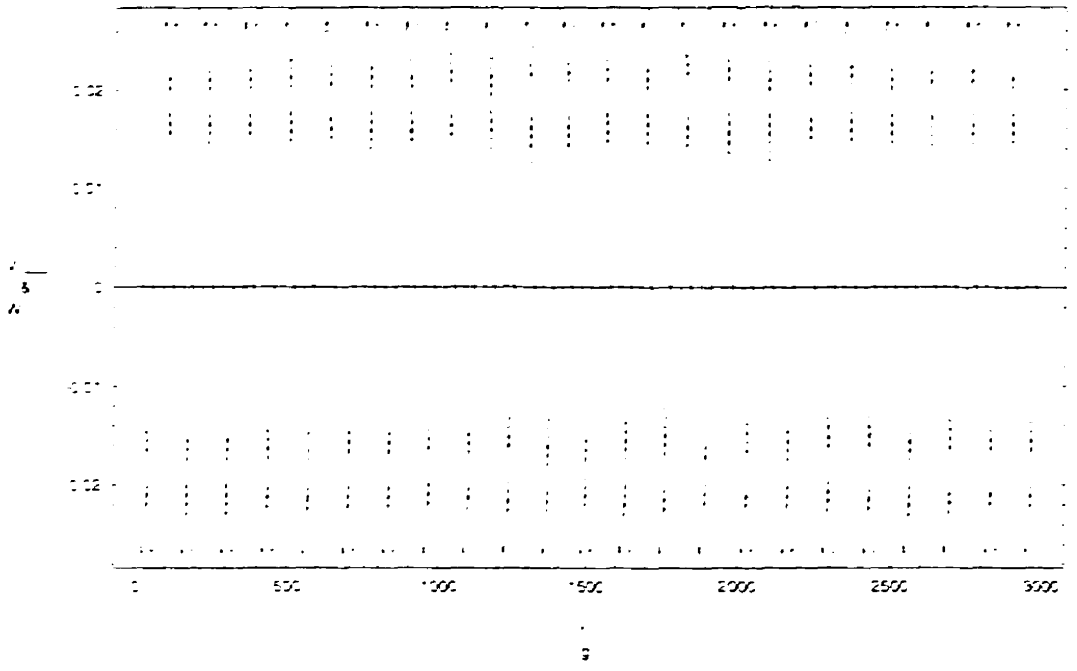

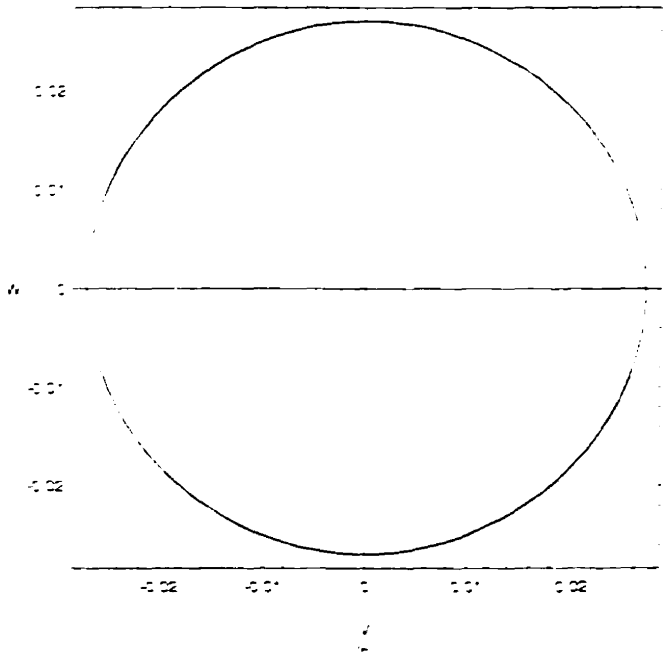

Figure 5.12 (continued)

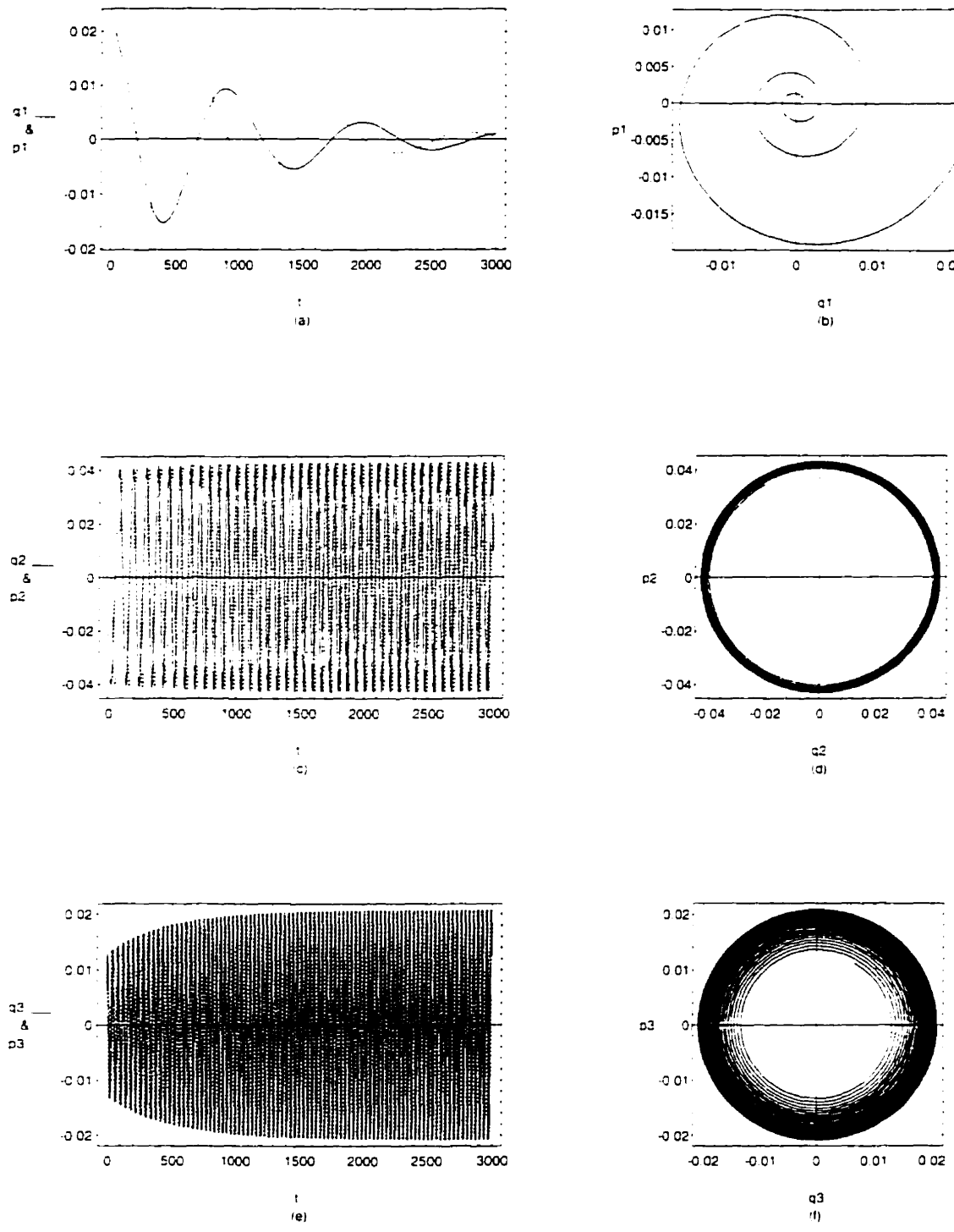

Figure 5.13 Phase-space response and transverse motion in steady state I.C.(-) with damping [case 10]

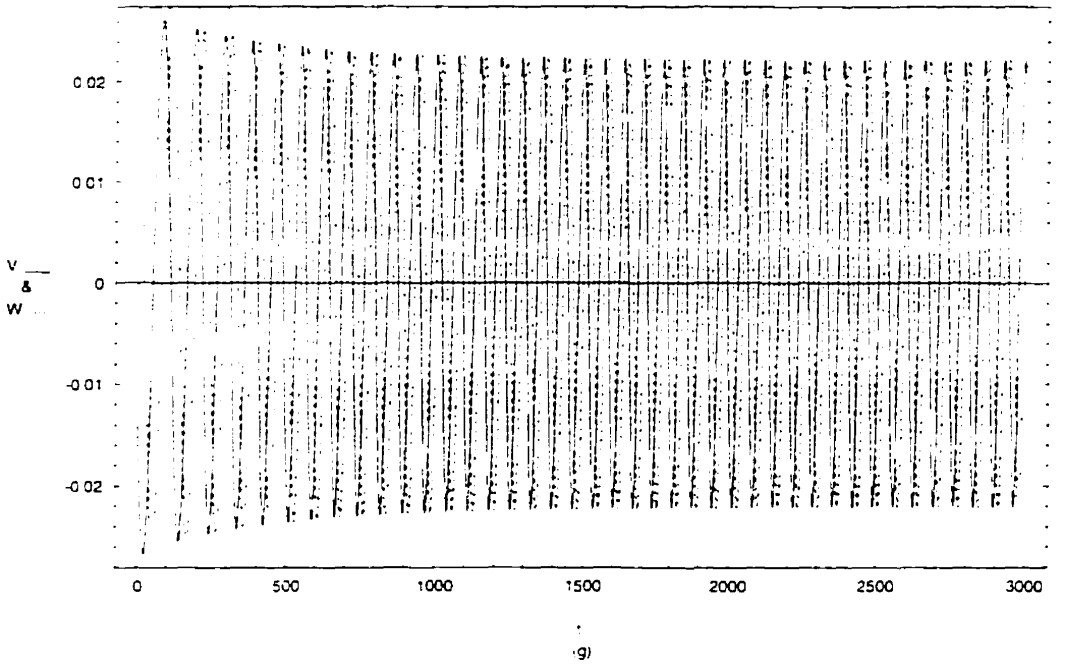

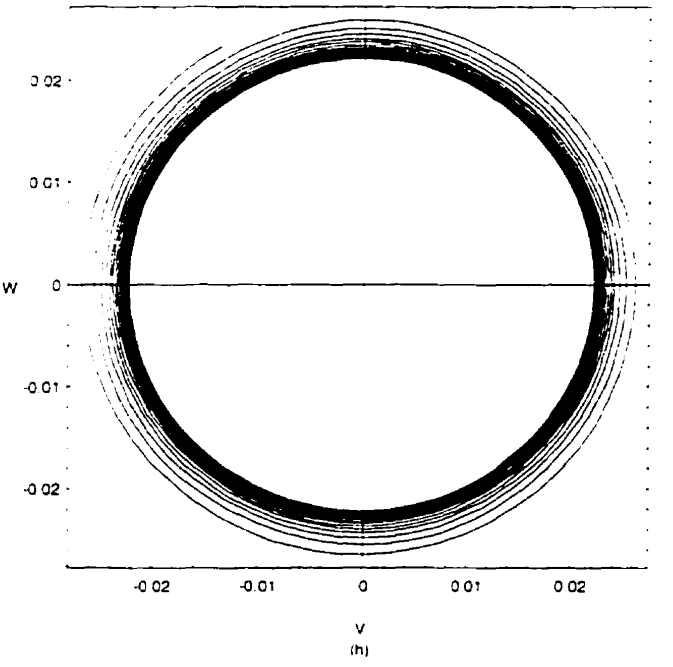

Figure 5.13 (continued)

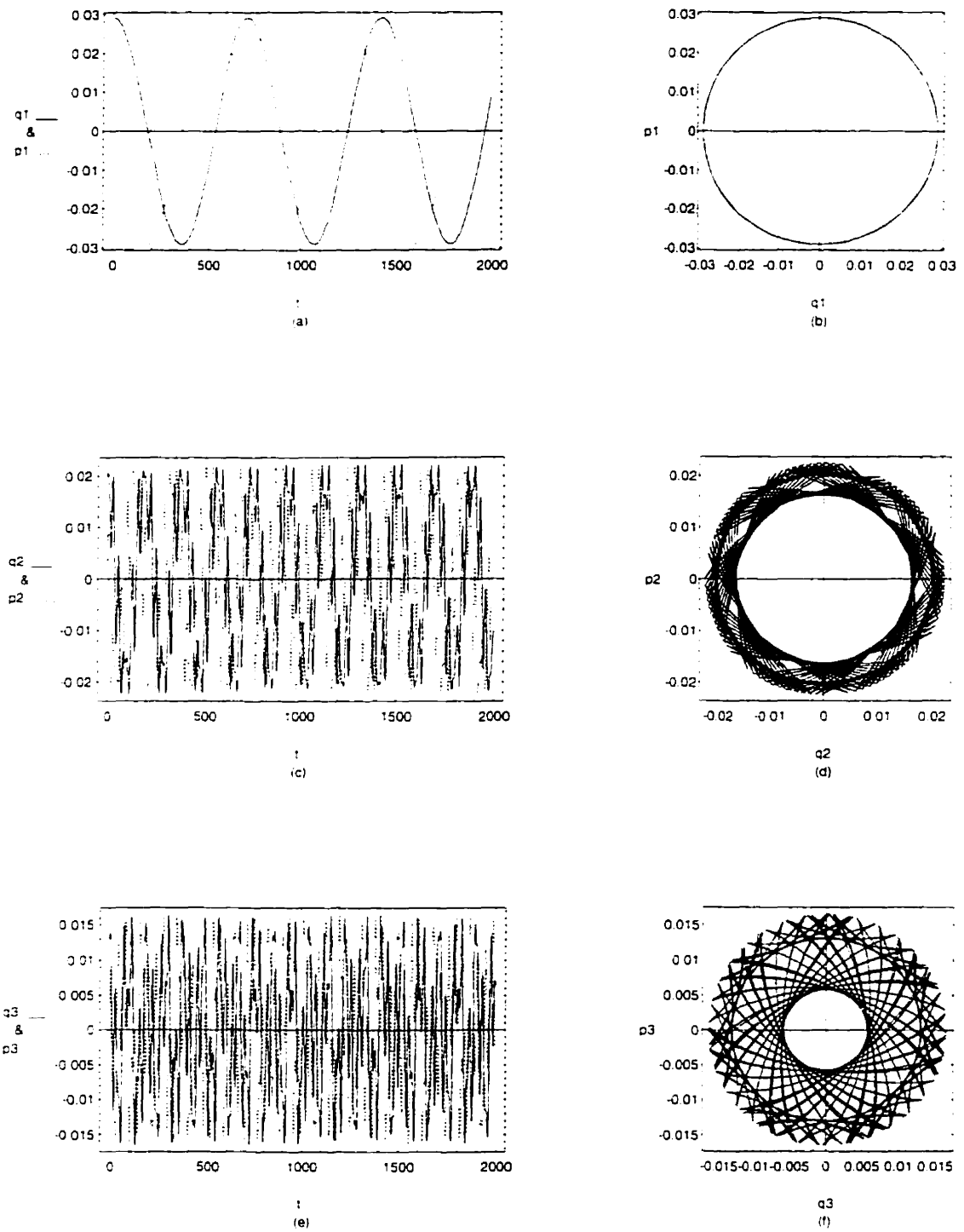

Figure 5.14 Phase-space response and transverse motion [case 11]

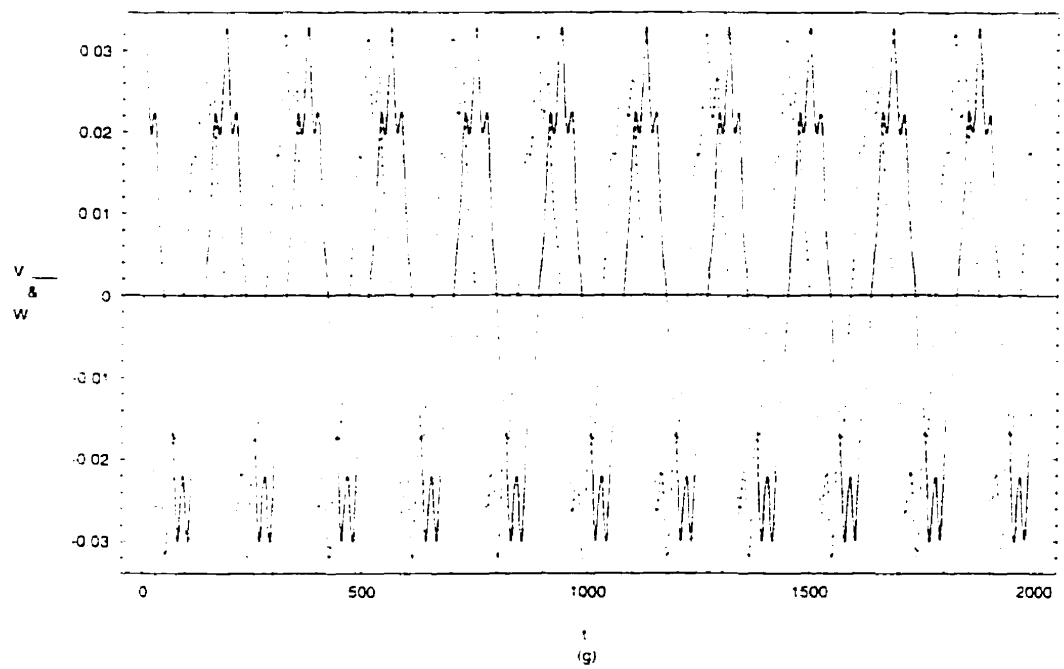

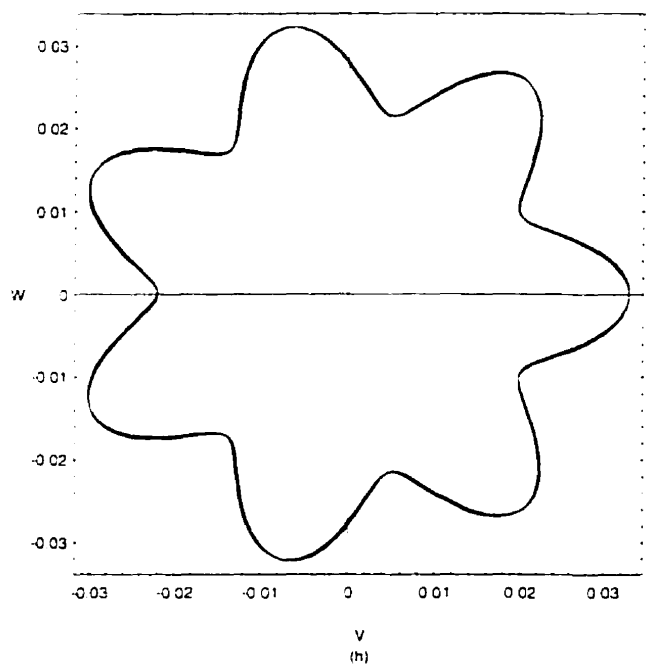

Figure 5.14 (continued)

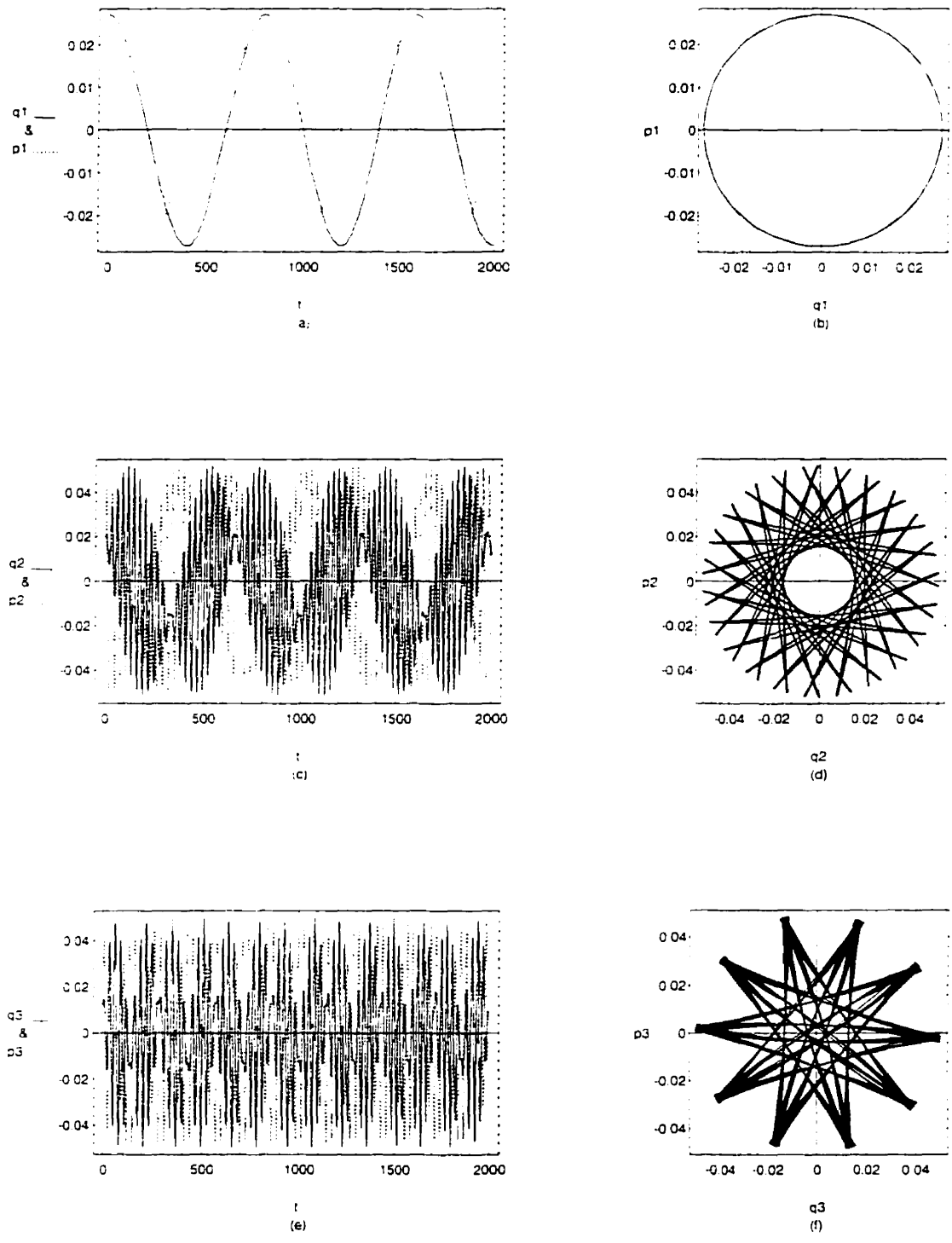

Figure 5.15 Phase-space response and transverse motion [case 12]

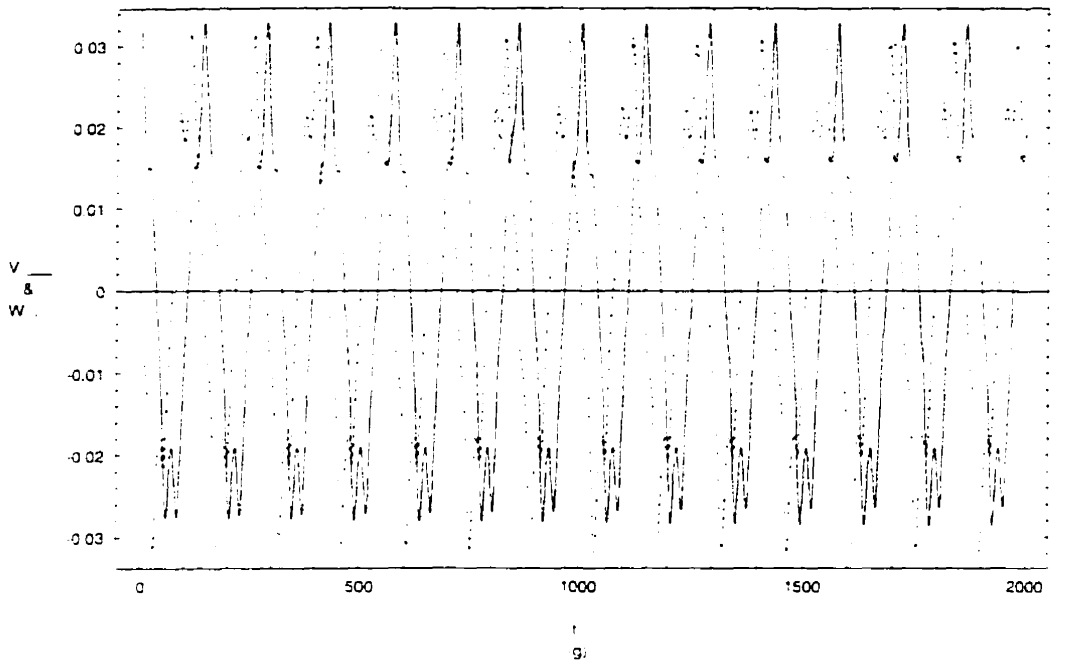

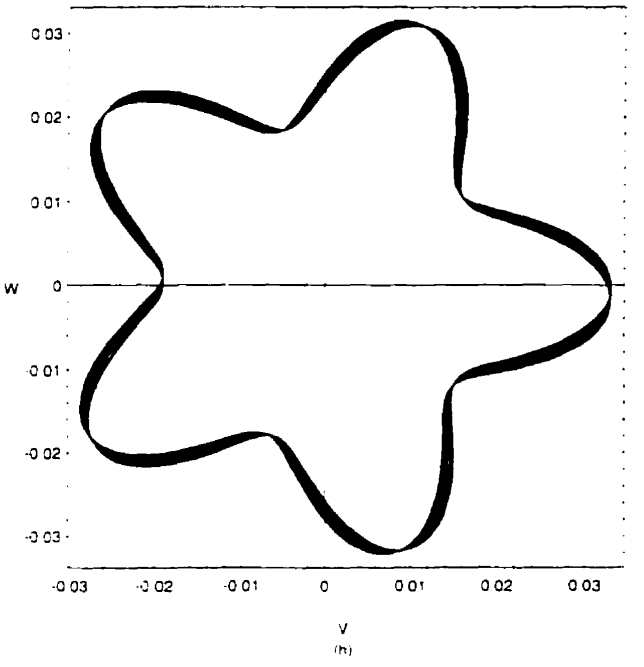

Figure 5.15 (continued)

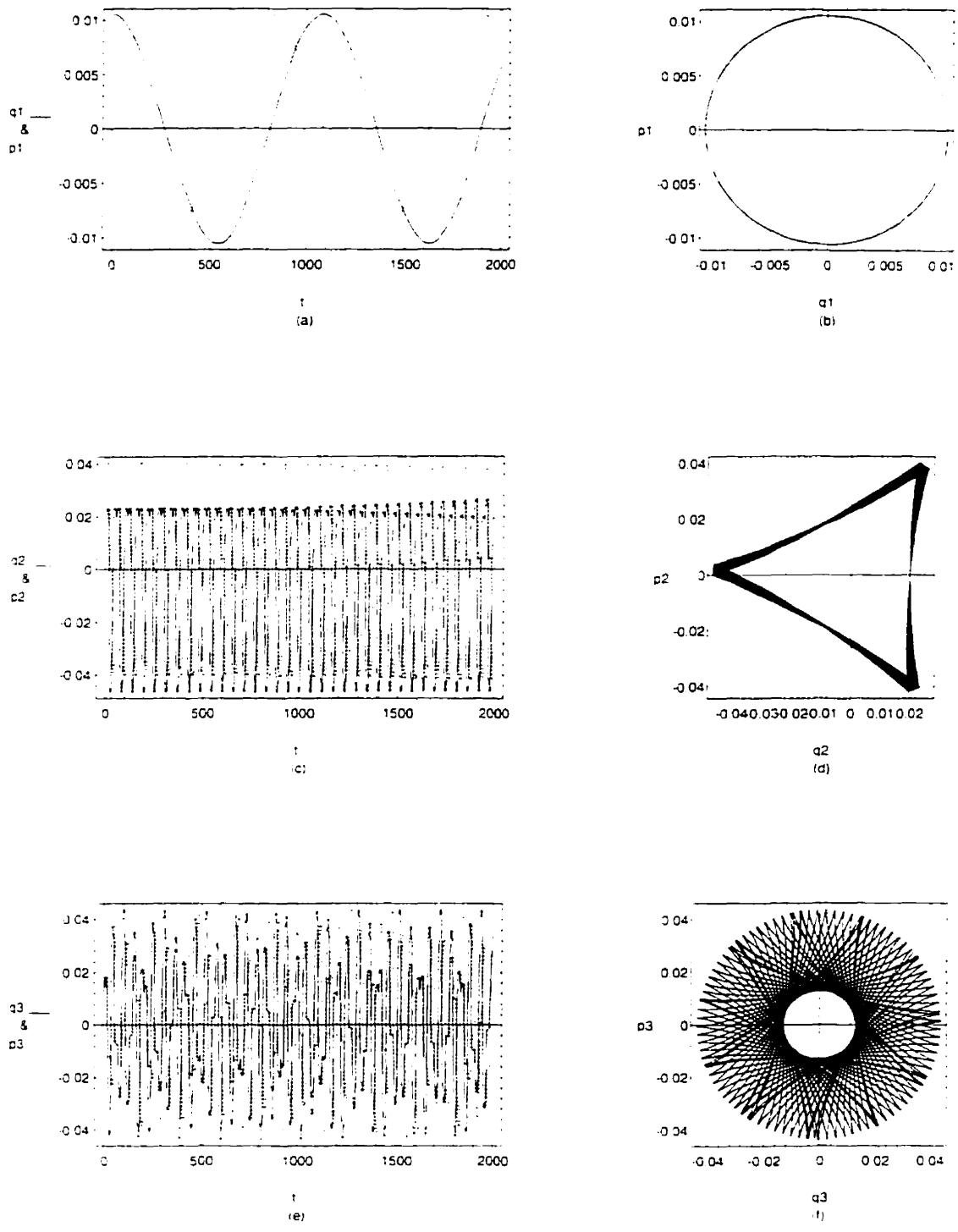

Figure 5.16 Phase-space response and transverse motion [case 13]

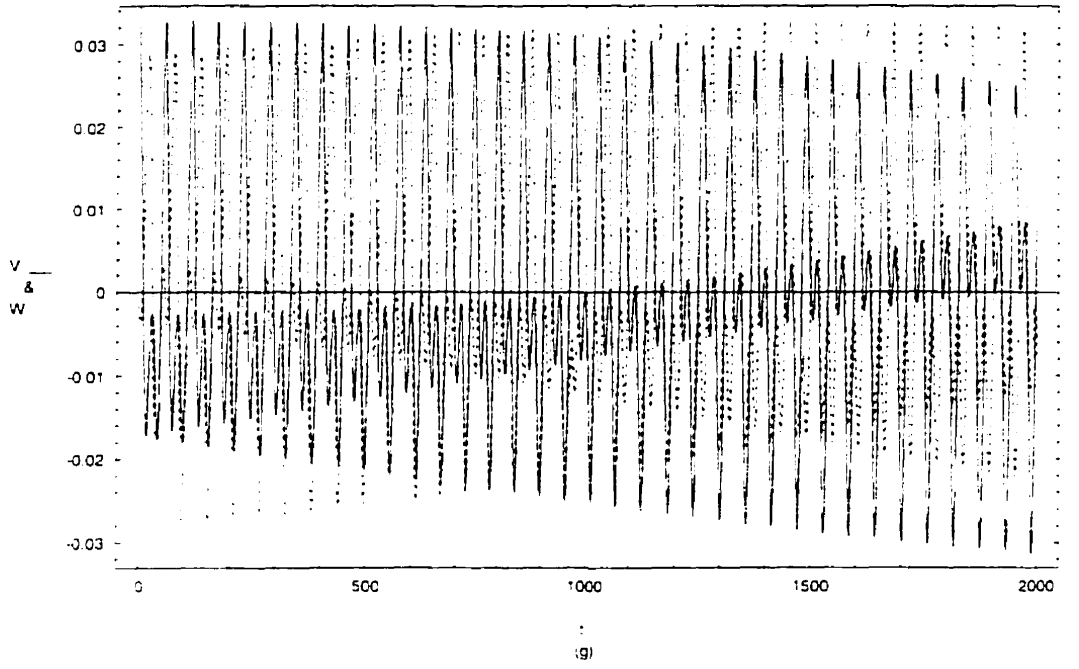

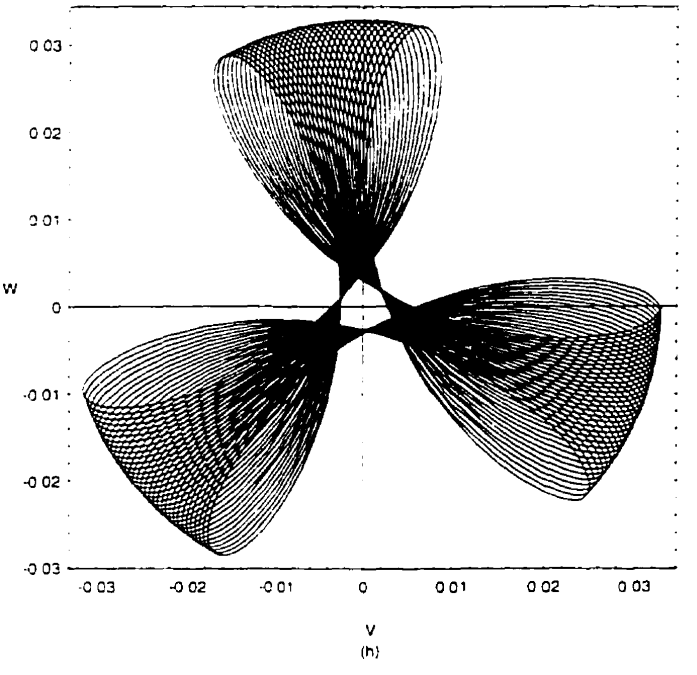

Figure 5.16 (continued)

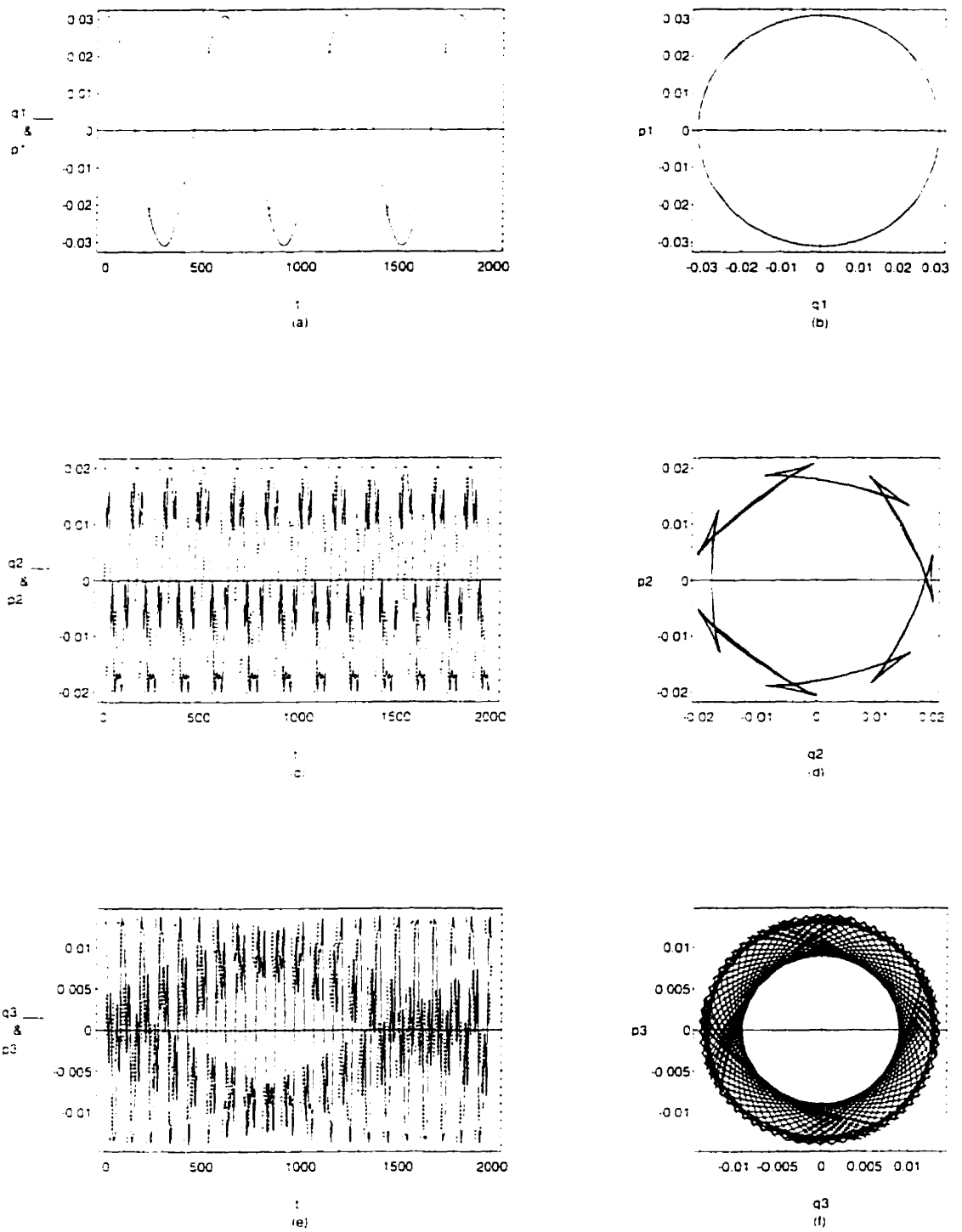

Figure 5.17 Phase-space response and transverse motion [case14]

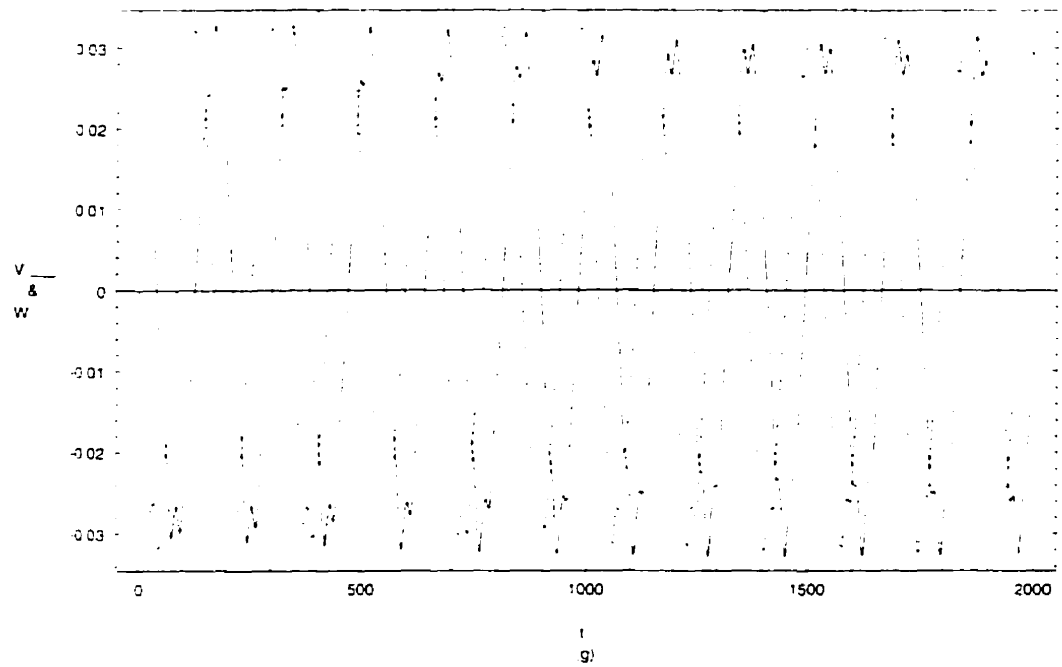

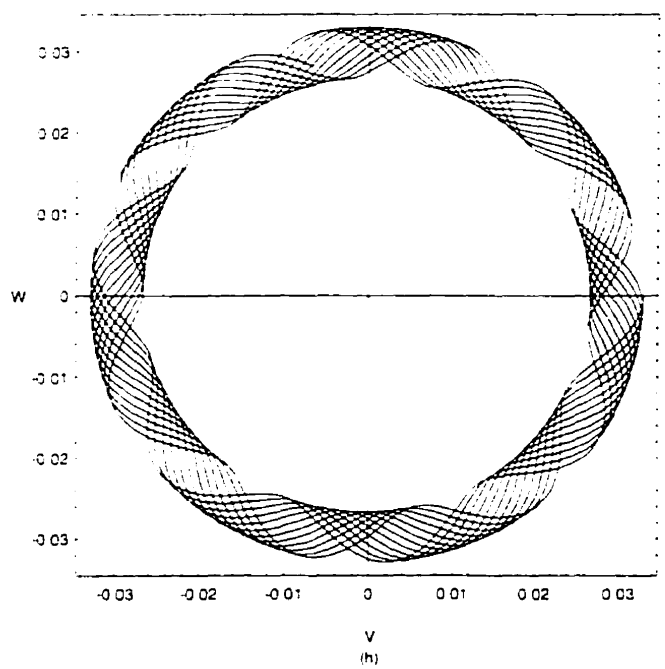

Figure 5.17 (continued)

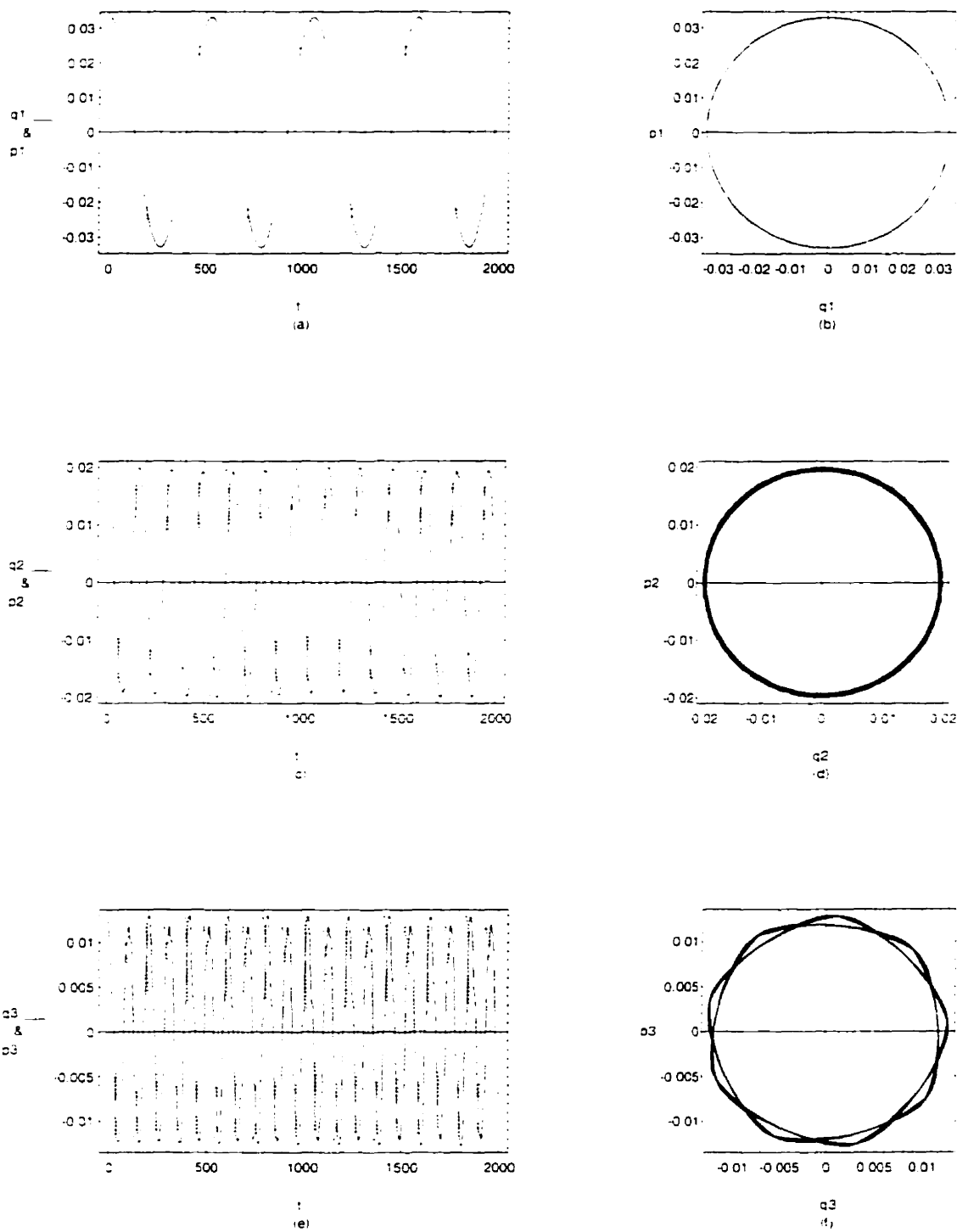

Figure 5.18 Phase-space response and transverse motion [case 15]

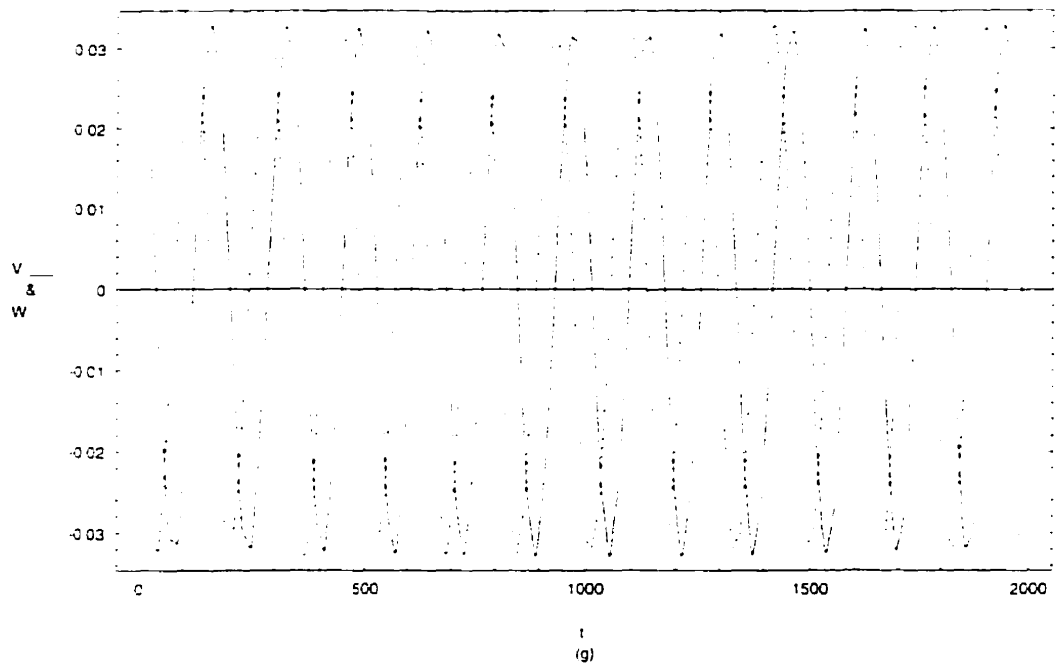

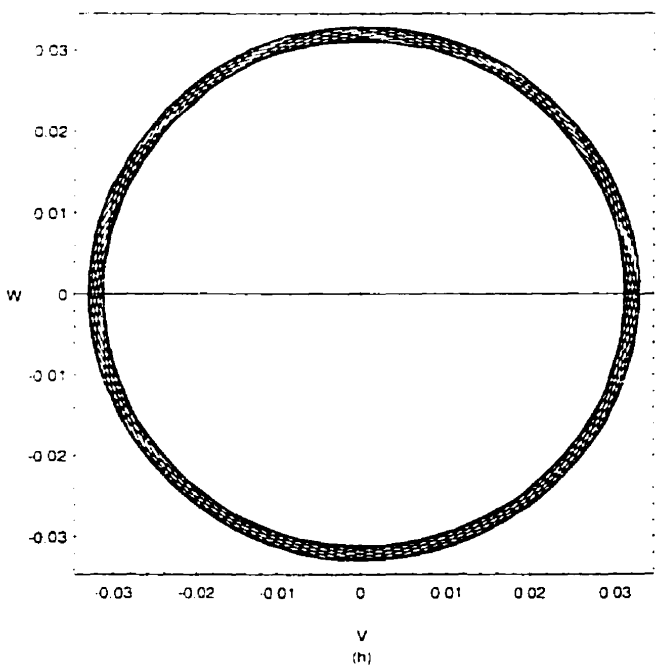

Figure 5.18 (continued)

APPENDIX A

DERIVATION OF THE EQUATIONS OF MOTION

The equations of motion of the system are derived by the extended Hamilton's principle, which is a variational method based on the energy of the system. Inserting the Lagrangian (2.11) of the system into the variational expression (2.12) results in

$$\begin{aligned} 0 = \int_{t_1}^{t_2}\int_0^l \big[\ & \rho u_t \delta u_t + \rho(v_t - \Omega w)(\delta v_t - \Omega \delta w) + \rho(w_t + \Omega v)(\delta w_t + \Omega \delta v) \\ & - N_o(\delta u_x + v_x \delta v_x + w_x \delta w_x) \\ & - \tfrac{1}{2} EA\{2u_x \delta u_x \\ & \quad + (v_x^2 + w_x^2)\delta u_x + u_x(2v_x \delta v_x + 2w_x \delta w_x) \\ & \quad + \tfrac{1}{2}(v_x^2 + w_x^2)(2v_x \delta v_x + 2w_x \delta w_x) \\ & \quad - 2u_x(v_x^2 + w_x^2)\delta u_x - u_x^2(2v_x \delta v_x + 2w_x \delta w_x)\} \\ & + Q_u \delta u + Q_v \delta v + Q_w \delta w \ \big] dx dt \end{aligned} \tag{A.1}$$

where Q_u, Q_v, and Q_w are the generalized forces per unit nominal length along the directions of the deformations, u, v, and w, respectively. Collecting terms corresponding to each variational variable together leads to

$$\begin{aligned} 0 = \int_{t_1}^{t_2}\int_0^l \big[\ & \rho u_t \cdot \delta u_t + \rho(v_t - \Omega w)\cdot \delta v_t + \rho(w_t + \Omega v)\cdot \delta w_t \\ & + Q_u \cdot \delta u + \{\rho(w_t + \Omega v)\Omega + Q_v\}\cdot \delta v + \{-\rho(w_t - \Omega v)\Omega + Q_w\}\cdot \delta w \\ & - \{N_o + EA(u_x\{1 - v_x^2 - w_x^2\} + \tfrac{1}{2}\{v_x^2 + w_x^2\})\}\cdot \delta u_x \\ & - \{N_o + EA(u_x - u_x^2 + \tfrac{1}{2}\{v_x^2 + w_x^2\})\}v_x \cdot \delta v_x \\ & - \{N_o + EA(u_x - u_x^2 + \tfrac{1}{2}\{v_x^2 + w_x^2\})\}w_x \cdot \delta w_x \ \big] dx dt \end{aligned} \tag{A.2}$$

Let us introduce the following substitutions into Eq. (A.2) for brevity.

$$\begin{cases} A = N_o + EA\left(u_x\left\{1 - v_x{}^2 - w_x{}^2\right\} + \frac{1}{2}\left\{v_x{}^2 + w_x{}^2\right\}\right) \\ B = \left\{N_o + EA\left(u_x - u_x{}^2 + \frac{1}{2}\left\{v_x{}^2 + w_x{}^2\right\}\right)\right\}v_x \\ C = \left\{N_o + EA\left(u_x - u_x{}^2 + \frac{1}{2}\left\{v_x{}^2 + w_x{}^2\right\}\right)\right\}w_x \end{cases} \tag{A.3}$$

Integration by parts results in

$$\begin{aligned} 0 = \int_{t_1}^{t_2}\int_0^l \Big[& \left(\rho u_t \delta u\right)_t + \left\{\rho\left(v_t - \Omega w\right)\delta v\right\}_t + \left\{\rho\left(w_t + \Omega v\right)\delta w\right\}_t \\ & - \rho u_{tt}\delta u \quad - \rho\left(v_{tt} - \Omega w_t\right)\delta v \quad - \rho\left(w_{tt} + \Omega v_t\right)\delta w \\ & - Q_u\delta u - \left\{\rho\left(w_t + \Omega v\right)\Omega + Q_v\right\}\delta v - \left\{-\rho\left(v_t - \Omega w\right)\Omega + Q_w\right\}\delta w \\ & - \left(A\delta u\right)_x - \left(B\delta v\right)_x - \left(C\delta w\right)_x \\ & - A_x\delta u \quad + B_x\delta v \quad + C_x\delta w \Big]\, dxdt \end{aligned} \tag{A.4}$$

The integrand in the above equation contains the terms that are exact differentials with respect to either time t or the nominal coordinate x. Integrating those terms, one can obtain

$$\begin{aligned} 0 = & \int_0^l \left[\rho u_t\delta u + \rho\left(v_t - \Omega w\right)\delta v + \rho\left(w_t + \Omega v\right)\delta w\right]_{t_1}^{t_2} dx \\ & + \int_{t_1}^{t_2}\int_0^l \Big[\left(-\rho u_{tt} + A_x + Q_u\right)\cdot\delta u \\ & \qquad + \left(\rho\left(v_{tt} - \Omega w_t\right) + \rho\left(w_t + \Omega v\right)\Omega + B_x + Q_v\right)\cdot\delta v \\ & \qquad + \left(-\rho\left(w_{tt} + \Omega v_t\right) - \rho\left(v_t - \Omega w\right)\Omega + C_x + Q_w\right)\cdot\delta w \Big]\, dxdt \\ & - \int_{t_1}^{t_2}\left[A\delta u + B\delta v + C\delta w\right]_0^l dt \end{aligned} \tag{A.5}$$

Eq. (A.5) is composed of the three integral terms. According to the Hamilton's principle, the first integral term becomes zero because the variational variables are assumed to be specified both at the beginning and at the end of the arbitrarily selected time interval. Also,

it can be easily seen that the third integral term is zero since the variational variables vanish at the ends of the tether according to the boundary conditions of the system, which is the case of both ends fixed. Finally, the variational expression becomes as follows:

$$
\begin{aligned}
0 = \int_{t_1}^{t_2}\int_0^l \Big[& \left(-\rho u_{tt} + EA\left\{u_{xx}\left(1-v_x^{\,2}-w_x^{\,2}\right)+\left(1-2u_x\right)\left(v_x v_{xx}+w_x w_{xx}\right)\right\}+Q_u\right)\cdot\delta u \\
& +\left(-\rho\left\{v_{tt}-2\Omega w_t-\Omega^2 v\right\}+N_o v_{xx}\right. \\
& \left.\quad +EA\left\{\left(u_x-u_x^{\,2}+\tfrac{3}{2}v_x^{\,2}+\tfrac{1}{2}w_x^{\,2}\right)v_{xx}+\left(u_{xx}-2u_x u_{xx}+w_x w_{xx}\right)v_x\right\}+Q_v\right)\cdot\delta v \\
& +\left(-\rho\left\{w_{tt}+2\Omega v_t-\Omega^2 w\right\}+N_o w_{xx}\right. \\
& \left.\quad +EA\left\{\left(u_x-u_x^{\,2}+\tfrac{1}{2}v_x^{\,2}+\tfrac{3}{2}w_x^{\,2}\right)w_{xx}+\left(u_{xx}-2u_x u_{xx}+v_x v_{xx}\right)w_x\right\}+Q_w\right)\cdot\delta w \\
& \Big] dx dt
\end{aligned}
\qquad \text{..... (A.6)}
$$

Eq. (A.6) must be true for any arbitrary variations δu, δv, and δw that vanish at the boundary of the system. Therefore, coefficient of each of the variations in the integrand should vanish. It results in the following governing equations:

P.D.E.

$$
u_{tt} - \frac{EA}{\rho}\left\{\left(1-v_x^{\,2}-w_x^{\,2}\right)u_{xx}+\left(1-2u_x\right)\left(v_x v_{xx}+w_x w_{xx}\right)\right\} = q_u \qquad \text{(A.7. a)}
$$

$$
\begin{aligned}
& v_{tt} - 2\Omega w_t - \Omega^2 v - \frac{N_o}{\rho} v_{xx} \\
& \quad - \frac{EA}{\rho}\left\{\left(u_x-u_x^{\,2}+\tfrac{3}{2}v_x^{\,2}+\tfrac{1}{2}w_x^{\,2}\right)v_{xx}+\left(u_{xx}-2u_x u_{xx}+w_x w_{xx}\right)v_x\right\} = q_v
\end{aligned}
\qquad \text{(A.7. b)}
$$

$$
\begin{aligned}
& w_{tt} + 2\Omega v_t - \Omega^2 w - \frac{N_o}{\rho} w_{xx} \\
& \quad - \frac{EA}{\rho}\left\{\left(u_x-u_x^{\,2}+\tfrac{1}{2}v_x^{\,2}+\tfrac{3}{2}w_x^{\,2}\right)w_{xx}+\left(u_{xx}-2u_x u_{xx}+v_x v_{xx}\right)w_x\right\} = q_w
\end{aligned}
\qquad \text{(A.7. c)}
$$

B.C.

$$
u = v = w = 0 \qquad \text{at} \qquad x = 0 \quad \text{and} \quad x = l \qquad \text{(A.8)}
$$

IMAGE EVALUATION
TEST TARGET (QA-3)

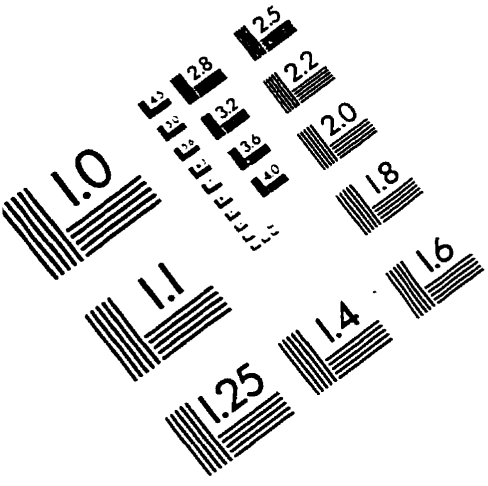

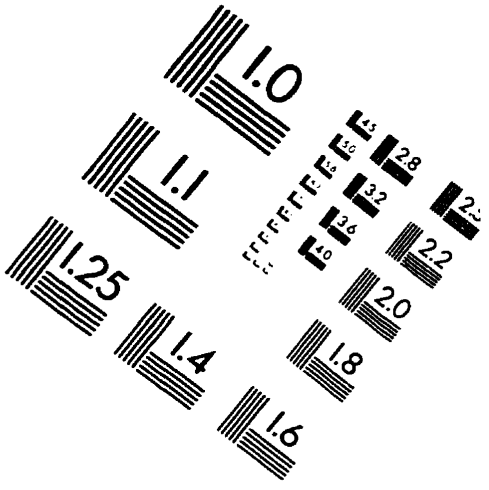

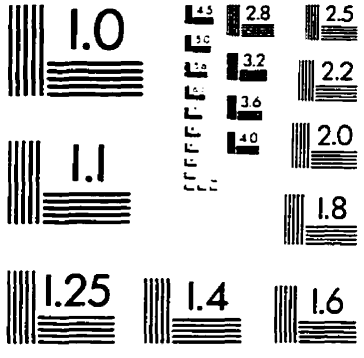

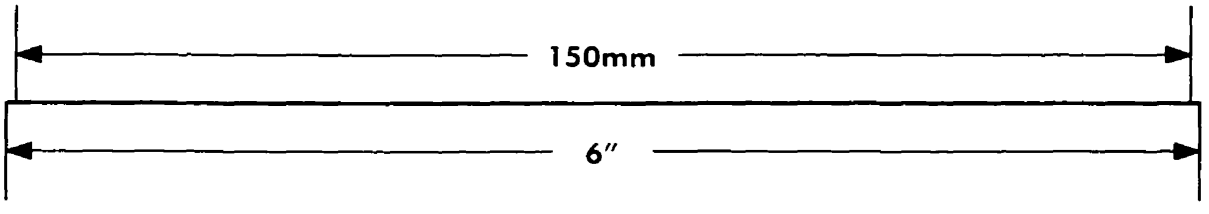

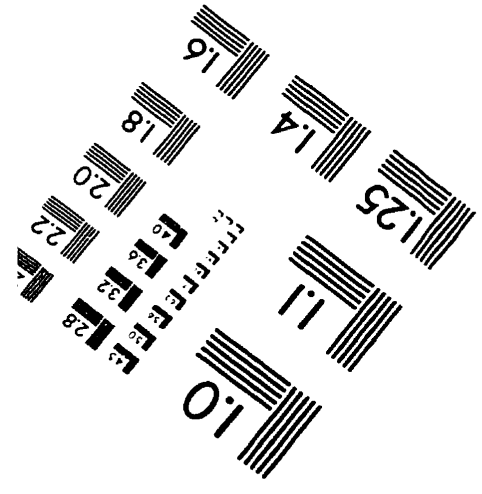

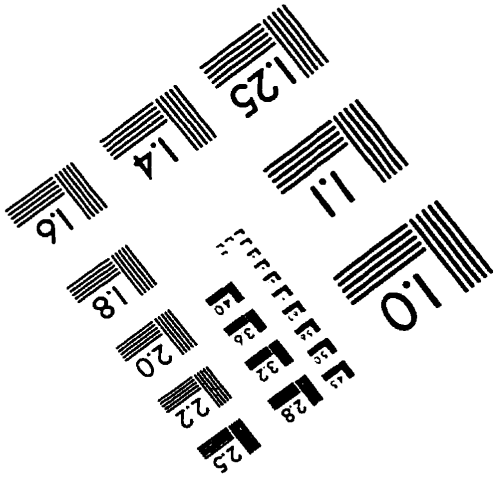

APPLIED IMAGE, Inc
1653 East Main Street
Rochester, NY 14609 USA
Phone: 716/482-0300
Fax: 716/288-5989